12-2014

ROLE OF PHOSPHORYLATION OF FOCAL ADHESION KINASE AT TYROSINE 861 IN PROSTATE CANCER METASTASIS

Tanushree Chatterji

ROLE OF PHOSPHORYLATION OF FOCAL ADHESION KINASE AT TYROSINE 861 IN PROSTATE CANCER METASTASIS

by

Tanushree Chatterji, M.S.

APPROVED:

_____

Gary E. Gallick, Ph.D., Supervisory Professor

_____

Menashe Bar-Eli, Ph.D.

_____

David J. McConkey, Ph.D.

_____

Jian Kuang, Ph.D.

_____

Scott E. Kopetz, M.D., Ph.D.

APPROVED:

_____

Dean, The University of Texas
Graduate School of Biomedical Sciences at Houston

ROLE OF PHOSPHORYLATION OF FOCAL ADHESION KINASE AT TYROSINE 861 IN PROSTATE CANCER METASTASIS

A

DISSERTATION

Presented to the Faculty of

The University of Texas

Health Science Center at Houston

and

The University of Texas

MD Anderson Cancer Center

Graduate School of Biomedical Sciences

in Partial Fulfillment

of the Requirements

for the Degree of

DOCTOR OF PHILOSOPHY

by

Tanushree Chatterji, M.S.

Houston, Texas

December 2014

DEDICATION

This dissertation is dedicated to my parents Priyabrata and Krishna, supportive husband Venky, my loving sister Anushree and brother-in law Dhanesh.

ACKNOWLEDGEMENTS

I would like to convey my deepest gratitude to my mentor, Dr. Gary Gallick for his tireless efforts and immense support, patience and encouragement during the duration of this degree.

I wish to thank my committee members Drs. Scott Kopetz, Menashe Bar-Eli, Jian Kuang, and David McConkey for their contribution, supervision, and ideas during this dissertation work.

I wish to thanks members of Dr. Gallick's laboratory, Nila Parikh, Andreas Varkaris, Jian Song, Lynnelle Thorpe, Sanchaika Gaur and Jung Kang Jin for their help, friendships, advice and encouragement during this degree.

I wish to thank the Genitourinary Medical Oncology Research program for providing me with the resources required to complete the dissertation work and the Graduate School of Biomedical Sciences for their financial support.

ROLE OF PHOSPHORYLATION OF FOCAL ADHESION KINASE AT TYROSINE 861 IN PROSTATE CANCER METASTASIS

Tanushree Chatterji, M.S.

Supervisory Professor: Gary E. Gallick, Ph.D.

Focal adhesion kinase (FAK) is a non-receptor tyrosine kinase that mediates interactions between the extracellular matrix and intracellular signaling pathways critical in promoting numerous cellular functions including adhesion, proliferation, survival and migration. Most FAK functions result from phosphorylation by Src family kinases, which trigger numerous signaling cascades. Overexpression of FAK is associated with metastasis in many solid tumors, including prostate cancer. Hence, understanding the mechanisms by which FAK is regulated in prostate cancer will better elucidate its role in prostate cancer metastasis. Work in this dissertation tested the hypothesis that altered phosphorylation of FAK is critical for cell migration and promotion of prostate cancer metastasis.

To address the hypothesis, I developed highly migratory variants of prostate cancer cells. These cells were increased in invasion, decreased in adhesion and had increased metastatic potential. A hallmark of the migratory variants was increased phosphorylation of FAK Y861. To examine the mechanism for this increased phosphorylation, expression and activity of Src family members were assessed. The migratory variants were increased in expression and total activity of the SFK, Yes, but no other members of the Src family kinases. I demonstrated that Yes was specifically responsible for the phosphorylation of FAK Y861 using both prostate tumor cells and *src-/-*, *yes-/-*, *fyn-/-* mouse embryo fibroblasts and that

increased Yes expression was directly responsible for increased migration of the selected migratory variants. Using shRNA plasmids directing knockdown of Yes, I further demonstrated that silencing Yes inhibits prostate cancer lymph node metastasis *in vivo* in an orthotopic model of prostate cancer tumor growth and metastasis. Furthermore, in human specimens, I demonstrated that Yes expression and phosphorylation of FAK Y861 was increased in lymph node metastases relative to primary tumors, with the latter correlating with decreased patient survival.

In summary, I have identified novel roles for Yes in selectively phosphorylating FAK relative to other SFKs, resulting in increased migration and metastasis of prostate cancer cells. Therefore, increased expression of phosphorylated FAK at tyrosine 861 and Yes kinase may be predictive markers for prostate cancer progression.

TABLE OF CONTENTS

LIST OF FIGURES

LIST OF TABLES

ABBREVIATIONS

AR	Androgen receptor
CRPC	Castration-resistant prostate cancer
ECM	Extracellular matrix
EMT	Epithelial to mesenchymal transition
FAK	Focal adhesion kinase
FAT	Focal adhesion targeting domain
FDA	Food and Drug administration
FERM	Ezrin, radixin, meosin domain
HBME	Human bone marrow endothelial
MAPK	Mitogen-activated protein kinases
MET	Mesenchymal to epithelial transition
PI3K	Phosphoinositide 3-kinase
PIN	Prostate intraepithelial neoplasia
PIP2	Phosphatidylinositol-4, 5-bisphosphate
PIP3	Phosphatidylinositol-3, 4, 5-trisphosphate
PSA	Prostate-specific antigen
SNPs	Single-nucleotide polymorphisms
SH2	Src Homology 2 domain
SFK	Src family kinase
USPTF	United States preventive services task force

Chapter-1

Introduction

Prostate Cancer (PCa) is the most commonly diagnosed form of cancer and the second leading cause of death due to cancer in men in the United States [1]. According to The American Cancer Society, there will be 233,000 estimated new cases of prostate cancer and 29,400 men are expected to die due to the disease in 2014. Localized disease is almost always curable, with a survival five-year rate exceeding 99% [2]. Hence, for patients with early stage localized disease, "active surveillance" is often recommended [3]. Nevertheless, many patients, even those diagnosed at a relatively early stage will choose radical prostatectomy, proton therapy or external radiation beam therapy because prediction of prognosis of prostate cancer is still unclear [4-6]. Additionally, many patients with early stage prostate cancer may choose to opt for androgen-ablation strategies as inhibition of the levels of androgens by androgen-ablation therapy leads to anti-tumor effects in early stage prostate cancer [6].

Prostate cancer, in its early stages, has few overt symptoms, hence, without performing a biopsy, diagnosis of prostate cancer in patients is challenging. Currently the biomarker used by some clinicians to guide diagnosis of prostate cancer is elevated levels of prostate-specific antigen (PSA) [7]. Presence of high serum levels of PSA (<4.0ng/mL) indicates, in some men, increased probability of having prostate cancer [8]. However, PSA is secreted by both normal and tumor prostate epithelial cells and increase in PSA concentration often occurs due to other factors such as increasing age and inflammation of the prostate [9]. On the contrary, low levels of PSA do not always indicate absence of prostate cancer [7]. The difficulty with PSA as a predictor of prostate cancer is illustrated by of two recent clinical trials by Andriole *et al.*, 2009 and Schröer *et al.* 2009. These trials have resulted in a controversial recommendation by the United States Preventive Services Task Force (USPSTF) against prostate cancer screening using PSA. However, regardless of the recommendation, The American Cancer Society

recommends that men at age 50 should discuss the benefits and limitations of PSA testing with their health care providers. High concentrations of PSA often lead to biopsies, which are more diagnostic.

If patient is biopsied, staging of the cancer is performed by the five-tier Gleason grading system [10]. The grading consists of the sum of two scores from well-differentiated pattern to most poorly differentiated pattern ranging 1-5, necessary because of the heterogeneity of the tumor. The most prevalent pattern (observed in more than 50% of the tumor) is the primary score and the second most prevalent pattern (observed in less than 50% but more than 5% of the tumor) is the secondary score ranging from 1-5. A low Gleason score of 2-6 has a five-year recurrence-free survival risk of 94.6%. As the Gleason score increases to 7 (3+4 or 4+3), recurrence-free survival risk drops to 82.7% and 65.5% respectively. Gleason score of >7 is considered high-grade cancer with the highest scores 9-10. Patients with Gleason scores of 9 or 10 have the five-year recurrence free survival of 34.5% [11]. While treatment for patients with Gleason scores >7 is always recommended, which lower grade tumors will progress and which may never progress during a man's lifetime is not clear. Thus developing better biomarkers to predict prostate cancer progression is of high priority. Considerable focus has been made on whole genome sequencing, SNP analysis, etc., to develop novel biomarkers, but these approaches have not led to an easily assayed serum marker.

Deaths from prostate cancer primarily arise from metastasis that can occur to several organs such as lungs, liver, brain and in 80% of prostate cancer cases, to the bone [12]. The five-year survival rate of metastatic prostate cancer drops drastically to 31% from 99% [2], as current therapeutic regimens have little effect on improving long-term survival of patients afflicted with metastasis [13]. Therefore, gaining a better understanding of the mechanisms by

which prostate cancer metastasizes is critical to developing novel therapies for this late-stage disease.

Some progress has been made in treatment of metastatic disease. In the last three years, several drugs that have been approved by the Food and Drug Administration (FDA) for treatment of metastatic prostate cancer, including Abiraterone Acetate [14], Enzalutamide [15] and Bicalutamide [16]. These drugs have been based on numerous studies that indicate that even late castrate-resistant metastatic disease are still "driven" by the androgen/AR pathways [17], and these drugs inhibit AR-driven genes by different mechanisms. More recently, advances in immunotherapy have led to considerable promise for the treatment of several tumors, including prostate cancer [18]. These include FDA approval of Siuleucel-T and Ipilimumab [2, 19-21]. These drugs have improved patient survival; however, few if any patients are cured by these new agents [22]. A major cause of short survival is development of resistance, in which compensatory signaling pathways still drive metastatic growth [23-25]. Hence, understanding both the mechanisms of resistance and mechanisms that lead to metastasis may provide new biomarkers and therapeutic targets. These advances in therapy may come from understanding the genetics and epigenetics of prostate cancer (discussed in the next sections), along with understanding the alterations in the androgen/AR pathway that drive prostate cancer progression (discussed later).

Genetic alterations in prostate cancer

Genetic changes in prostate cancer are fewer than in many other solid tumors, although many have been identified as summarized in a recent review by Boyd *et al*.[26]. Through several strategies, gains and losses of chromosomes have been observed. Gain of chromosome 8q is observed in 34% of prostate cancer cases and losses at chromosomes 3p, 8p, 10q, 13q, and 17p are observed in 30-50 % of prostate cancer cases [27-29]. Some of the key regulatory genes that are located within this region, including *NKX3.1* at 8p21, *PTEN* at 10q23, *MYC* at 8q24, and fusion of *TMPRSS2* and *ERG* both located at 21q22.3 to form *TMPRSS2:ERG* [30]. Some of their roles in prostate cancer initiation and progression will be discussed below briefly.

Loss of NKX3.1

NKX3.1 is a tumor suppressor gene and a transcription factor that is a critical regulator of prostate epithelial differentiation. It is located on chromosome 8p21.2 *NKX3.1* shows loss of heterozygosity (LOH) in 20% of high-grade intra epithelial neoplasia (PIN), a precursor to prostate adenocarcinoma and 78% of metastases [31]. Evidence that it is important in prostate cancer progression has been developed from genetically engineered mouse models that indicate that deletion of a single *NKX3.1* allele or complete knockout results in hyperplasia or dysplasia in prostate cancer mouse models [32, 33]. Studies have indicated that prostate glands of *NKX3.1* null mutant transgenic mice resemble histopathological alterations of human PIN [34-36] and *NXX3.1* null mice have the characteristics of early stages of prostate cancer [37]. Hence, these findings strongly suggest *NKX3.1* is a tumor suppressor gene that prevents prostate cancer initiation.

Loss of PTEN

Phosphatase and tensin homolog (*PTEN*) is a lipid-phosphatase that de-phosphorylates the 3 position of the inositol ring of PtdIns (3,4,5)P3 and thus inactivates several pathways, one of the major ones is the protein kinase B/AKT kinase pathway, critical in survival and growth of prostate cancer [38]. It was identified as a tumor suppressor gene and is located on chromosome10 q23 normal epithelial cells [38-41]. *PTEN* undergoes allelic loss in observed in 20-30% prostate cancers[42] and epigenetic silencing of *PTEN* is observed in 60% prostate cancers[40]. Studies with genetically engineered mice with knock out of *PTEN* have indicated that deletion of *PTEN* in mice causes PIN, followed by progression to invasive adenocarcinoma [43]. Additionally, loss of PTEN also promotes progression to castration-resistant prostate cancer [44]. These data indicate that *PTEN* loss promotes prostate cancer progression.

TMPRSS2:ERG

TMPRSS2:ERG is a fusion gene consisting of the *TMPRSS2* located on 21q22.3, regulated by androgens, which can be fused to the transcription factor *ERG* located on chromosome 21q22.2 from the ETS family [45]. This fusion gene is found in 50% of prostate cancers, implicating that presence of *TMPRSS2:ERG* fusion can be a critical event in prostate cancer progression leading to androgen-regulated high expression of a transcriptionally active, N-terminal truncated ERG protein that contributes to prostate cancer development and progression [46]. Transgenic expression of this fusion gene in mouse models results in PIN lesions, loss of *PTEN* and activation of the PI3K pathway leading to prostate cancer initiation [47]. Together, these data indicate that *TMPRSS2:ERG* fusion is critical in prostate cancer initiation and progression.

MYC upregulation

MYC is a transcription factor that regulates variety of cellular processes [48]. It is located on chromosome 18q24 which is amplified ~40% of the primary tumors and ~90% in prostate cancer metastases [49]. Studies using genetically engineered mouse models indicate that overexpression of MYC in the prostate of transgenic mice induces formation of PIN, leading to invasive prostate adenocarcinoma[50]. Transgenic mice overexpressing MYC when crossbred with *PTEN*-null mice developed high-grade PIN, which progressed to prostate cancer [51]. Collectively these data indicate that upregulation of *MYC* is associated with prostate cancer initiation and progression. In summary, while these genetic alterations may lead to biomarkers important in prostate cancer initiation or progression, none to date has resulted in targeted therapies.

Androgen signaling in prostate cancer progression

Although genetic alterations are required for prostate cell transformation and cancer initiation, AR signaling is the driver of prostate cancer at early stages. Binding of androgen to AR leads to formation of an androgen/AR receptor complex that translocates to the nucleus and binds to AR-responsive elements, and orchestrates transcription of androgen-regulated genes [52]. Activation of androgen-regulated genes promotes cell survival, proliferation and prevention of apoptosis of cancer cells [53]. Hence, inhibition of the levels of androgens by androgen-ablation therapy leads to anti-tumor effects in early stage prostate cancer also known as the “endocrine-phase” of prostate cancer [54].

As prostate cancer progresses under androgen-ablation selection pressure, the tumor evolves and escapes dependence on androgen entering the “paracrine-phase” [54]. In this phase,

the disease is not only driven by androgens but also numerous stimuli/molecules secreted from the microenvironment [54]. Hence, the "paracrine-phase" of tumor development involves both the tumor and the microenvironment to promote metastasis. Collectively, the "endocrine-phase" and the "paracrine-phase" lead to development of prostate cancer metastasis, which does not respond to chemotherapeutics leading to mortality of patients. Therefore, in the next section, I will briefly describe the metastatic process in prostate cancer and the selected signaling pathways that are associated with metastasis relevant to my thesis work that may lead to novel therapeutic approaches.

Prostate cancer metastasis

As the vast majority of deaths due to prostate cancer result from metastases, mostly to the bone but also to the viscera and a better understanding of the metastatic process is required to develop novel therapies that will prolong survival. The metastatic process is extremely inefficient but selective, with less than 0.1% of the cells that enter the circulation, surviving to form metastasis at the distant sites [55]. The classical model of metastasis, the "seed and soil" hypothesis was first proposed by Stephen Paget in 1889, which states that tumor cells (seeds) only metastasize to specific organs (soil) that facilitate their growth [56]. Work that is much more recent has led to the understanding that the tumor microenvironment at the metastatic site plays an important role in the development of the "soil" that facilitates the process of metastasis.

Classically, as defined by Fidler *et al.*[57], the metastatic process has been described as a series of individual but linked steps including angiogenesis, migration, invasion, intravasation, circulation, extravasation and finally, colonization in distant organs [58]. Several models have been described to understand the progression of these steps. One model is the "linear progression model" that states that cancer cells pass through multiple successive rounds of

mutations to select for cells with competitive fitness in the context of the primary tumor to go through above mentioned steps in metastasis [59]. The tumor cells that can survive and proliferate at a competitive rate, expand and subsequently leave the primary tumor sites to colonize on the secondary sites [59]. However, dissemination of tumor cells can occur early (when the primary tumor is small). The second model is the "parallel progression model", that states that metastasis can occur in parallel to the development of the primary tumor and this model does not consider the occurrence of dissemination of cells as a later phenomenon after development of primary tumor [60]. Moreover, dissemination of cells can occur during the development of primary tumor as the cells adapt to the tumor microenvironment [59].

In spite of the presence of the different models that define cancer progression, a critical process that facilitates metastasis in both these above-described models is bidirectional interactions between tumor cells and microenvironment, occurring both at the primary and metastatic sites. At the primary site, one of the adaptations is epithelial to mesenchymal transition (EMT), which allows cells to acquire a more mesenchymal phenotype, increasing their abilities to migrate and invade through the ECM. However, the cancer cells later revert to the mesenchymal phenotype by mesenchymal to epithelial transition (MET) allowing adherence to ECM and growth at the metastatic site. This ability of cancer cells to switch between different phenotypes through EMT and MET is a feature of "epithelial plasticity" [61, 62].

A recent study demonstrated that switching between different modes of cell migration is required for epithelial plasticity and metastasis [63], indicating the role of migration of cells in metastasis. In prostate cancer, a number of studies have demonstrated a strong correlation between increased migration of prostate cancer cells and metastasis [64-66]. However, the

molecular mechanisms that regulate the process of migration remain unclear. Hence, a principal focus of this thesis was to understand the role of migration in metastasis of prostate cancer.

Migration signaling in prostate cancer

While there multiple modes of migration, classified as amoeboid migration, mesenchymal migration, multicellular streaming and collective migration [67], the underlying process in all the modes of migration results in changes in cytoskeletal dynamics. These are highly complex processes that involve many signaling pathways [68].

Relevant to my work, Focal Adhesion Kinase (FAK) is a critical mediator of migration signaling. FAK is a non-receptor tyrosine kinase that localizes to focal adhesions, which mediate interactions between the extracellular matrix and intracellular signaling through integrin activation upon cell attachment to the extracellular matrix [69]. The role of FAK in migration is demonstrated in FAK-null mouse embryonic fibroblasts, which form irregular focal adhesion complexes in which FAK turnover does not occur and cells do not migrate; the first demonstration that FAK turnover was essential to migration [70]. The next section of this thesis briefly describes the structure and activation of FAK followed by the role of FAK in the process of cell migration.

Focal adhesion kinase (FAK)

Structure of FAK

FAK is a 128 KDa non-receptor tyrosine kinase that, as described above, localizes to focal adhesions. X-ray crystallography has revealed that FAK consists of an N-terminal four-point-one ezrin radixin moesin (FERM) domain, a central kinase domain, proline-rich regions,

and a C-terminal focal-adhesion targeting (FAT) domain (Figure 1) [71]. These domains are arranged as a tripartite globular structure with the FERM domain organized in a compact cloverleaf conformation connected by an unstructured linker to the catalytic domain, which in turn is connected to a four-helix bundle structure of FAT domain by an unfolded proline-rich region (Figure 2). Each of these domains and their functions are briefly described below.

N-Terminal domain

The N-terminal is also known as the FERM domain that has three lobes, the F1, F2 and F3 subdomains. The F1 subdomain consists of a five-strand β sheet capped by and α-helix. The F2 subdomain is entirely α-helical with a core similar to acyl-CoA-binding protein. This region of the protein docks with the catalytic domain of the FAK itself and forms the auto-inhibited conformation. The F3 subdomain is a β-sandwich capped by a C-terminal α-helix. The linker between the FERM and the kinase domain consists of an anti-parallel β-sheet that binds on a groove on the F3 subdomain. Two important features of the linker are tyrosine 397, the major autophosphorylation site and the nearby "PxxP" motif that acts as and SH3-domain binding site [72] as shown in Figure 2. The FERM domain facilitates interaction of FAK with other receptor tyrosine kinases such as MET, EGFR, PDGFR and also some integrins [73]. These interactions are required to activate signaling cascades that promote migration, as well as invasion, survival, proliferation, adhesion and anti-apoptosis[73].

Kinase domain

This is the primordial conserved domain related to all tyrosine kinases. The crystal structure of FAK kinase domain reveals a bilobed structure with the N-terminal lobe containing a single α-helix with a five-stranded β-sheet and the larger C-terminal lobe that is mostly α-

helical [72]. In the kinase domain itself are three tyrosine phosphorylation sites (Y407, Y576 and Y577). Phosphorylation of these sites results in formation of a β hairpin loop confirmation, as observed in other active kinases [74].

C-Terminal domain

The C-terminal of FAK contains the focal adhesion targeting (FAT) domain contains four amphipathic α-helices that assemble into an antiparallel four helix bundle. The FAT domain also consists of two hydrophobic patches that bind to the FAK-associated proteins containing the leucine-rich (LD) domain. The α- helix 1 of the FAT domain contains tyrosine 861 and tyrosine 925 [75]. Specific functions of the C-terminal domain of FAK include association of the FAT domain to integrins and localization of FAK to focal adhesion complexes, which is required for migration of cells [72, 75]. Additionally, tyrosine 861 and tyrosine 925 upon phosphorylation by Src family kinases (SFKs) recruit Grb2 via the Grb2 SH2 domain, leading to activation of the Ras/Raf/MAPK/ERK proliferation pathway.

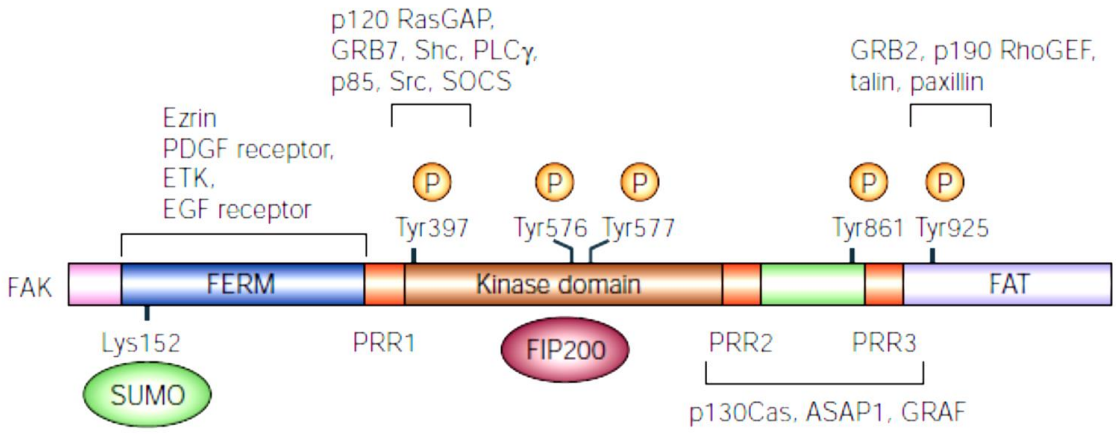

Figure 1: Structure of FAK. FAK consists of an N-terminal FERM domain, a C-terminal FAT domain and a kinase domain. Multiple tyrosine phosphorylation sites present on FAK include Y397, Y401, Y576, Y577, Y861 and Y925. FAK contains three proline-rich regions PRR1, PRR2 and PRR3 that bind to SH3 domain containing proteins.

From Mitra SK, Hanson DA, Schlaepfer DD (2005) Focal adhesion kinase: In command and control of cell motility. Nat Rev Mol Cell Biol 6: 56-58. Reproduced with permission.

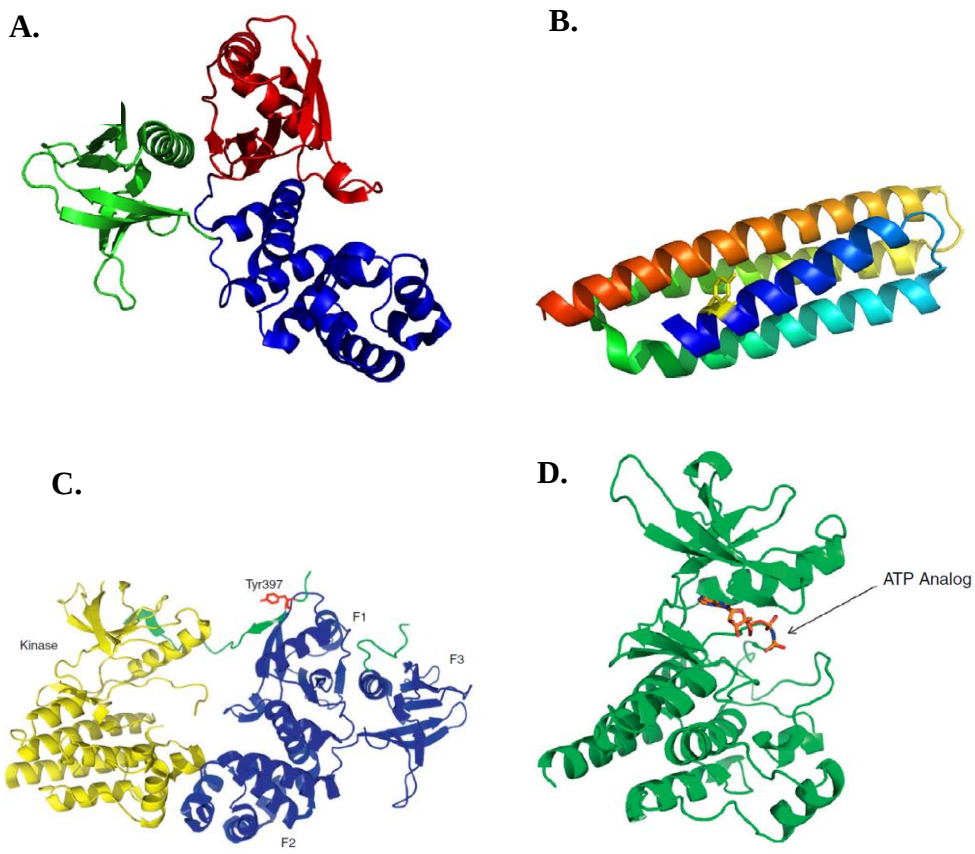

Figure 2: Crystal structure of FAK A. Three lobes FERM domain with subdomains F1 (Red), F2 (Blue) and F3 (Green) **B.** Kinase domain with a small N-terminal lobe with single α-helix and β strands **C.** FAT domain of FAK with the containing four-helix bundle (colors indicate different helices) **D.** Structure of auto-inhibited FAK FERM domain, the FERM domain is indicated blue, the linker segment is green and the kinase domain is yellow. Tyrosine 397 autophosphorylation residue is on the linker segment represented by sticks colored in red. Association of p130Cas to the tyrosine 861 and tyrosine 925 leads to recruitment of Crk/DOCK complexes, that regulate signaling pathways involved in migration of cells [76-78].From Hall JE, Fu W, Schaller MD. (2011) Focal Adhesion Kinase: Exploring FAK Structure to Gain Insight into Function. Int Rev Cell Mol Biol. 288-185-225. Reproduced with permission.

Activation and regulation of FAK

As stated above, FAK can be activated by multiple mechanisms, principally including integrin clustering or growth factor receptor activation [72]. FAK activation occurs through sequential steps starting with release of the FERM-kinase domain from the intramolecular interaction after binding to a heterologous FERM binding partner. After the FERM domain is released, activation of FAK occurs upon autophosphorylation of tyrosine 397 [79]. Phosphorylated tyrosine 397 then binds to SH2-domain containing proteins including Src family kinases (SFKs), PI3-Kinase, PLCγ, SOCS, Grb7, Shc and p120RasGAP. SFK binding to pFAK Y397 (through the SFK SH-2 domain) leads to activation of the interacting proteins (Figure 4), and phosphorylating each of the other tyrosine phosphorylation sites on FAK, specifically Y577, Y576, Y407, Y861 and Y925 [80]. As stated above, phosphorylation of FAK Y576 and FAK Y577 is required for complete activation of the FAK kinase, and the activated FAK kinase domain adopts a conformation that cannot be inhibited by FERM-mediated intramolecular interactions, as the phosphorylated activation loop precludes the inhibitory docking of the FERM domain (Figure 2) [80].

Role of FAK and cell migration

For migration to occur, the leading edge of the cells must attach to the ECM, a process that results in formation of focal contacts [81]. During the formation of focal contacts, FAK is recruited to the focal contacts and associates with the Arp2/3 complex to promote actin polymerization and causes cell spreading [82]. The cell then elongates to form cell protrusions called pseudopods, which result in distinct polarity differences between the cell “front” and “rear” as shown in Figure 4 [83]. The cell protrusions that associate with ECM are called

lamelipodia, which are broad, flat sheet like structures and filopidia, which are thin, elongated, needle-like structures [84]. In the next stage of migration, the growing protrusions containing integrins bind to the ECM resulting in integrin clustering leading to autophosphorylation of FAK Y397 and subsequently phosphorylation of FAK at Y401, Y576, Y577, Y861 and Y925 [85]. Specific to migration signaling, phosphorylation of FAK Y397 leads to recruitment of PI 3-kinase and activation of Rac GTPases required for lamelipodia formation and migration (Figure 5) [86]. Phosphorylation of FAK Y 861 and FAK Y 925 leads to recruitment of p130Cas and formation of complexes with Crk/DOCK 180 and activation of Rac GTPases, which are also essential in lamelipodia formation, and cell migration [87]. Simultaneously, FAK phosphorylates both the guanine nucleotide exchange factor (GEF), that activate Rho proteins and GTPase activating protein (GAP) that deactivate Rho proteins necessary to generate contractile forces and induce cell polarity required for migration [88]. In the final stages of migration, tyrosine phosphorylation of FAK results in disassembly of focal adhesion complexes [89], detachment of the trailing edge leading to turnover of FAK and forward movement of the cell.

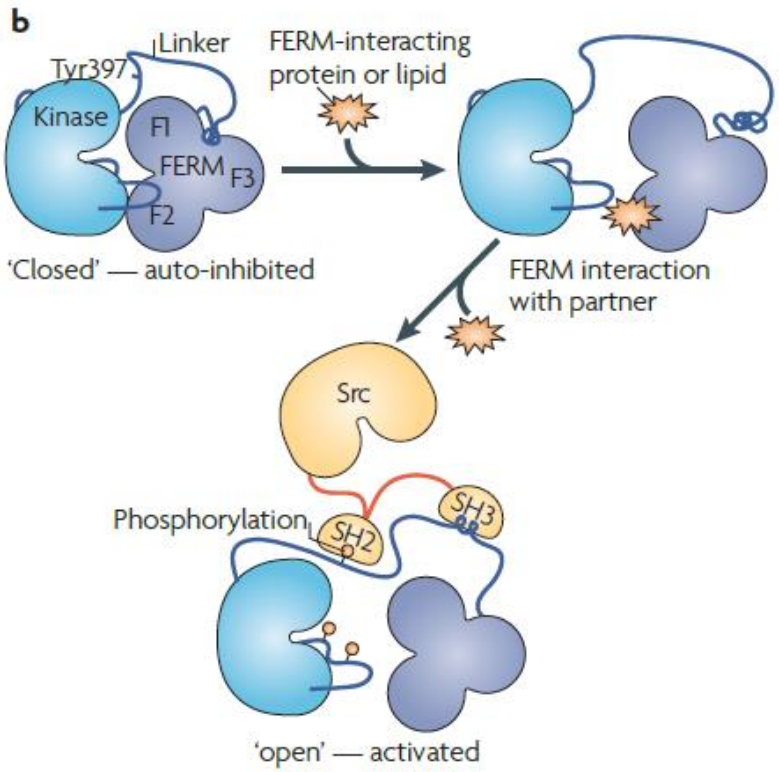

Figure 3: Activation of FAK. The FERM domain directly binds to the kinase C-lobe when FAK is auto-inhibited, impeding access to the FAK active site and protecting FAK activation loop from phosphorylation by SFKs. Binding of a protein or a lipid-partner to the FAK FERM domain leads to conformational change in FAK and release of the auto-inhibited "closed" state. This conformational change allows binding of SFKs leading to tyrosine phosphorylation of FAK and increases its kinase activity.

From Frame MC, Patel H, Serrels B, Leitha D, Eck MJ (2010). The FERM domain: organizing the structure and function of FAK. Nat Rev Mol Cell Biol.11 (11):802-14. Reproduced with permission.

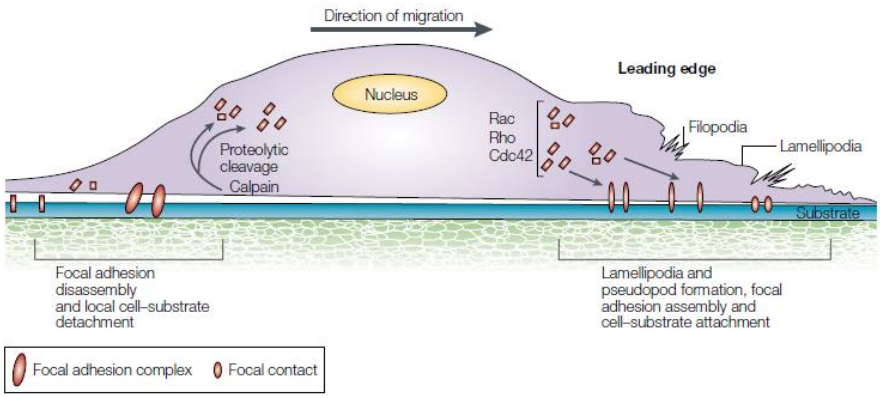

Figure 4: Cell migration. Directed cell migration occurs upon coordinated formation of focal adhesion complexes in the leading edge of the cell followed by simultaneous detachment of the focal complexes in the trailing edge of the cell. Several molecules like integrins, FAK, Rho/Rac GTPases are required for the cell to migrate.

From Mitra SK, Hanson DA, Schlaepfer DD (2005) Focal adhesion kinase: In command and control of cell motility. Nat Rev Mol Cell Biol 6: 56-58. Reproduced with permission.

FAK in prostate cancer progression

FAK is overexpressed in many solid tumors; including prostate cancer and increased FAK expression is associated with prostate cancer progression [90, 91]. However, the existing studies on FAK overexpression and prostate cancer are correlative; and whether overexpression of FAK plays a casual role of FAK in prostate cancer progression still remains to be established [92].

In addition to lack of knowledge about the role of FAK overexpression in mediating prostate cancer metastasis, considerable information is lacking with respect to potential roles of differential phosphorylation of different FAK tyrosine residues. While FAK phosphorylation and the signaling pathways mediating proteins interacting with these tyrosine residues have been well described, few studies have addressed whether altered phosphorylation at one or more sites contribute to tumorigenicity and progression of prostate cancer. Recent work from Slack JK *et al.* has indicated that phosphorylation of FAK Y861 is associated with more migratory prostate cancer cells [78]. Additionally, phosphorylation of FAK Y861 is also associated with oncogenic transformation of fibroblasts [93]. However, these observations are only associations, and mechanisms of increased phosphorylation of specific FAK tyrosine phosphorylation sites and their biological relevance is unclear. Hence, this thesis focused on the unanswered questions in FAK regulation that might mediate biological properties of prostate cancer progression.

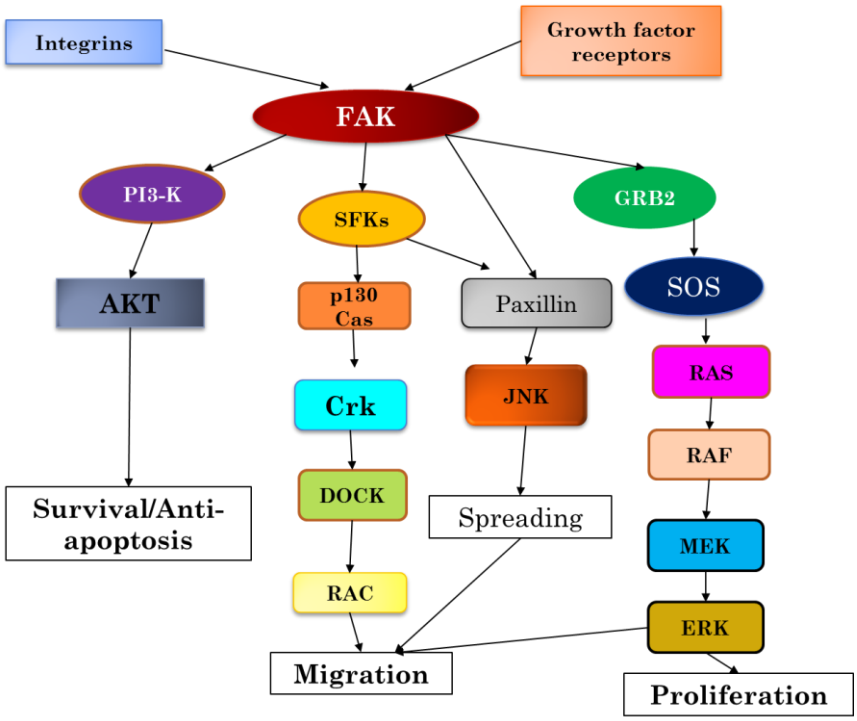

Figure 5: FAK is the central mediator of migration pathway. Multiple molecular pathways regulate migration of cells including integrins and growth factor receptors and non-receptor tyrosine kinases. The FAK/SFK signaling pathway is the central mediator of migration signaling. Additional pathways that regulate migration, survival and proliferation of cells include, PI3-K /AKT and the Ras/Raf/MEK/ERK pathway.

Src family kinases- Structure, Activation and Function

As discussed in the previous sections, after the initial autophosphorylation of FAK, SFKs are required for the additional phosphorylations. These phosphorylations are critical to all FAK functions, including migration, invasion, angiogenesis, cell survival, cell proliferation, cell cycle regulation, epithelial to mesenchymal transition and resistance to anoikis [94-99]. As SFKs are required for FAK-mediated migration, it is not surprising that Src family members themselves are also associated with migration, as activation of Src increases migration [100-103] and *src-/-* cells are impaired in migration [104]. Therefore, understanding the relationship among SFKs and FAK is critical in understanding the migration process.

Structure and activation of the SFK family

SFKs are a group of nine structurally highly related non-receptor tyrosine kinases consisting of Src, Yes, Fyn, Lyn, Lck, Blk, Fgr, Yrk and Hck [100]. SFKs mediate signals from numerous cellular stimuli including integrins, receptor tyrosine kinases, cytokine receptors, ion channels, G-protein coupled receptors, polypeptides, and hormones that activate downstream signaling pathways that regulate numerous cellular functions. To better understand the role of SFKs in prostate cancer migration, a brief introduction to the structure and activation of SFKs are described below.

The structure of SFKs is composed of an N-terminal membrane-targeting region that is myristoylated. Many Src family kinases (the exception being Src itself) are also palmitoylated at the N-terminal glycine residue. The Src homology-4 (SH-4) domain residues at the amino terminus function for membrane localization; Src homology-3 (SH3) domain involved in intermolecular binding by recognizing prolines in the Pro-xx-Pro motif of the substrates; the

Src homology-2 (SH2) domain interacts with numerous phospho-tyrosine containing proteins, including its own C-terminal tyrosine 530 residue that leads to a closed conformation (see below); the kinase domain or Src homology-1 (SH-1) is the primordial tyrosine kinase domain [105].

Activation of SFKs occur when the SFK-SH2 domain of FAK has higher affinity to the phospho-tyrosine domains of numerous factors that it can interact with relative to the negative-regulatory tyrosine 530 (human nomenclature) residue on its own SH2 domain [100]. Upon binding of the activated growth factor receptors to SFK-SH2 domain, a conformational change occurs that increases the accessibility to phosphatases that dephosphorylate the C-terminal phospho-tyrosine residue (tyrosine 530 in human Src). Once in the "open" conformation, autophosphorylation of the tyrosine 419 residue (human Src) occurs leading to "complete" catalytic activation of Src (Figure 6) [106].

As numerous proteins that interact with SFKs are aberrantly expressed or activated in several solid and hematological tumors [107-110], SFKs themselves are also frequently activated as well [110, 111].

SFKs in Prostate cancer

SFKs have aberrantly increased activity in prostate cancer cells and they have various functions in prostate cancer progression as described above. Additionally, different members of the SFK family are also suggested to play important roles in prostate cancer progression. Jensen AR *et al.*, demonstrated that Fyn plays important roles in prostate cancer cell growth and chemotaxis, required for metastasis [112]. Additionally, Lyn kinase regulates androgen expression and activity in castrate-resistant prostate cancer and mice in which Lyn is

functionally deleted showed abnormal morphogenesis of the prostate gland [113-115]. Interestingly, a recent study by Cai H *et al.* indicates that ectopic expression of Src, Fyn and Lyn kinase in primary prostate cancer cells isolated from *Src−/−Fyn+/−, Fyn+/−, Fyn−/−, or Lyn−/−* knockout mice have different transformation capacities, with Src inducing the strongest oncogenic phenotype, followed by Fyn and then Lyn [116]. Regenerated tissue from *Lyn-/-* epithelium on transformation displayed neoplastic growth, whereas transformation of tissues from *Fyn-/-* epithelium exhibited PIN lesions. In contrast, transformation of tissue from *Src−/−Fyn+/−* mice resulted in normal glandular structures [116]. These data strongly suggest that different SFK members have different roles in mediating prostate cancer progression.

Understanding these roles may be of critical importance because of the recent failure of an SFK inhibitor, Dasatinib in an international phase-3 clinical trial [117]. Numerous investigators have suggested that this failure may be due to lack of understanding of specific and overlapping roles of SFKs in tumor progression and bone metastasis [118-120]. Strikingly, there have been no studies published on specific roles of Yes in these processes; the work in my thesis has provided an understanding of some of its critical functions.

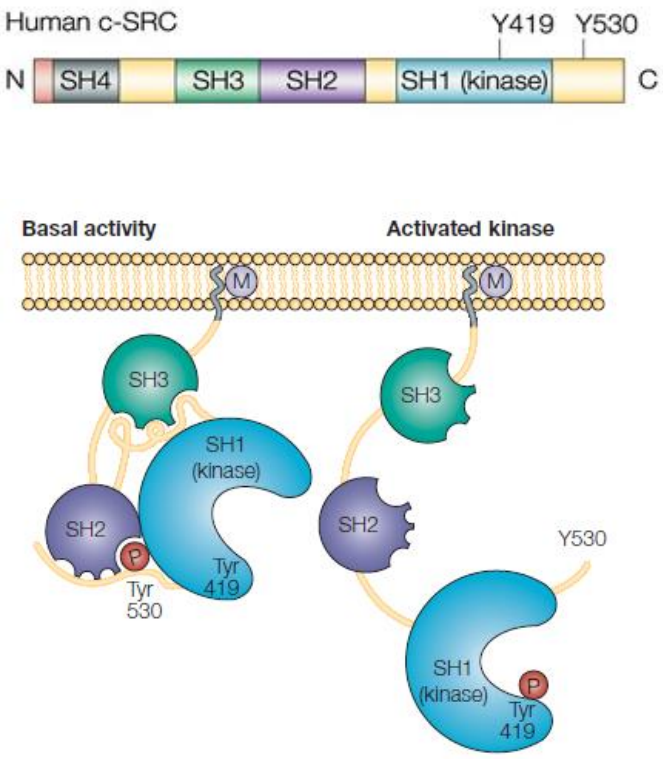

Figure 6: Structure and activation of SFKs. In an inactive status, SFKs are in a "closed" conformation by intramolecular interactions between SH-3 domain and Pro-X-X-Pro domain and between SH-2 domain and negative regulatory phosphorylated tyrosine 527 residue. This closed conformation limits accessibility of the kinase domain active site for substrates. SFKs attains a more "open" conformation through phosphatase-mediated dephosphorylation of the Y527 residue and higher affinity of SH-2 and SH-3 domains to activated binding partners and also through phosphotyrosine residues and Pro-X-X-Pro motifs. Further phosphorylation at tyrosine 416 in SH-1 kinase domain is required for “complete” kinase activity of SFKs, leading to open accessibility of substrates to the active binding sites of the kinase domain.

From Yeatman TJ (2004) A renaissance of SRC. Nat Rev Cancer 4(6):470-480. Reproduced with permission.

Differential roles of Yes kinase in regulating cellular signaling

Since, Src and Yes kinase are the two most structurally similar members with about 90% structural homology, there are signaling and functional redundancies in between these two kinases[121]. However, there are also specific structural and functional differences between Yes and Src kinase indicating a possibility of different roles in tumor progression [121, 122]. These structural differences suggest the possibility of different roles and indeed a previous study from our lab has indicated that Yes activation portends poorer survival in colorectal metastases than does Src activation [123]; however, these correlative studies have not defined specific roles for Yes. As indicated above, a potential role for Yes activation in promoting prostate cancer progression or metastases was unknown before the work performed in my thesis.

Summary of problems and hypothesis

Prostate cancer is the second leading cause of cancer-related deaths in men in the Unites States [1]. Although, the five-year survival rate of patients with early-stage disease is ~99%, the survival rate of patients with metastatic disease including to the lymph node and bones, drastically decreases to 31% [124]. Thus, understanding the molecular mechanisms that drive prostate cancer metastasis could lead to development of novel therapeutic strategies to prevent metastasis.

The goal of this PhD. thesis was to focus on specific aspects of migration, an early step in the metastatic cascade [81]. One of the mediators of migration of cells is FAK [85]. Additionally, FAK is overexpressed in prostate cancer [91, 125]. However, whether FAK has a role in increased metastasis of prostate cancer remains unknown. FAK is phosphorylated by SFKs and SFK-mediated FAK phosphorylation is one of the mechanisms that regulate

migration of cells [94, 106]. SFKs also regulate numerous biological properties that promote metastasis of prostate cancer including migration of cells and increased SFK activity is associated with prostate cancer progression [100, 106]. However, a novel small molecule inhibitor of SFK has failed to show significant improvement in overall survival in patients with metastatic castrate resistant prostate cancer [117], indicating the need for a deeper understanding of the molecular mechanisms that are regulated by different SFK members. Current knowledge implicates, Src (a member of the SFK) as the major kinase that phosphorylates FAK [126]. However, recent evidence indicates that different SFK members have different role in prostate cancer progression [113, 116, 127]. Hence, the emphasis was to understand if specific changes in the FAK-SFK complexes could be identified that promote migration and affect important processes of metastasis.

Recent studies have demonstrated increased phosphorylation FAK Y861 in migration of prostate cancer cells [78]. However, the cause and effect of this phenomenon is still unclear. Therefore, the first question addressed in this dissertation is whether all the tyrosine residues on FAK are phosphorylated equally in the PC3 Mig-3 and DU145 Mig-3 cells and specifically understanding the role of increased phosphorylation of FAK Y861 in highly migratory prostate cell models, which were developed by me. The second question was what is the association of increased phosphorylation of FAK Y861 in survival of patients? The third question was what is the mechanism of increased phosphorylation of FAK Y861, leading to understanding the roles of Yes kinase in preferential phosphorylation of FAK Y861? In addition, the fourth question was whether Yes kinase promotes prostate cancer metastasis and if increased Yes expression is associated with prostate cancer progression in patients.

The hypothesis tested in this dissertation was that changes in the FAK/SFK complexes dictate the increased migration in prostate cancer cells and promotes prostate cancer metastasis. To test this hypothesis, I first isolated highly migratory variants of prostate cancer cells named PC3 Mig-3 and DU145 Mig-3 from parental PC3 and DU145 cells. I then examined the role of pFAK Y861 in migration of these cells by overexpressing its non-phosphorylatable form FAK Y861F in the PC3 Mig-3 cells and then investigated the relevance of pFAK Y861 expression with survival of prostate cancer patients. Then, I investigated the mechanism of increased phosphorylation of FAK Y861 by silencing Yes in PC3 Mig-3 and overexpressing Yes kinase in parental PC3 cells. Finally, I assessed the role of Yes kinase in prostate cancer metastasis *in vivo* and investigated the clinical relevance of Yes expression in matched primary tumor and lymph node metastasis from patients. Together, this work addressed the mechanism and biological function of FAK Y861 phosphorylation and providing a better understanding of the mechanism for prostate cancer metastasis.

Chapter-2

Materials and Methods

Cell culture

Human prostate cancer cells lines; PC3 cells were a gift from Dr. Isaiah J. Fidler's laboratory and were maintained in DMEM F-12 (Hyclone) supplemented with 10% FBS (Hyclone). DU145 cells were a gift from Dr. Renata Pasqualini's laboratory and were maintained in RPMI 1640 (Corning cell gro) supplemented with 10% FBS (Hyclone). SYF *(Src-/-, Yes-/-, Fyn-/-)* mouse embryonic fibroblasts were bought from ATCC and grown in DMEM media containing 10% FBS, glutamine and pyruvate. Cell cultures were incubated in 5% CO_2/95 % air tissue culture incubators at 37^{o}C. Cells were checked every three months to be mycoplasma free. Fingerprinting analysis was performed on these cell lines by the M.D Anderson Cancer Center Department of Systems Biology and the identities of these cell lines were confirmed. The analysis was performed using the AmpF_STR Identifier kit according to the manufacturer's instructions (Applied Biosystems #4322288). The STR profiles were compared to known ATCC DNA fingerprints (ATCC.org) and to the cell line integrated molecular authentication database (CLIMA) version 0.1.200808 (http:// bioinformatics.istge.it/clima/) (Nucleic Acids Research 37:D925-D932 PMCID: PMC2686526).

Migration assay

Migration abilities of the PC3 and DU145 cells were determined by the modified Boyden chamber migration assay as described by Lesslie *et al*. [98]. Briefly, PC3 and DU145 cells were trypsinized and plated ($0.05 \text{ X } 10^6$) in the upper well of the 8.0µm pore size polyethylene terephthalate membrane culture inserts for 24 well plates (BD Biosciences, Medford MA) in 500µL DMEM/F12 media without FBS. The lower chamber was filled with 750µLof DMEM/F-12 supplemented with 10% FBS as a chemo attractant. After 24 hours, the non-migratory cells from the upper chamber were scraped using a cotton swab. The cells that had migrated in the lower chamber were fixed and stained with HEMA-3 stain kit (EMD, Millipore) according to the manufacturer's protocol. Migrated cells were counted in 100X magnification under the microscope in five random fields/inserts in triplicates. Each experiment was performed in triplicates.

Time-lapse microscopy and quantification of cell migration

Subconfluent tumor cells were detached with 2mM EDTA (Ambion #AM9260G), embedded (33,000/100 µl) in bovine collagen (PureCol, Advanced BioMatrix, Catlog #5005-B; final concentration 1.7 mg/ml), and afterwards incorporated into a self-constructed chamber. To construct the migration chamber an object slide and a coverslip were connected by a spacer composed of vaseline / paraffin (1:1), resulting in an approximate chamber size of 20 x 20 x 0.5 mm and a volume of ~200 µl. After addition of medium, spontaneous migration was monitored by digital time-lapse, bright-field inverse microscopy (air objectives, 10×, NA 0.20; Leica) at 37°C using CCD cameras (Sentech) and the 16-channel frame grabber software (Vistek) for 24 hr. with 4-min frame intervals. Migration speed was quantified by computer-assisted cell tracking (Autozell 1.0 software; Centre for Computing and Communication Technologies

[TZI], University of Bremen, Bremen, Germany) of xy paths with 12-min step intervals (tumor cells). The average speed per cell was calculated from the length of the path divided by time, including "go" and "stop" phases.

Invasion assay

Invasion abilities of the PC3 and DU145 cells were determined by the modified Boyden chamber invasion assay as described by Lesslie *et al*.[98]. . Briefly, parental PC3 cells (0.5 X 10^6) were suspended in the upper well of the 8.0µm pore size polyethylene terephthalate membrane culture inserts for 24 well plates coated with matrigel (BD Biosciences) in 500µL DMEM/F12 media without FBS. The lower chamber was filled with 750µLof DMEM/F-12 with 10% FBS as a chemo-attractant. After 24 hours, the non-invasive cells from the upper chamber were scraped using a cotton swab. The cells that had invaded in the lower chamber were fixed and stained with HEMA-3 (Biochemical Sciences) according to the manufacturer's protocol. Invasive cells were counted in 100X magnification under the microscope in five random fields/inserts in triplicates.

Adhesion assay

PC3 and DU145 cells (5 X 10^4 cells/ 100µL) were seeded into each well of a 96 well plate. The plates were incubated for 30 minutes in 37^{o}C; the wells were washed with PBS three times and incubated with 1µmol/L Calcein AM (Invitrogen Life Technologies, Grand Island, NY, USA) for 3 minutes. The cells that adhered to the plate were quantified by measuring the fluorescence intensity at 458/528 nm in each well on a Synergy HT fluorescent plate reader (BioTeK).

Proliferation assay

3 x 10^4 cells / well were cultured in 6-well dishes for up to 96 hours. For cell counting, at various time points, the media was removed, cells were washed with once PBS (Gibco), and 500µl TrypLE dissociation reagent (Gibco) was added to each well. Cells were then incubated for 5 minutes at 37ºC. Complete media (1ml) was then added to each well, and cells were resuspended with a micropipette. 500µl cell suspension was transferred into a separate cup (Beckman Coulter) and cells were counted using an automated cell viability analyzer Vi-Cell XR (Beckman Coulter). All experiments were performed in triplicate.

Immunoblotting

Clarified cell lysates (50µg/lane) were separated by SDS-PAGE on 8% gels and electroblotted onto PVDF (Immobilin-P) membranes (EMD Millipore, Billerica, MA,USA) as described previously(). Membranes were blocked with 5% skimmed milk in TBS-T and incubated with primary antibodies (listed in table) overnight at 4ºC. All mouse monoclonal antibodies were followed by horseradish peroxidase-conjugated rabbit anti-mouse IgG (ICN Biochemicals Inc., Costa Mesa, CA, USA); rabbit polyclonal antibodies were followed with horseradish peroxidase conjugated goat anti-rabbit IgG. Specific binding was determined using the Pierce ECL western blotting substrate (Thermo Fisher Scientific, Waltham, MA, USA).

Immunoprecipitation

Cells were rinsed with ice cold PBS, then detergent lysates were made in a standard Radio Immuno Precipitation Assay ‘A’ buffer (Garcia et.al 1991). Cells were homogenized and clarified by centrifugation at 10000g. Cell lysates (500 µg protein) were reacted for 12 hours with the monoclonal antibody for anti-Src (Cell Signaling Technologies, Inc., Danvers,

MA,USA), Yes, Fyn and Lyn (Santa Cruz Biotechnology, Dallas, TX,USA). The next day, 50µL of 1:1 slurry of protein 'A' or protein 'G' agarose beads (Millipore) in NP-40 buffer was added to the protein lysate- antibody mixture and incubated for an additional 2 hours in 4^{o}C. Bound proteins were pelleted by centrifugation, washed three times with Np-40 buffer, and eluted by boiling in 1X Lamelli's sample buffer. Bound proteins were subjected to western blot analysis as described above.

RNA isolation and quantitative RT-PCR

RNA was isolated from the cells using RNAeasy™ mini kit (Catalog # 74104, Qiagen, Valencia, CA, USA) according to the manufacturer's instructions. Briefly, total RNA (200ng) was reverse transcribed by using a cDNA synthesis kit (Invitrogen, Life Technologies, Grand Island, NY, USA) according to the manufacturer's instructions. Gene expression was determined by quantitative PCR (qPCR) using KiCq Start SYBR Green kit (Sigma). The primer sequences for Yes were forward- TCCTGCTGGTTTAACAGGTGGTG and reverse- TGCTTCCCACCAATCTCCTTCC

Rho-A activation assay

Rho-A activation was determined by Rho G-LISA™ assay kit according to the manufacturer's instructions (Cytoskeleton Inc., Denver, CO, USA). Samples were prepared according to the instructions. Briefly, PC3, PC3 Mig-3, and Mig-3 FAKY 861-F cells were grown in subconfluent conditions for 3 days. The cells were then counted and plated in 12 well plates in serum-free media overnight. The cells were then stimulated with 10% FBS containing media and lysates were made from the cells immediately after 0, 6, 12, and 30 minutes. Protein assay was performed and an equal amount of protein was added to the wells of the Rho G-LISA

plate coated with Rho-GTP binding protein. The plate was placed in a cold micro plate shaker at 300rpm at 4^{o}C for 30 minutes. The plate was then washed 3 times with wash buffer at room temperature. Then anti-Rho an antibody (1:250 dilution) was added to each well and the plate was placed on the shaker for an additional 30 minutes. After three washes, the horseradish peroxidase reagent was added to the wells. The luminescence signal from the wells was read @490 nm using a microplate spectrophotometer. Results are shown as absorbance over the background signal (background signal is incubation from the assay reagent only).

Lentiviral-mediated pFAK Y861F expression

The FAK Y861F, WT FAK and empty vector plasmids were constructed by Dr. Rebecca Schweppe's lab (University of Colorado, USA). These plasmids contain a blasticidin resistant gene and a gene encoding V5 tagged mutant FAK Y861F. The lentivirus was infected (MOI: 11) into the PC3-Mig 3 cells using 4µg/mL polybrene. After 24 hours of infection, the media was replaced with DMEMF12 and RPMI 1640 containing 10µg/ml Blasticidin Hcl.

Lentivirus-mediated Yes silencing

Mission shRNA bacterial glycerol stock plasmids for Yes were purchased from Sigma-Aldrich. Sequences used for Yes were TRCN0000001611:CCGGACCACGAAAGTAGCAATCAAACTCGAGTTTGATTGCTACTTTCGTGGTTTTT,TRCN0000010006:CCGGTGGTTATATCCCGAGCAATTACTCGAGTAATTGCTCGGGATATAACCATTTTT. A non-targeting control was used along with the shRNA plasmid. The knockdown of Yes using both the sequences was confirmed by immunoblotting. For lentivirus production, the pLKO.1-puro plasmid (3 µg) was co-transfected with the packaging plasmid pCMV-dR8.2 dvpr (3 µg) and the envelope plasmid pCMV-VSV-

G (0.6 µg) in a ratio of 5:5:1 into 293FT cells in one 100-mm plate (Life Technologies) using Lipofectamine 2000 (Life Technologies). After 24 hours incubation in culture, medium was replaced with 20% FBS. The viral supernatant was collected after 24 hours and again at 48 hours, filtered through 0.45 µm filters followed by centrifugation at 20,000 rpm for 2 hours at 4 ℃. The viral pellet was resuspended in 200 µl of RPMI medium and stored at -80 ℃. Cells were cultured in 48-well plates were incubated with 20 µl of virus supernatant in the present of 8 µg/ml of polybrene (Sigma) and centrifuged at 500 ×g for 20 min and further incubated for 24 hr. The medium was changed after 24 hours and replaced again with 5 µg/ml puromycin after 48 hours and incubated for one week to select stable silenced cells.

Yes kinase overexpression

Yes was transiently overexpressed in the PC3-P cells using the PCMV6-XL5 Yes overexpression plasmid. (Catalog # SC116734, OriGene Technologies, Inc., Rockville MD, USA). The negative control was provided by the manufacturer (Catalog # PCMV6-XL5). The Yes plasmid was sequenced using VP1.5 (forward) 5' GGACTTTCCAAAATGTCG 3' and XL39 (reverse) 5' ATTAGGACAAGGCTGGTGGG 3'

Src kinase overexpression

Full-length c-Src was cloned in PCDNA3.1 plasmid as described by Trevinio JG *et. al.* [128] . 2µg of the plasmid was used to transfect the SYF cells and the PC3 cells using the jetPRIME (Polyplus-transfection, Illkirch, France) according to the manufacturer's instructions. The cells were selected with 100 µg/mL of G418 antibiotic containing DMEMF-12 media containing 10% FBS. The PC3-Src cells were selected and cultured to get a stable cell line overexpressing Src.

Immunohistochemical staining

Immunohistochemistry was performed as described previously. Briefly, paraffin embedded tissue sections were heated at 65^{o}C overnight before deparaffinization in xylene, followed by treatment with graded series of alcohols (100%,95%,80% ethanol [vol/vol] in double distilled H_2O) and rehydration with PBS (pH 7.5). For antigen retrieval, tissues were submerged in 0.1 M EDTA and Citrate buffer for pFAK Y861 and pFAK Y397 respectively in a pressure cooker for a total of 40 minutes (4 minutes actual cook time). After washing with PBS endogenous peroxidases were blocked with 3% hydroxyl peroxide (H_2O_2) in PBS for 12 minutes, followed by three washes in PBS. The sections were blocked with cyto Q background buster for 30 minutes followed by incubation with the primary antibodies in Immunodiluent (Innovex) overnight at 4^{o}C. After washing with PBS, the slides were incubated with HRP Mach-4 polymer anti-rabbit antibody (Bio care, Concord, CA, USA) for 1 hour. After 3 washes with PBS the chromogenic reaction was visualized using 3-3' diaminobenzidine (DAB) solution (Invitrogen, Life Technologies, Grand Island, NY, USA) for 3 minutes or until good color formation was observed by monitoring the reaction under the microscope. The sections were counter stained with Gill's hematoxylin solution for 1 minute, and mounted with universal mount (Research Genetics, Inc. AL,USA).

Quantification of immunohistochemical staining

Quantification of immunohistochemical staining for expression of Yes and pFAK Y861 was performed using the NIH ImageJ software. The tumor tissue was scanned under bright field (magnification 100X, 0.14 mm^2) using Sony DXC-990 three chip charged-coupled device color video camera mounted on Nikon-Microphot-FX microscope (Nikon Co.). Five representative

images were selected randomly analyzed. Images were then processed and quantified using Image J, a public domain Java image-processing program (U. S. National Institutes of Health, Bethesda, Maryland, USA). Briefly, brown-colored images specific for DAB stain were extracted by the color deconvolution macro, inversed and measured for intensity using NIH ImageJ internal commands. All intensity values in the group were averaged to calculate intensity of pFAK Y861 and Yes expression in primary tumors and lymph node metastasis tissue as described by Park SI *et al.* [114].

In vivo tumorigenicity assay

PC3-P and PC3 Mig-3 cells were detached from subconfluent cultures and a desired number of cells were centrifuged and resuspended in $Ca2^{+}$-free and $Mg2^{+}$-free HBSS (Life Technologies, Austin, TX, USA). For implantation of the cells in prostate, the procedure of Kim et al. was followed. Male athymic nude mice (Ncr *nu/nu*; ages 8-12 weeks; the National Cancer Institute-Fredrick Animal Production Area) were anesthetized with pentobarbital sodium i.p (0.5mg/1gm of body weight; Nembutal (Abbott laboratories, Abbott Park, IL, USA) and placed in a supine position. A midline incision was made in the lower abdomen and the prostate was exteriorized. 50µL of HBSS containing 125,000 PC3-P cells and (125,000, 500,000 and $1X10^{6}$) Mig-3 PC3 cells were injected to the dorsolateral side of the prostate. The incision was closed with surgical metal clips (Braintree Scientific, Inc., Braintree, MA, USA).

Statistics:

Statistical analyses for differences of tumor weight were performed using the GraphPad Prism software. ANOVA and Tukey's test was conducted to compare differences in tumor weight. Incidences of tumors and lymph node metastases were compared between groups with the Fisher's exact test. Migratory cell numbers in modified Boyden chamber migration assay were compared by Student's t-test. Statistical analysis for pFAK Y861 and Yes immunohistochemistry was performed using one-way ANOVA and unpaired t-test. P values of less than 0.05 were considered statistically significant.

Chapter-3

Biological characterization of PC3 Mig-3 and DU145 Mig-3 cells

Isolation of PC3 Mig-3 and DU145 Mig-3 subclones from parental cells

50,000 PC3 and DU145 cells (PC3-P and DU145-P) were seeded on the upper chamber of the Boyden chamber for 24 hours. The cells that migrate through the chamber for 24 hours were collected from the bottom chamber and grown in culture. This process was repeated for 3 cycles to isolate the more migratory from both PC3 Mig-3 and DU145 Mig-3 cells. The selection was continued again for one more time to get PC3 Mig-4 cells; however, there was no further increase in migration in the PC3 Mig-4 cells. Hence, the PC3 Mig-3 and DU145 Mig-3 population from both the cell lines was used for further investigation. The PC3 Mig-3 and DU145 Mig-3 cells were grown in culture for < 30 passages and the migration abilities for the cells were found to be consistent.

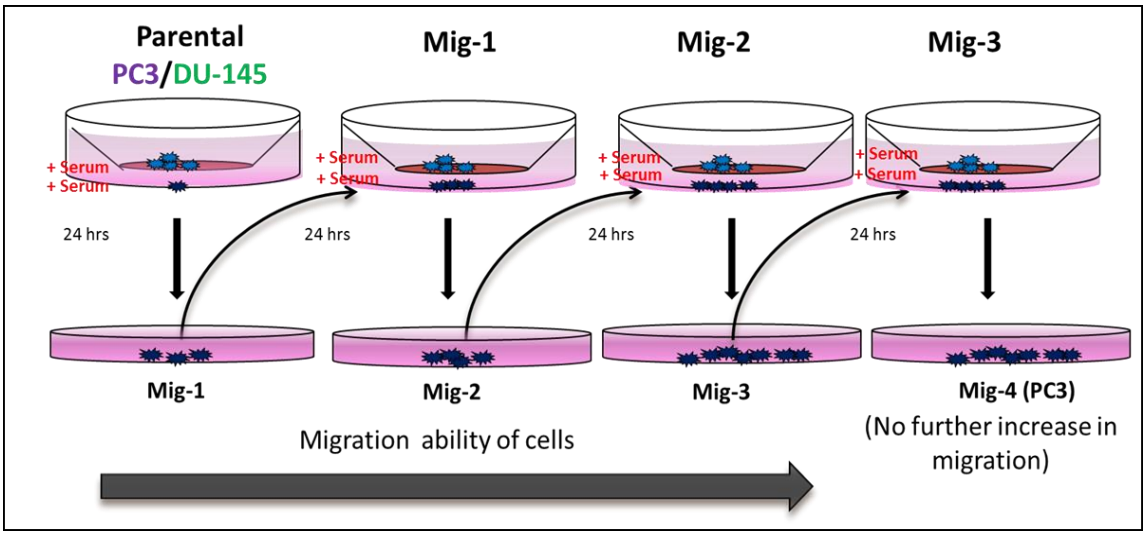

Figure 7: Schema for isolation of PC3 Mig-3 and DU145 Mig-3 cells. Modified Boyden chamber migration assay was used to isolate highly migratory prostate cancer cells. The cycle of isolation was repeated three times to get a subclone of highly migratory cells. The PC3 Mig-3 and DU145 Mig-3 cells were stable for more than 30 passages after multiple free-thaw cycles.

Morphology

To examine the morphology of the PC3-P, PC3 Mig-3, DU145-P and DU145 Mig-3 cells, equal number of cells were plated in culture overnight and bright field microscopy was performed to document morphological differences between the cell lines. Bright field microscopy at 10X magnification indicated no significant changes in morphology in the PC3 Mig-3 cells relative to the PC3-P cells. Similarly, there were no significant morphological differences observed in the DU145 Mig-3 cells relative to the DU145-P cells. However, consistent to the literature we observed that DU145 cells were more mesenchymal and PC3 cells were more epithelial (Figure 8).

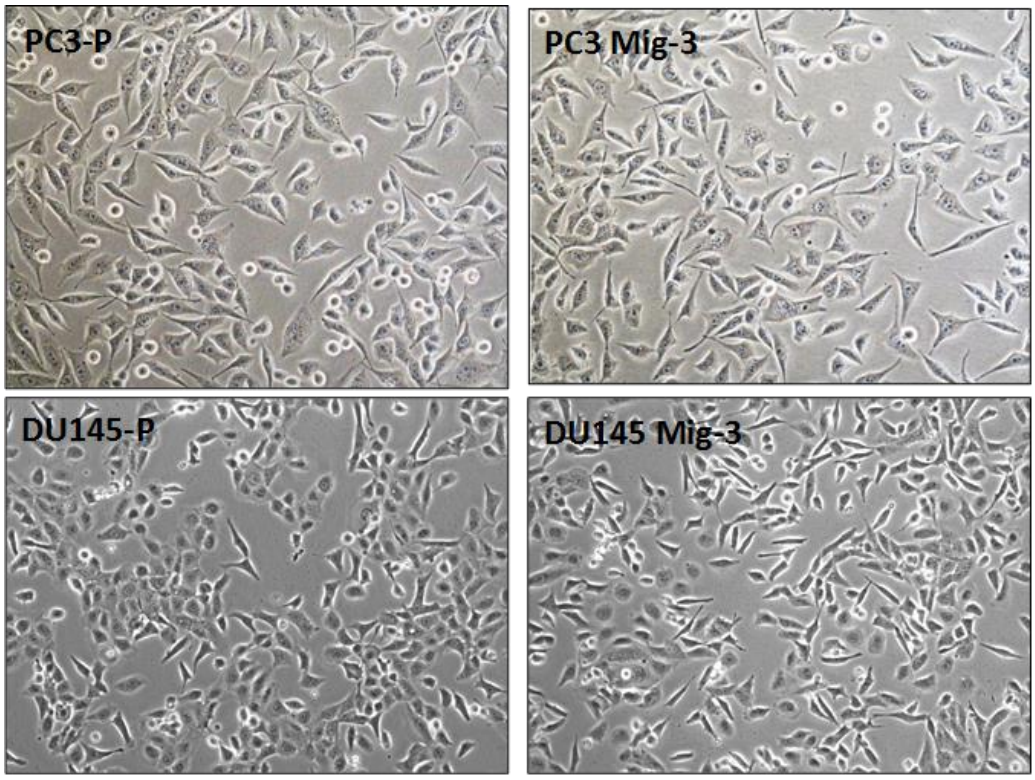

Figure 8: Morphology of PC3 and DU145 cells. Morphology of PC3 Mig-3 and DU145 Mig-3 cells were compared to PC3-P and DU145-P cells after examination under a light microscope.

Migration

To examine whether PC3 Mig-3 and DU145 Mig-3 have increased migration relative to the parental cells, I performed an *in vitro* Boyden chamber migration assay for 24 hours. As shown Figure 7, PC3 Mig-3 had 94% ($p<0.0001$) increase in migration of PC3-P cells. Consistently, DU145 Mig-3 cells had an 83% ($p<0.0001$) increase migration field in DU145-P cells (Figure 9). The increase in migration of the PC3 Mig-3 and DU145 Mig-3 cells were stable for more than 30 passages with repeated freeze-thaw cycles. To test the increased migratory abilities of the PC3 Mig-3 using a second assay, we used time-lapse microscopy to determine the speed of migration after plating them on the cell culture plate.

Time-lapse microscopy was performed on the PC3 Mig-3 cells and the data was quantified using the Auto Zell software. The speed of migration was calculated by dividing the distance travelled by a cell from point "A" to "B" divided by the time required to do so. On comparing the speed of migration within the two groups, PC3 Mig-3 had an increased migration speed of 0.170µm/min relative to 0.078µm/min in PC3-P cells (2-fold increase) 24 hours after plating the cells al PC3 cells consistent with the Boyden chamber assay data (Figure 10). To further characterize the molecular changes associated with migration in PC3 Mig-3 cells, we performed a DNA microarray using the Illumina platform. On performing an Ingenuity pathway analysis using the data, I observed that migration and motility pathways were the most differentially altered pathways at the mRNA levels (Figure 52). These data confirmed that PC3 Mig-3 and DU145 Mig-3 cells had increased *in vitro* migration relative to the parental cells.

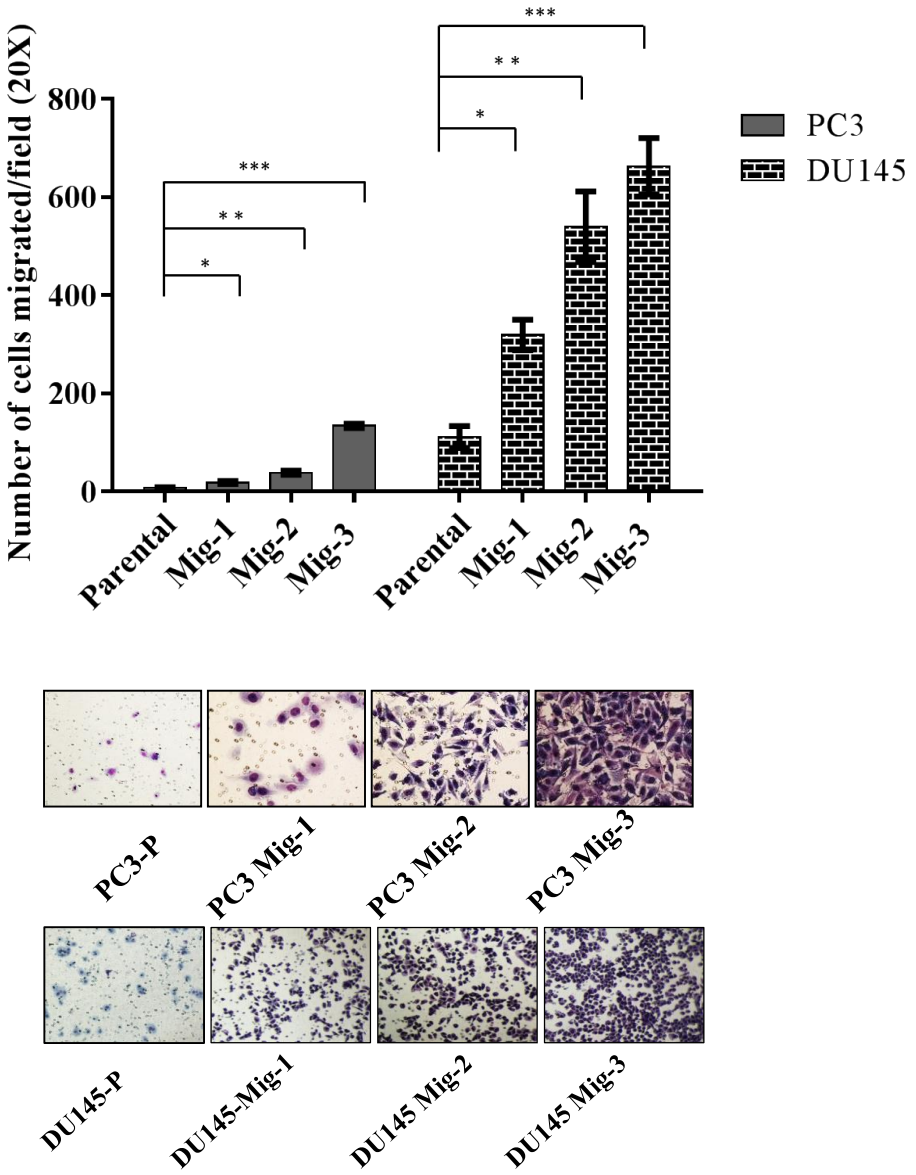

Figure 9: Migration assay of PC3 Mig-3 and DU145 Mig-3 cells. Migration assay was performed for 24 hours. Pictures were taken of migrated cells after fixation and staining. The cells were counted at 20X magnification. Graph illustrates number of cells that have migrated. Bars represent the average number of cells migrated from triplicate wells. *$p<0.002$, ** $p<0.0002$, ***$p<0.0001$ by Student's t-test, compared to the control group. Representative images are used to show the number of cells migrating per field.

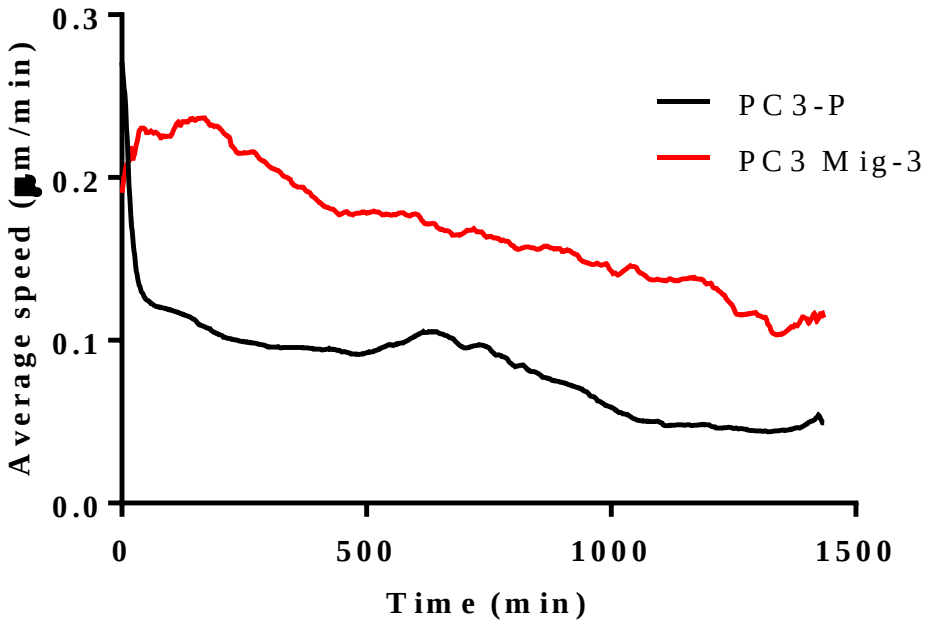

Figure 10:Time-lapse microscopy to determine speed of migration. PC3-P and PC3 Mig-3 cells were plated in bovine albumin containing chamber as described in the materials and methods. Spontaneous migration was recorded using time-lapse microscopy at 10X magnification and the speed of migration was calculated using the Auto Zell software**.**

Invasion

Invasion of cell through the extracellular matrix is crucial for metastasis to occur. Since, PC3 Mig-3 and DU145 Mig-3 cells had increased migration *in vitro*, I further investigated whether, the *in vitro* selection for migration, selects for cells with increased invasive properties. To test this hypothesis, I performed an *in vitro* invasion assay using a modified Boyden chamber, coated with matrigel. As shown in Figure 10, PC3 Mig-3 cells had 95% ($p<0.0001$) increase in invasion relative to PC3-P cells. Consistently, DU145 Mig-3 cells had a 70% ($p<0.0001$) increase in invasion compared to DU145-P cells (Figure 11) correlating with the increased migration in both cell models.

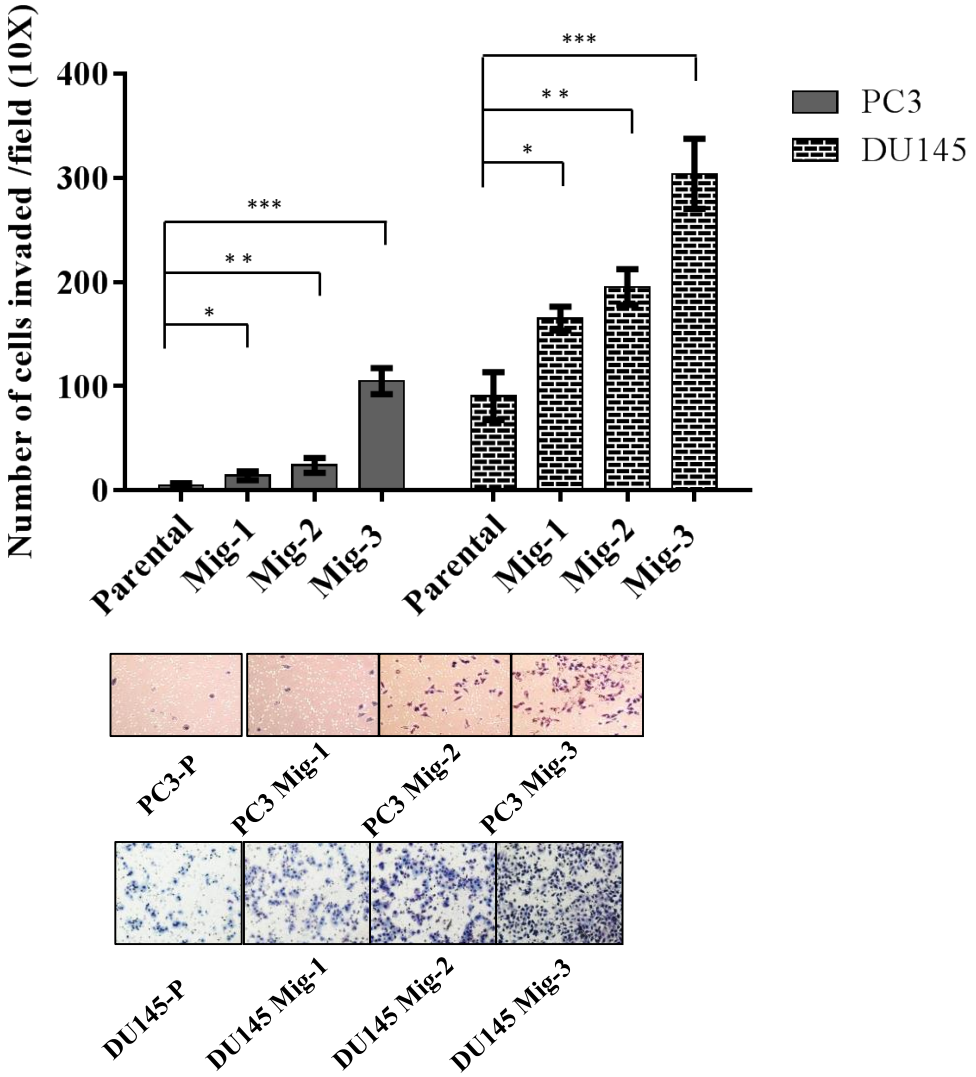

Figure 11: Invasion assay of PC3 Mig-3 and DU145 Mig-3 cells. Invasion assay was performed for 24 hours. Pictures were taken of migrated cells after fixation and staining. The cells were counted at 10X magnification. Graph illustrates number of cells that have migrated. Bars represent the average number of cells migrated from triplicate wells. *p<0.002, ** p<0.0002, ***p<0.0001 by Student's t-test, compared to the control group. Representative images are used to show the number of cells invading per field.

Proliferation

To determine whether increased migration and invasion were due to differences in proliferation; I examined the proliferation rates of PC3 Mig-3 and DU145 Mig-3 cells relative to the parental cells. Viable cells were enumerated as described in materials and methods. As shown in Figure 12, the doubling time for PC3-P cells was 19 hours relative to 22 hours for PC3 Mig-3 cells. The doubling time for DU145-P cells was 19 hours and for DU145 Mig-3 cells, 24 hours. These data are consistent with more migratory cells having reduced proliferation rates [129].

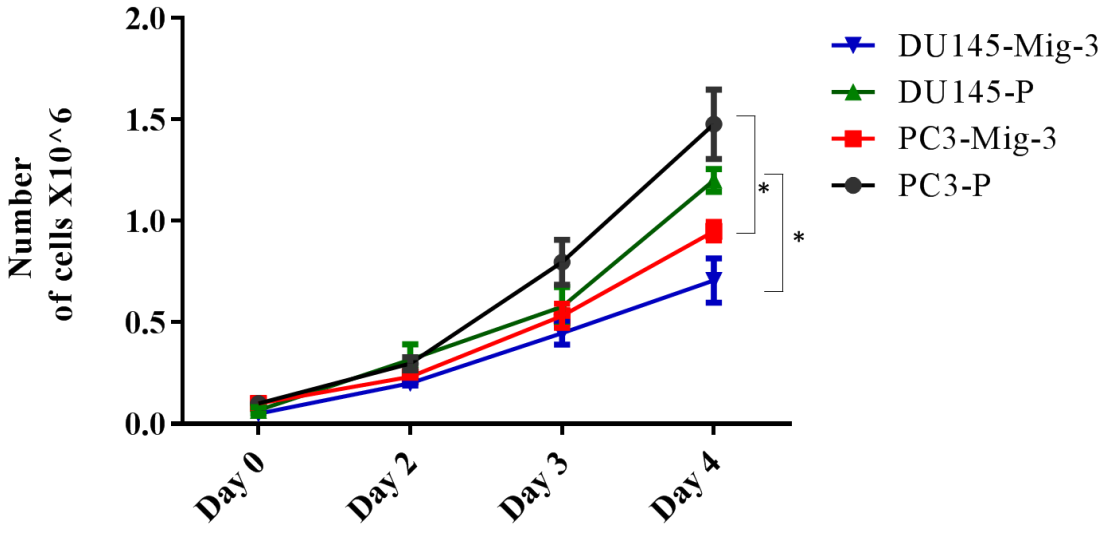

Figure 12: Proliferation of PC3 and DU145 cells. PC3-P, PC3 Mig-3, DU145-P, and DU145 Mig-3 cells were plated $5X10^4$ and cultured for indicated times. The cells were then stained with tryphan blue and counted. *$p<0.005$ by Student's t-test, compared to the control group.

Adhesion

Another property of a more metastatic cell is its ability to detach from the primary tumor site and enter the circulation. Adhesion was determined by plating 5 $X10^4$ cells in each well of a 96-well plate and washing with PBS after 30 minutes. The number of viable cells bound to the cell culture plate was determined using Calcein AM staining as described in the materials and methods. As shown in Figure 13, our results demonstrate that PC3 Mig-3 cells had a 33% decrease in adhesion relative to PC3-P cells ($p<0.005$). Likewise, DU145 Mig-3 cells had a 63% decrease in adhesion relative to DU145-P cells ($p<0.003$). These results indicate that PC3 Mig-3 and DU145 Mig-3 have decreased adhesion relative to the parental cells.

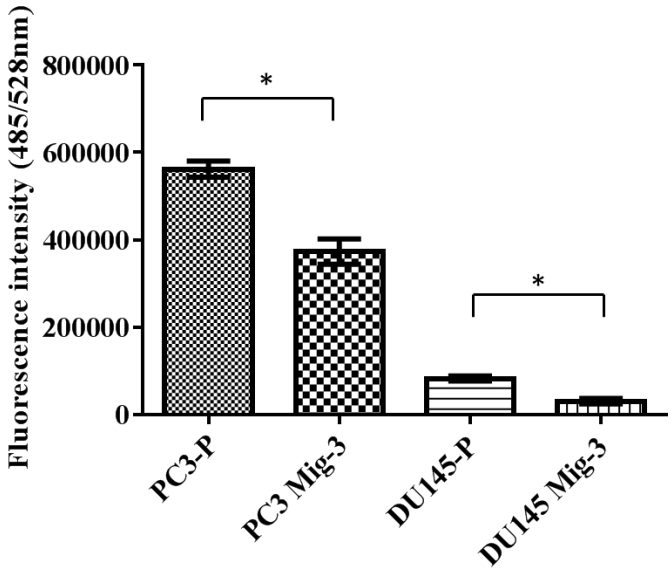

Figure 13: Adhesion assay of PC3 and DU145 cells. PC3-P, PC3 Mig-3, DU145-P, DU145 Mig-3 cells were plated 50 X 10^4 for 30 minutes and washed with PBS. The cells were stained with Calcein AM and fluorescence intensity was measured indicating the viable cells remaining on the plate. The graph represents average fluorescence intensity of triplicates. *$p<0.005$ by Student's t-test, compared to the control group**.**

PC3 Mig-3 cells are more metastatic to the lymph node relative to the parental cells in the prostate cancer spontaneous metastasis model

Because of the differences in growth rate, we first examined tumor growth *in vivo*. We performed an *in vivo* tumorigenicity assay using the orthotopic nude mouse model. 500,000 PC3-P and 500,000 PC3 Mig-3 cells were orthotopically implanted in the prostate of nude mice as described in the methods. The tumors were allowed to grow for 4 weeks and the mice were sacrificed to evaluate the incidence of lymph node metastasis and size of the primary tumor. As shown in Figure 14, PC3 Mig-3 cells were found to form significantly smaller primary tumors relative to parental PC3 cells ($p<0.0006$); however the number of lymph node metastases was similar. The slow *in vivo* growth rate of the PC3 Mig-3 was consistent with the *in vitro* results and further confirmed with Ki67 staining, which is a marker for cellular proliferation. PC3 Mig-3 tumors had significantly less Ki67 positive cells relative to the parental primary tumors, represented in Figure 15.

To perform metastasis assays, it was desirable to measure metastasis when primary tumors were of similar size. Therefore a titration experiment was performed. To accurately examine *in vivo* tumorigenicity, an increasing number of PC3 Mig-3 and PC3-P cells were intraprostatically implanted in the nude mice, which were then sacrificed after 4 weeks to evaluate the size of the primary tumors and incidence of lymph node metastases. All mice developed primary tumors; however due to differences in proliferation rates, similar sized primary tumors were obtained implanting 125,000 PC3-P cells and 500,000 PC3 Mig-3 cells (Table 1). Lymph node metastases were assessed by identifying solid, opaque and enlarged iliac lymph nodes as represented in Figure 18.

As shown in Figure 16, similar sized primary tumors were obtained from 125,000 PC3-P cells and 500,000 PC3 Mig-3 cells. Additionally, the PC3 Mig-3 tumors formed 4.1±0.3 lymph node metastases relative to 1.5±0.29 lymph node metastases in PC3-P ($p<0.005$) tumors as shown in Figure 17. These data, collectively, indicate that PC3 Mig-3 cells are significantly more metastatic to the lymph node relative to PC3-P cells.

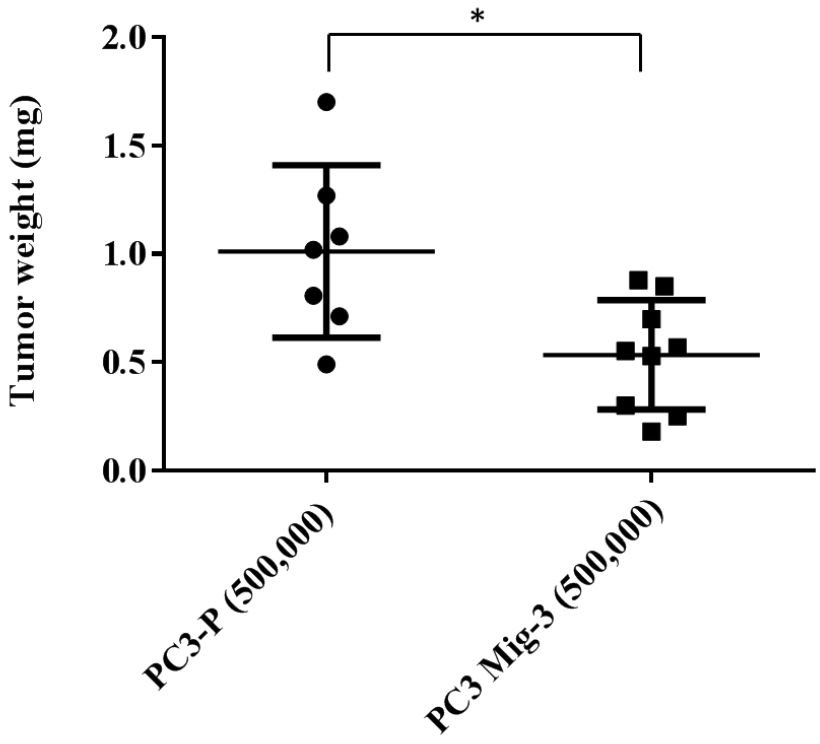

Figure 14: *In vivo* growth of PC3-P and PC3 Mig-3 cells. 500,000 PC3-P and 500,000 PC3 Mig-3 cells were injected intraprostatically. The tumors were grown for 4 weeks and the tumor weight was determined after sacrificing the mice. *$p<0.005$ by ANOVA and Tukey's test, compared to the control group.

Group	Average tumor weight (mg)	Incidence of primary tumor	LN metastasis incidence
PC3-P (500,000)*	1.01 (0.49-0.8)	7/7	7/7
Mig-3 (500,000)*	0.53 (0.18-0.8)	7/7	7/7

Table 1: Average tumor weight and incidence of lymph node metastasis

*ANOVA and Tukey's test, PC3 Mig-3 compared to PC3-P, *$p<0.005$

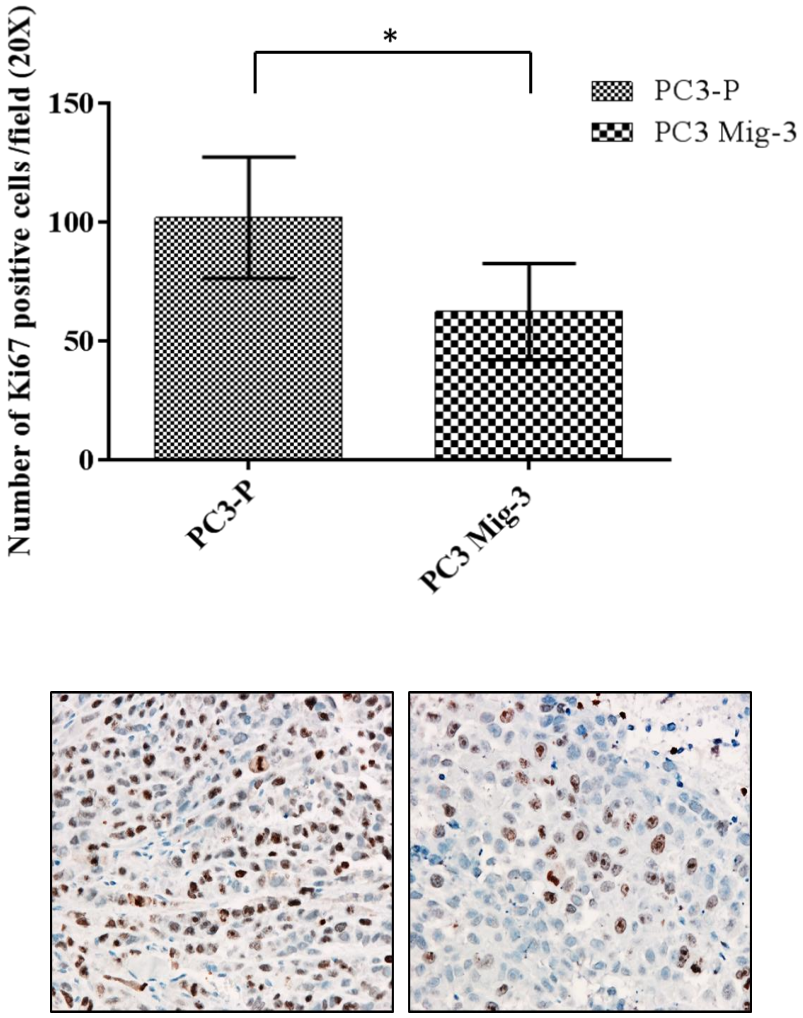

Figure 15:Ki67 staining on PC3-P and PC3 Mig-3 tumors. Ki67 staining in fixed sections from the primary tumors from the PC3-P and PC3 Mig-3 cells. *p<0.005 by Student's t-test, compared to the control group.

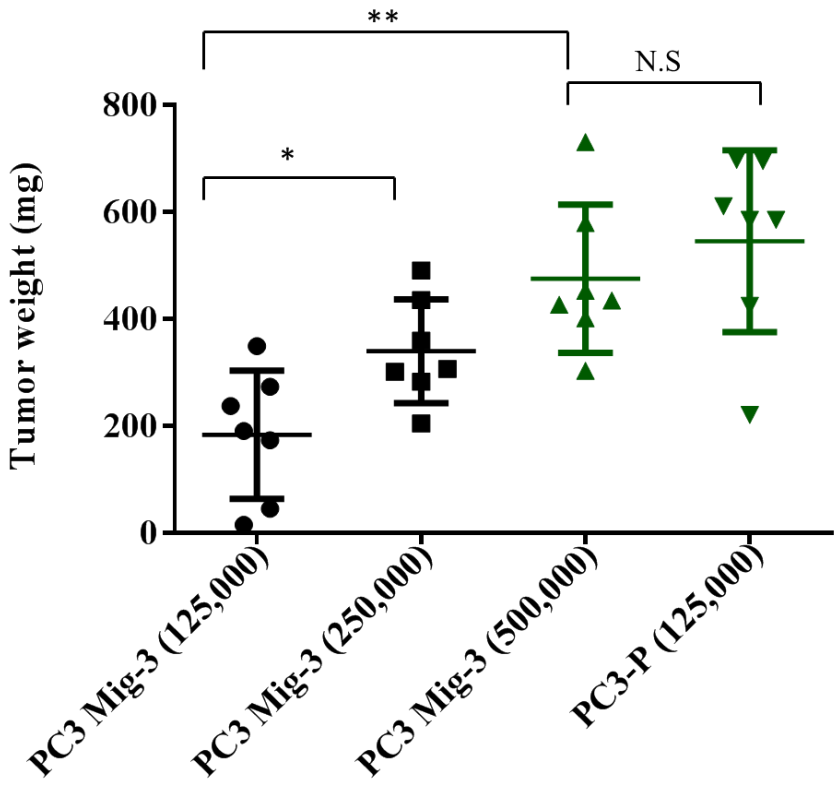

Figure 16: Tumor weight of PC3-P and PC3 Mig-3 cells. Variable amounts of PC3 Mig-3 cells (125000, 250000 and 500000) and 125,000 PC3-P cells were injected intraprostatically in the nude mice. The tumors were grown for 4 weeks and the tumor weight was determined after sacrificing the mice. *$p<0.05$, ** $p<0.005$ by ANOVA and Tukey's test, compared to the control group.

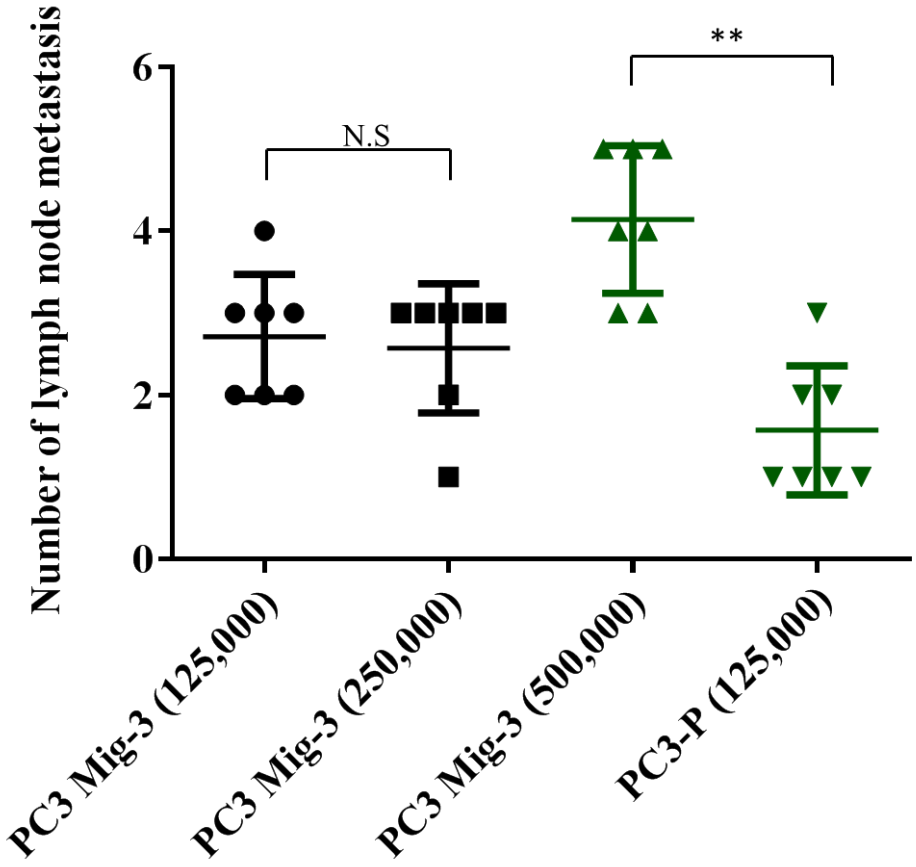

Figure 17: Incidence of lymph node metastasis of PC3-P and PC3 Mig-3 cells. Variable amounts of PC3 Mig-3 cells (125000, 250000 and 500000) and 125,000 PC3-P cells were injected intraprostatically in the nude mice. The tumors were grown for 4 weeks and the incidence of metastasis was determined after sacrificing the mice. ** $p<0.005$ by ANOVA and Tukey's test, compared to the control group.

Group	Average Tumor wt. (mg)/ range	Incidence of primary tumor	Average incidence of LN mets/ range	Incidence of LN Metastases
PC3-P (125,000)	598.5 (220-875)*	9/9	1.8 (1-3)**	9/9
PC3 Mig-3 (125,000)	183.1 (45-349)	7/7	2.7(2-4)	7/7
PC3 Mig-3 (250,000)	339.5 (204-490)	7/7	2.6(1-3)	7/7
PC3 Mig-3 (500,000)	423.5 (303-730)*	7/7	4.1(3-5)**	7/7

Table 2: Average weight of primary tumor and lymph node metastases following different numbers of PC3 Mig-3 cells injected intraprostatically

ANOVA and Tukey's test, PC3 Mig-3 compared to PC3-P, *$p<0.005$, **$p<0.001$

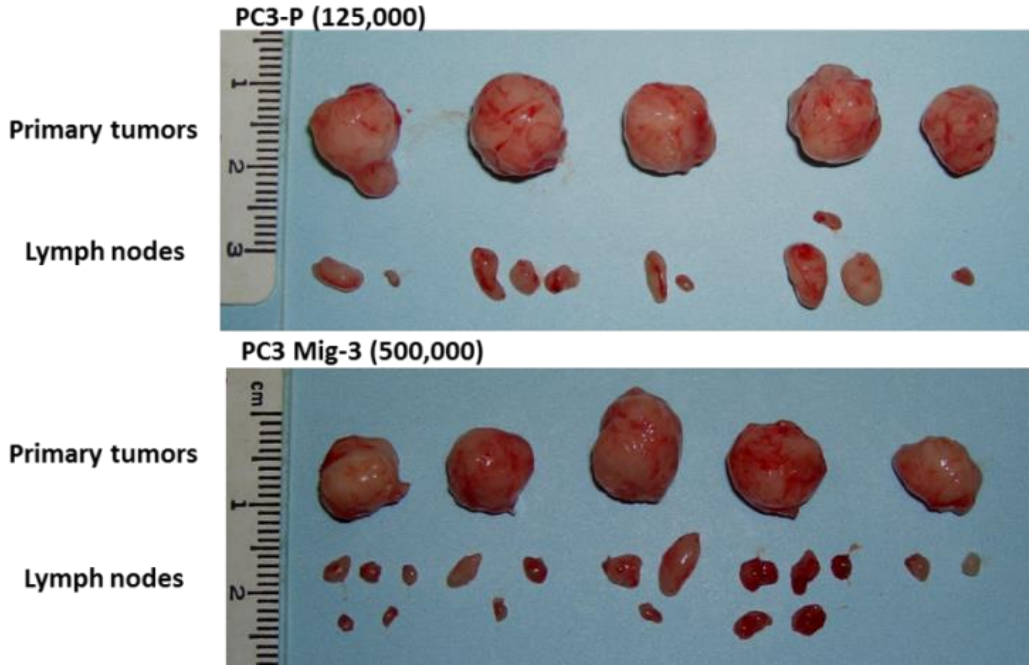

Figure 18: Tumor weight and incidence of lymph node metastasis of PC3-P and PC3 Mig-3 cells. Representative images of the primary tumors and lymph node metastasis isolated from after intraprostatic injections.

Chapter-4

Molecular characterization of FAK in PC3 Mig-3 and DU145 Mig-3 cells

Increased expression of pFAK Y861 is associated with increased migration in PC3 Mig-3 cells

To examine the role of FAK in increased migration of PC3 Mig-3 and DU145 Mig-3 cells, levels of FAK expression and phosphorylation were determined by immunoblotting as described in material and methods. As shown in Figure 19 and 20, total levels of FAK expression in PC3 Mig-3 and DU145 Mig-3 cells were similar. However, in both the PC3 Mig-3 and DU145 Mig-3 cells, there was no increase in FAK Y397 phosphorylation (the autophosphoryation site) and there was no increase in phosphorylation of the SFK-dependent phosphorylation sites FAK Y401, FAK Y577, FAK Y576 and FAK Y925). In contrast, in both PC3 Mig-3 and in DU145 Mig-3, an increase in pFAK Y861 expression was observed relative to the cognate parental cell lines.

Phosphorylation of FAK Y861 is critical to migration

To determine if pFAK Y861 increases were likely the most important alterations to migratory potential, I examined two additional proteins known to promote prostate cancer cell migration and overexpressed during tumor progression, Met and Axl [130, 131]. Roles of Axl and Met were potentially important as in my uncloned population of Mig-3 cells (both PC3 and DU145), were increased in expression of these proteins (as well as Yes, discussed below). To examine if Axl and/or Met to contributed to migration, single cell cloning of PC3 Mig-3 was performed and individual cell lines were isolated. Expression of key proteins under investigation from five clones is shown in (Figure 21). Each clone consistently overexpressed Yes and FAK pY861. However, Met and Axl were variably expressed with some clones overexpressing both proteins, some failing to overexpress either protein, and other clones overexpressing either Met or Axl but not both. To determine the potential contribution of Met and Axl to subclones of PC3 Mig-3 cells, representative examples were chosen in which Met and/or Axl were overexpressed (see Figure 21 with differential expression of these proteins), and migration assays were performed as previously described. As shown in Figure 21, neither increased expression of Met, nor Axl nor both led to increase *in vitro* migration of PC3 Mig-3 clones relative to parental cells. Importantly, the only consistent alteration that correlated with increased migration in all of the clones of PC3 Mig-3 cells was increased levels of pFAK Y861 (Figure 22). The significance of Yes kinase in PC3 Mig-3 cells will be discussed in the next chapter. These results indicated that increased expression of pFAK Y861 is independent of Axl or Met expression and is most associated with increased of PC3 Mig-3 cells by the selection procedure used.

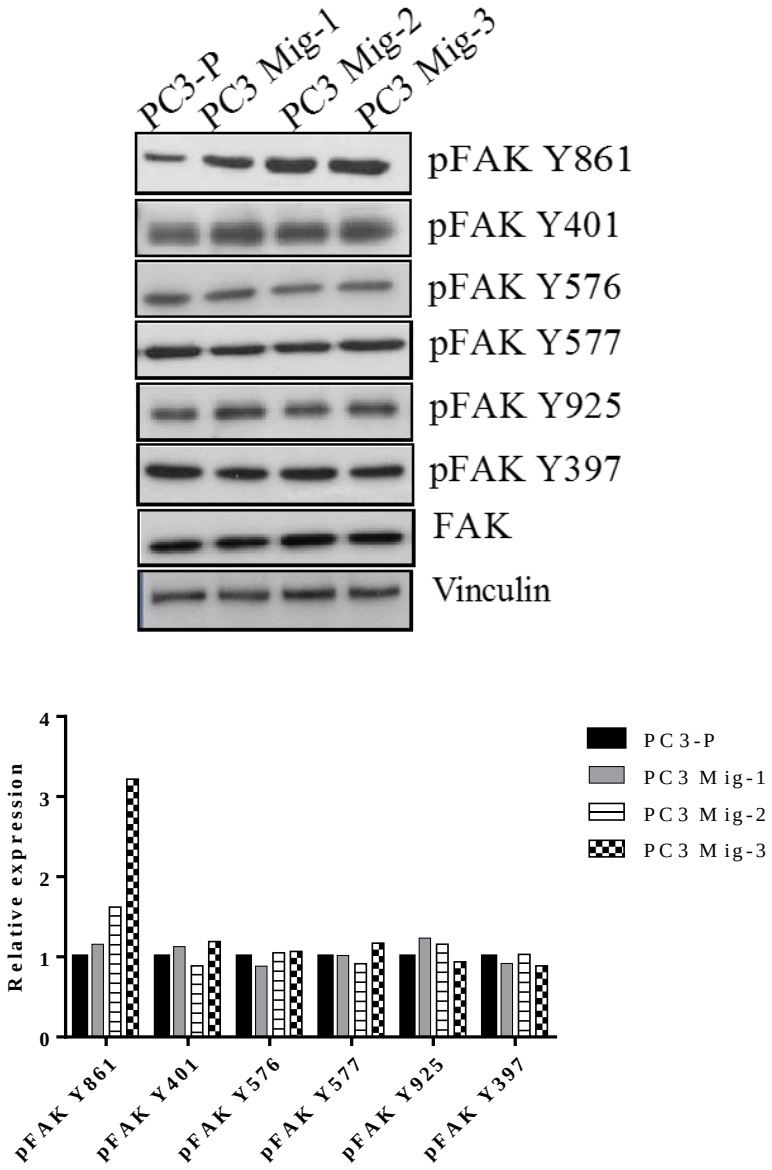

Figure 19: Phosphorylation of FAK in PC3 cells after migration selection. PC3-P, PC3 Mig-1, PC3 Mig-2, PC3 Mig-3 cells were grown in culture. The cells were lysed and subjected to immunoblot analysis to determine expression of pFAK Y861, pFAK Y397, pFAK Y577, pFAK Y401, pFAK Y576, pFAK Y925 and total FAK expression. Relative expression was determined after normalization against total FAK expression using NIH ImageJ.

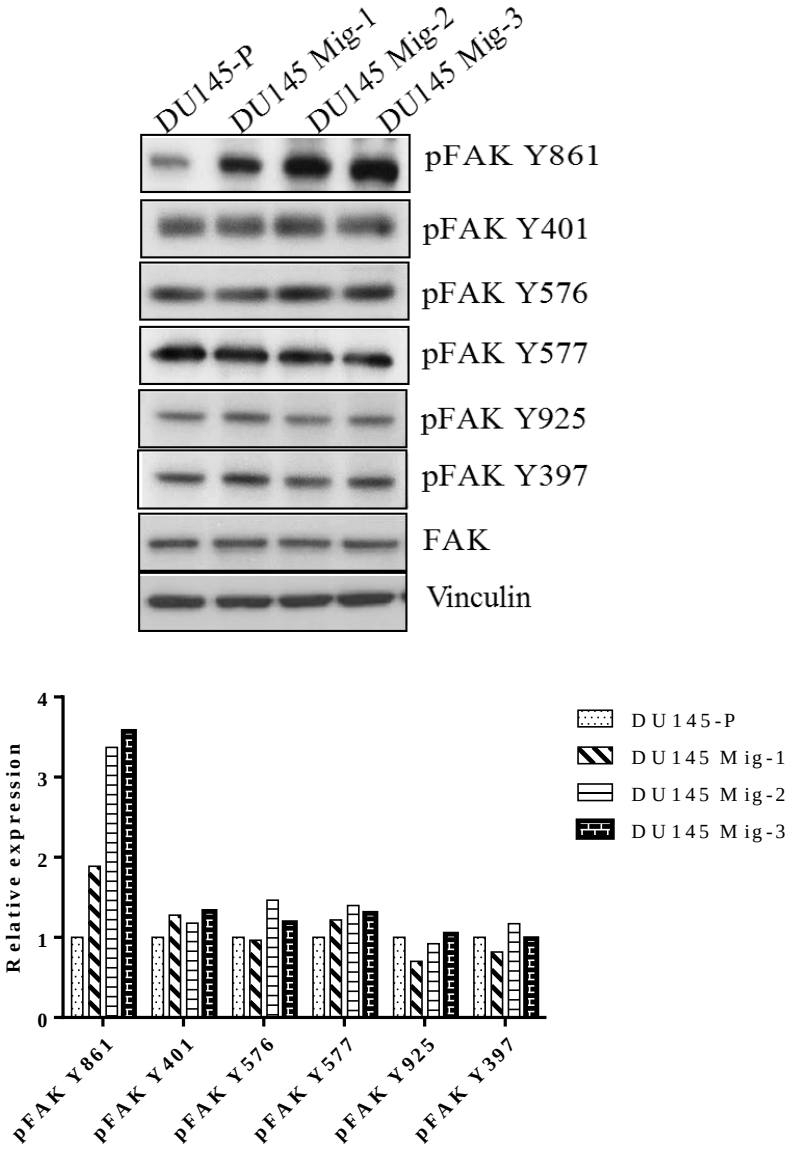

Figure 20: Phosphorylation of FAK in DU145 cells after migration selection. DU145-P, DU145 Mig-1, DU145 Mig-2 and DU145 Mig-3 cells were grown in culture. The cells were lysed and subjected to immunoblot analysis to determine expression of pFAK Y861, pFAK Y397, pFAK Y577, pFAK Y401, pFAK Y576, pFAK Y925 and total FAK expression. Relative expression was determined after normalization against total FAK expression using NIH ImageJ.

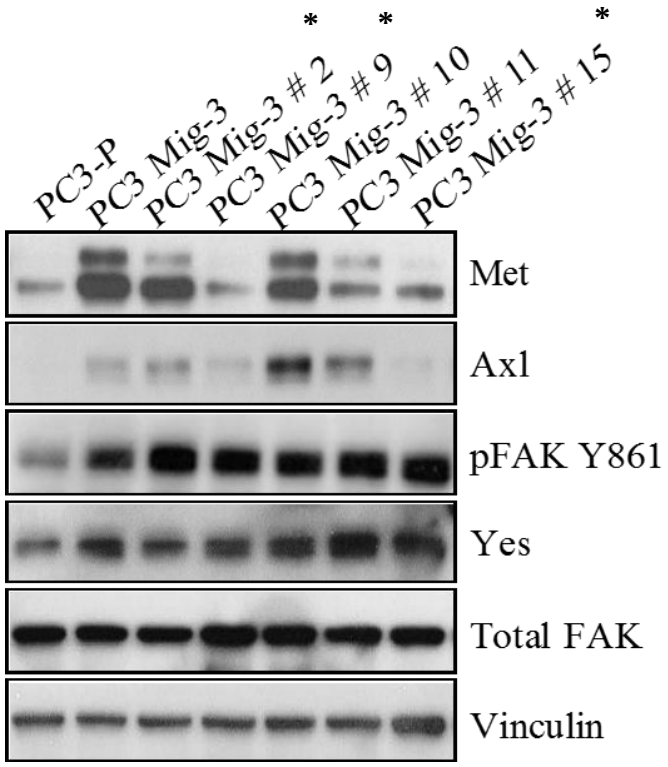

Figure 21: Expression of proteins involved in migration after subcloning in PC3 Mig-3 cells. PC3 Mig-3 cells were subjected to single cell cloning and subpopulations of PC3 Mig-3 cells were grown in culture. The clones were lysed and the protein was subjected to immunoblot analysis for expression of Met, Axl, Yes and pFAK Y861.

* indicate the clones used for migration assay

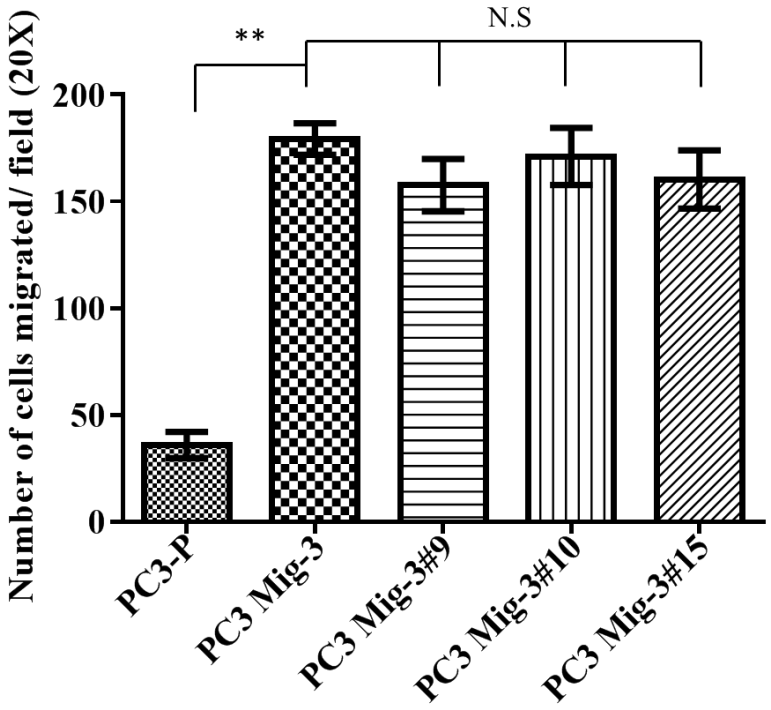

Figure 22: Migration of the clones of PC3 Mig-3 cells. Specific subclones of PC3 Mig-3 cells, which had differential expression of Axl, and Met, were tested for migration abilities using a modified Boyden chamber. The cells were allowed to migrate for 24 hrs. The cells after fixation and staining were stained counted under 20X magnification Significance of differences within the cell lines were calculated and statistics represent migration relative to PC3 Mig-3 cells. **$p<0.0005$ by Student's t-test, compared to the control group.

Phosphorylation of FAK Y861 is associated with increased migration of PC3 Mig-3 cells

To determine if pFAK Y861 is required for migration of PC3 Mig-3 cells, I overexpressed a non-phosphorylatable form of FAK (FAK Y861F) (Figure 23) as described in the materials and methods. As shown in Figure 24, no effect on proliferation of PC3 Mig-3 FAK Y861F cells was observed. As shown in Figure 25, i*n vitro* migration of PC3 Mig-3 FAK Y861F cells was reduced by 90% compared to the empty vector control in a 24 hour Boyden chamber migration assay ($p<0.0001$), consistent with results from other cell lines demonstrating the importance of FAK Y861 phosphorylation in migration [78] [93]. These data confirm that phosphorylation of FAK Y861 regulates migration of PC3 Mig-3 cells.

A.

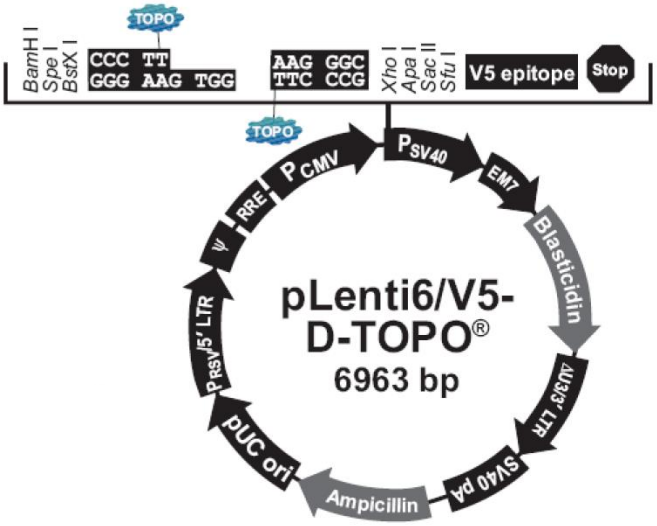

B.

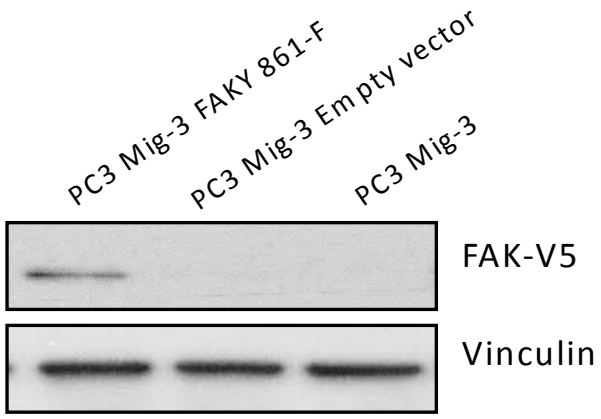

Figure 23: Overexpression of FAK Y861F plasmid in the PC3 Mig-3 cells A. Map of the plenti6/V-5D-TOPO vector used for expression of pFAK Y861F mutant. **B.** Immunoblot analysis of FAK Y861F cells to determine the expression of V5-FAK.

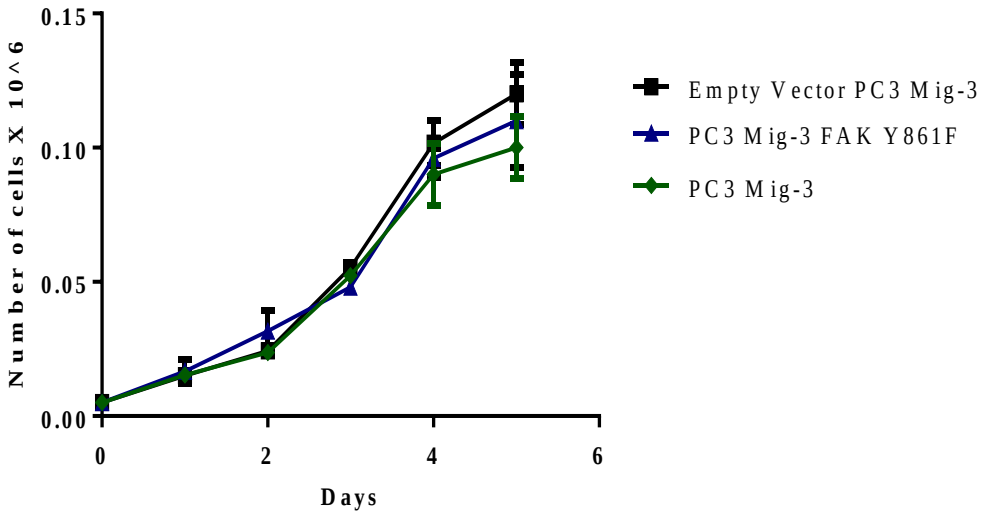

Figure 24: Effects of FAK Y861F expression on cell growth of PC3 Mig-3 cells. PC3 Mig-3, PC3 Mig-3 Vector control and FAK Y861F Mig-3 cell lines were equally plated in culture. The cells were trypsinized and counted after tryphan blue staining for 6 days. The cell numbers were plotted and the growth rate was determined.

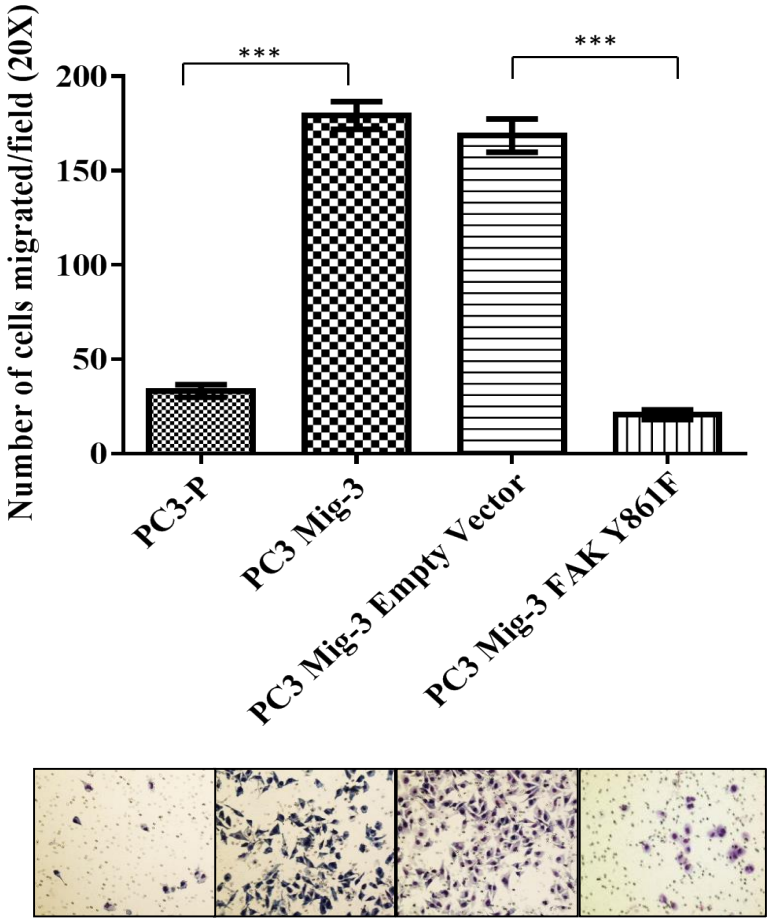

Figure 25: Effect of FAK Y861F expression in PC3 Mig-3 cells. Migration assay was performed for 24 hours. Pictures were taken of migrated cells after fixation and staining. The cells were counted at 20X magnification. Graph illustrates number of cells that have migrated. Bars represent the average number of cells migrated from triplicate wells. ** $p<0.0005$, ***$p<0.0001$ by Student's t-test, compared to the control group. Representative images are used to show the number of cells migrating per field**.**

Rho-A activation is associated with increased migration of PC3 Mig-3 cells

Rho-A is activated downstream of FAK phosphorylation to induce migration of PC3 cells [132]. To investigate the activation of Rho-A in the PC3 Mig-3 cells, G-LISA Rho-A activation assay was used. On stimulation of the cells with 10%, FBS had significantly PC3 Mig-3 cells had significantly higher Rho-A activation relative to PC3-P cells. Additionally the PC3 Mig-3 FAK Y861F cells were used as a negative control, since they were found to be low migratory *in vitro*. As shown in Figure 26, PC3 Mig-3 FAK Y861F cells had significantly less Rho-A activation relative to the PC3 Mig-3 cells. These data confirmed activation of Rho-A is one of the downstream pathways that is associated with increased migration in PC3 Mig-3 cells, consistent with many studies demonstrating the role of Rho-A in mediating FAK migration.

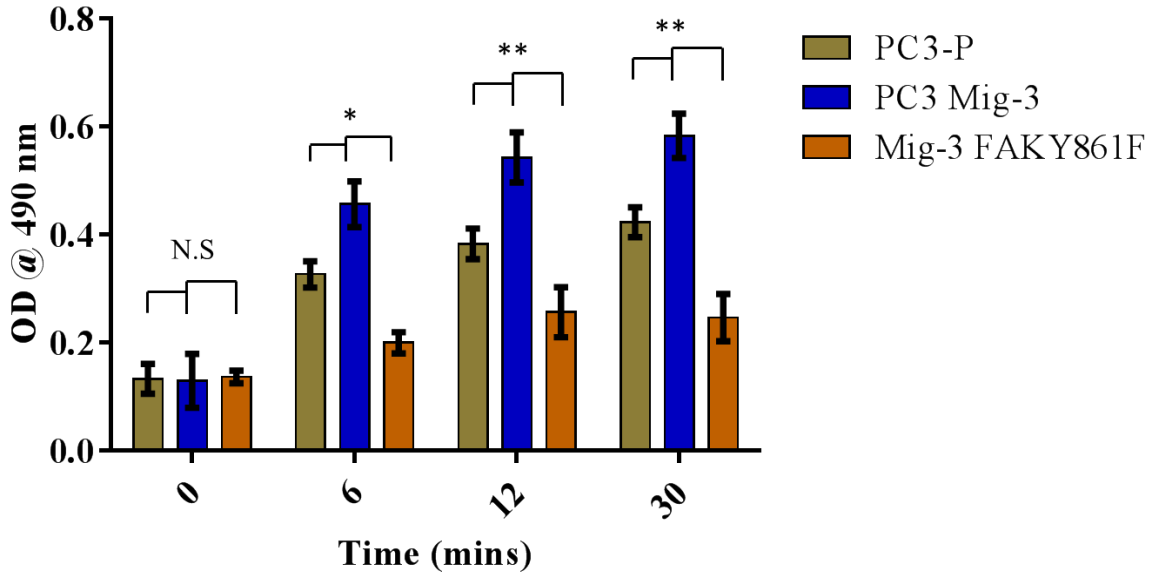

Figure 26: Rho-A activation status in PC3 Mig-3 cells. PC3-P, PC3 Mig-3 and FAKY861F Mig-3 cells were equally plated in culture overnight. Rho-A activation was determined using the G-LISA Rho-A activation assay kit after serum stimulation for 6 mins, 12 mins and 30 mins. Error bars represent average Rho-A activity from triplicate wells.*$p<0.005$, **$p<0.001$ by Student's t-test, compared to the control group.

Spontaneous metastases of PC3 Mig-3 cells to the lymph nodes are increased in expression of pFAK Y861

As discussed before, PC3 parental cells are able to metastasize to the lymph node following orthotopic injection. I therefore determined if the lymph node metastases from PC3-P were also increased in pFAK Y861. Which would suggest that increased pFAK Y861 is a general property of lymph node metastasis development. In PC3 Mig-3 cells and PC3-P cells, pFAK Y861 expression in the primary tumors was estimated by immunohistochemistry. As shown in Figure 27, a 2.5-fold increase was observed in expression of pFAK Y861 in the PC3 Mig-3 primary tumors relative to the PC3-P primary tumors. As PC3-P tumors also form lymph node metastases, we next examined if these lymph node metastases were selected for increased pFAK Y861 expression. Immunohistochemistry for pFAK Y861 was performed on tumor-positive lymph nodes harvested from the metastasis experiment described above. Lymph node metastasis in PC3-P tumors had a 2.3-fold increase in pFAK Y861 expression relative to the PC3-P primary tumors. These results demonstrate that lymph node metastases are increased in expression of pFAK Y861. As expected, in PC3 Mig-3 cells in which pFAK Y861 was already increased, both primary tumors and lymph node metastases showed high levels of pFAK Y861. Similar to what was observed in PC3 Mig-3 tumors, pFAK Y861 was also increased in lymph node metastases, suggesting that overexpression of pFAK Y861 may promote lymph node metastasis.

A.

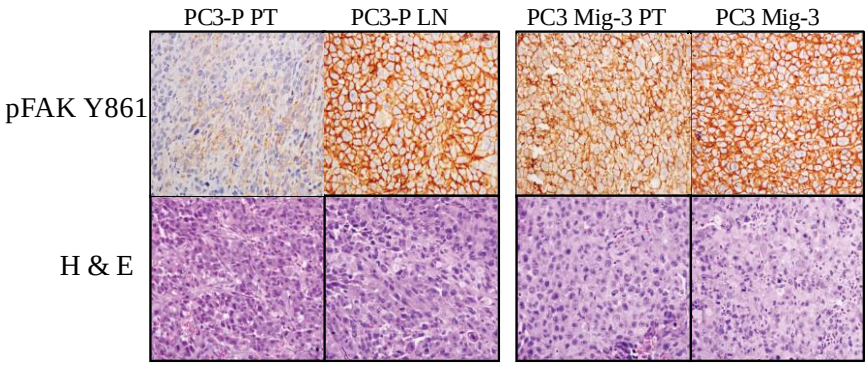

B.

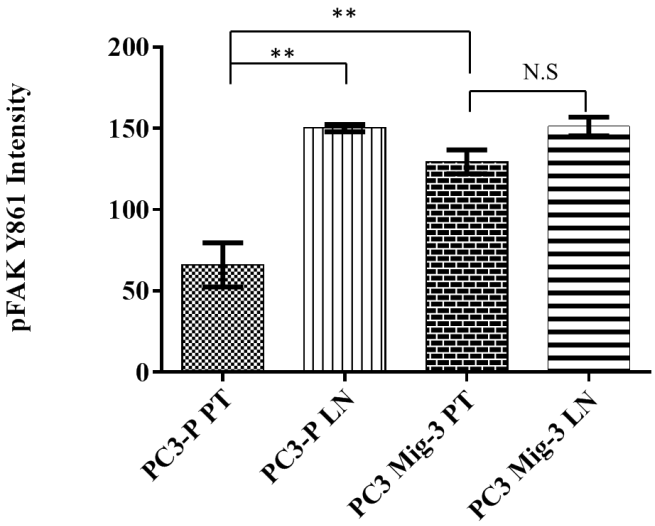

Figure 27: pFAK Y861 expression in mice prostate cancer samples.

A. Immunohistochemical staining for pFAK Y861 expression in primary tumor and lymph node metastases after orthotopic implantation of PC3-P and PC3 Mig-3 cells in prostate of the nude mice. **B.** The staining was quantified after DAB extraction using NIH ImageJ. *$p<0.008$, **$p<0.001$ by Student's t-test, compared to the control group. PT=parental tumor; LN=lymph node metastases

Chapter-5

Elucidating the mechanism of increased migration in PC3 Mig-3 and DU145 Mig-3 cells

Candidate approach to identify proteins associated with increased phosphorylation of FAK Y861

Phosphorylation of FAK Y861 is one of the signature alterations associated with the PC3 Mig-3 and DU145 Mig-3 cells. My next goal was to determine whether this increased phosphorylation was due to increased kinase expression, or decreased phosphatase expression. The cDNA microarray data performed in collaboration with Woonyoung, Ph.D. and David McConkey, Ph.D. demonstrated downregulation of Src homology-domain containing tyrosine phosphatase (Shp-2) in PC3 Mig-3 cells relative to the PC3-P cells. However, immunoblot analysis indicated that Shp-2 levels were not altered after translation at the protein levels, as shown in Figure 28 A. These data suggested that Shp-2 was unlikely to be responsible for altered FAK Y861 phosphorylation in the PC3 Mig-3 phenotype. We next investigated a kinase (PTK6) reported to associate with pFAK Y861 [128]. As shown in Figure 28 B, immunoblot analysis indicated that PTK6 was not altered in expression PC3 Mig-3 cells relative to PC3-P cells. Collectively, these data indicated no alterations in expression levels of Shp-2 and PTK6 are associated with the PC3 Mig-3 cells.

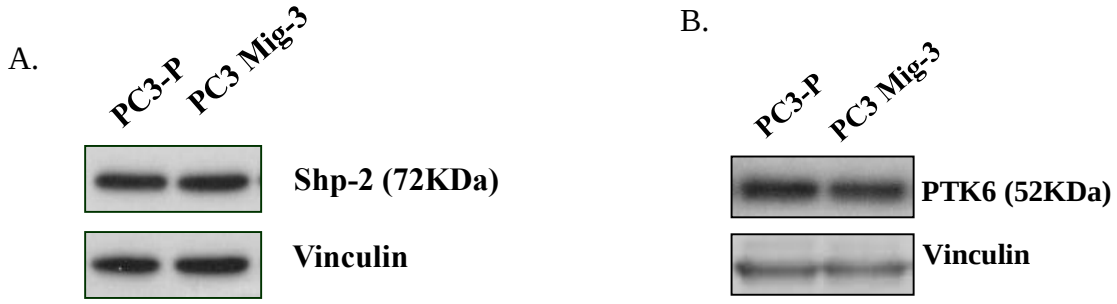

Figure 28: Shp-2 and PTK6 expression in PC3 and DU145 cells.

A. Immunoblotting of Shp-2. PC3-P and PC3 Mig-3 were grown in culture. The cells were lysed and subjected to immunoblot analysis **B. Immunoblotting of PTK6.** PC3-P and PC3 Mig-3 cells were grown in culture, lysed and 15µg of total protein lysate was subjected to immunoblot analysis.

Yes kinase overexpression and increased activity correlates with increased migration in PC3 Mig-3 cells

Src family kinases (SFK's) phosphorylate all of the FAK tyrosine phosphorylation sites excluding the autophosphorylation site (FAK Y397) [126]. Hence, I investigated the expression and activity of SFK's in PC3 Mig-3 and DU145 Mig-3 cells relative to parental cells. Expression of SFKs was examined by immunoblot analysis. As shown in Figure 29, no increased expression of Src, Fyn and Lyn were observed. However, a 2.5-fold increase in Yes expression was observed in PC3 Mig-3 cells relative to PC3-P cells. Similarly, the DU145 Mig-3 cells had a 2-fold increase in Yes expression relative to DU145-P cells, but no increase in other Src family members expressed in these cells as shown in Figure 30. As determined by rt-qPCR, c-*yes* mRNA was also increased 1.5-fold in the PC3 Mig-3 and DU145 Mig-3 cells relative to the PC3-P and DU145-P cells, as shown in Figure 31. As FAK is phosphorylated by SFKs, we next examined kinase activity of Src family members. As antibodies specific to the autophosphorylation sites (indicative of active forms of these enzymes) to specific SFKs have not been generated), to examine kinase activity of SFKs expressed in these cells, immunoprecipitation of individual SFKs was performed using specific antibodies to each and then blotted with antibody against the autophosphorylation site. This was necessary because the antibody to the autophosphorylation site recognizes this site in all the SFKs studied. As shown in Figure 32, no increase in expression or autophosphorylation (indicative of an activated form of the kinase) was observed for of Src, Lyn and Fyn (Figure 32 B, C, D) in PC3 Mig-3 cells relative to the PC3-P cells. However, Yes activity was increased by 3-fold in the more migratory PC3 Mig-3 cells relative to the parental cells (Figure 32 A).

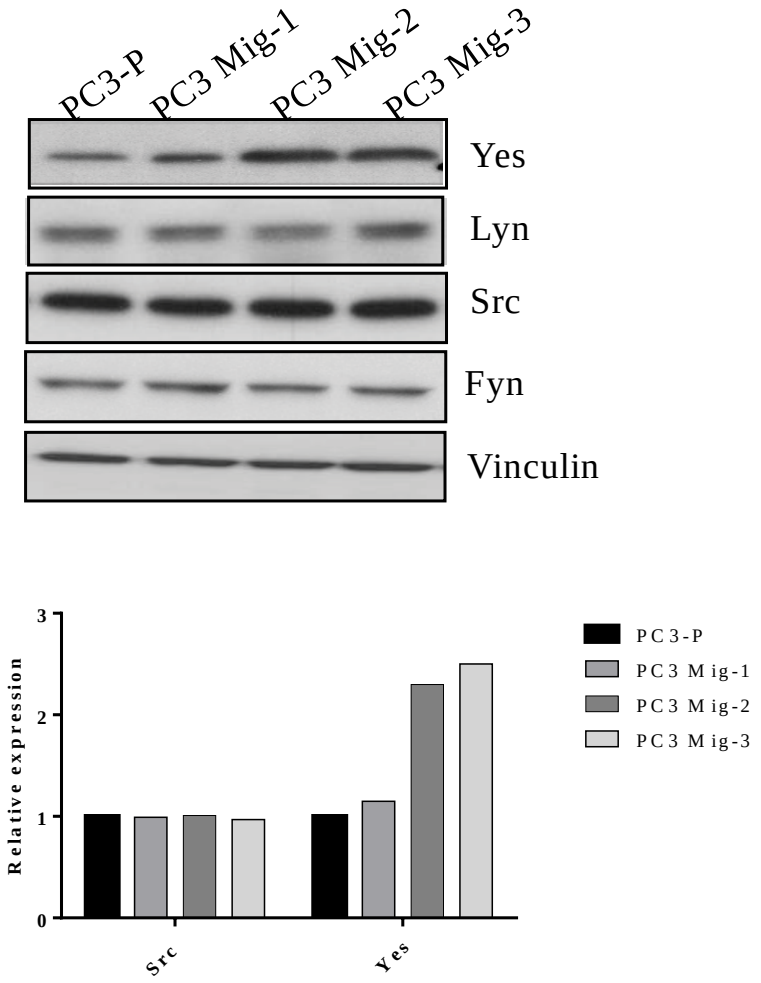

Figure 29: SFK expression in PC3 cells. A. Immunoblotting of SFK expression PC3-P, PC3 Mig-1, PC3 Mig-2 and PC3 Mig-3 cells were grown in culture and lysed. Total protein was subjected to immunoblot analysis. **B.** Quantification of the immunoblot analysis using NIH ImageJ normalized to the loading control.

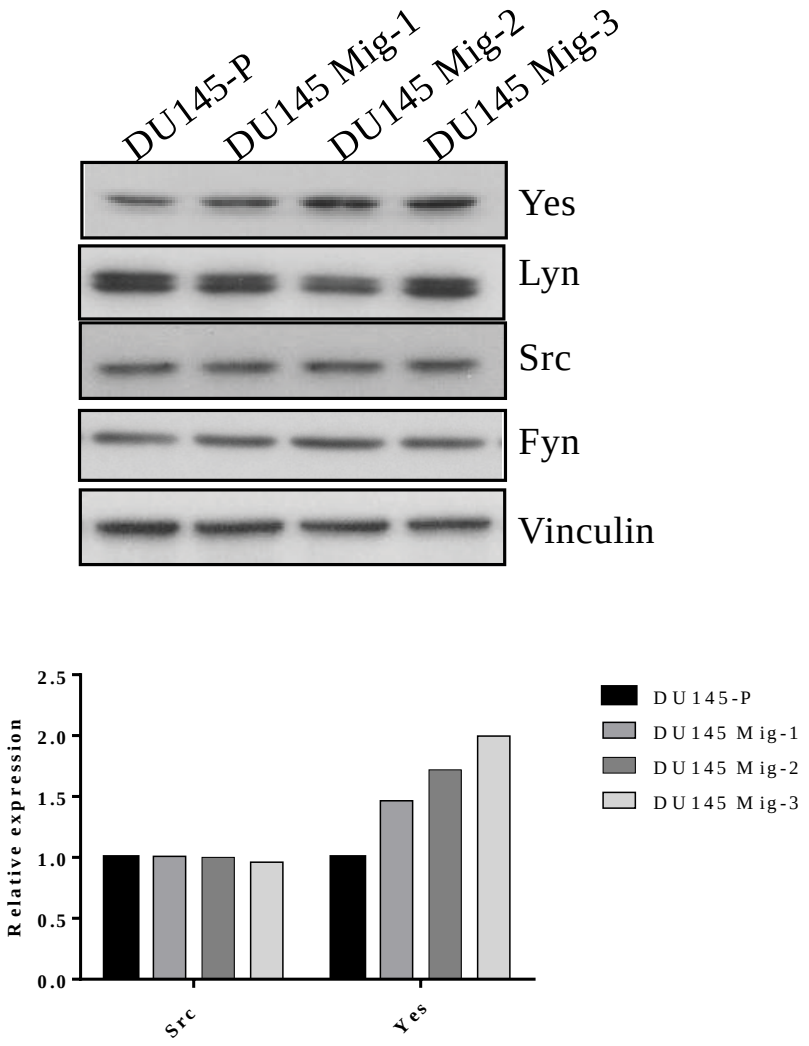

Figure 30: SFK expression in DU145 cells. A. Immunoblotting of SFK expression. DU145-P, DU145 Mig-1, DU145 Mig-2 and DU145 Mig-3 cells were grown in culture and lysed. Total protein was subjected to immunoblot analysis. **B.** Quantification of the immunoblot analysis using NIH ImageJ normalized to the loading control.

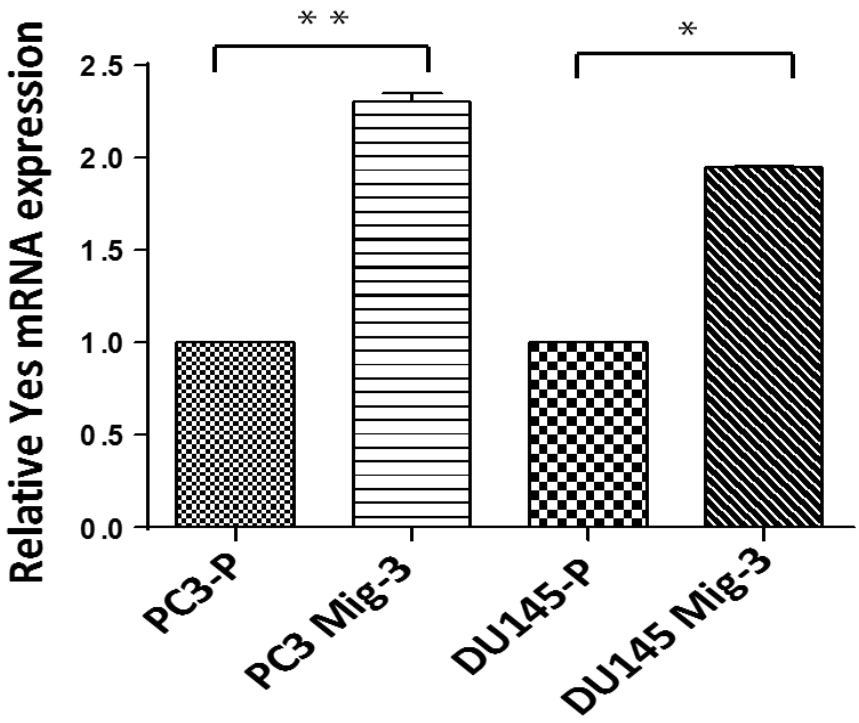

Figure 31: Yes mRNA expression in PC3 and DU145 cells. PC3-P, PC3 Mig-3, DU145-P and DU145 Mig-3 cells were grown in culture. Total RNA from the cells was extracted and subjected to RT-qPCR using primers specific to Yes kinase. The expression levels are presented relative to actin control levels **p=0.006, *p=0.002 by Student's t-test, compared to the control group.

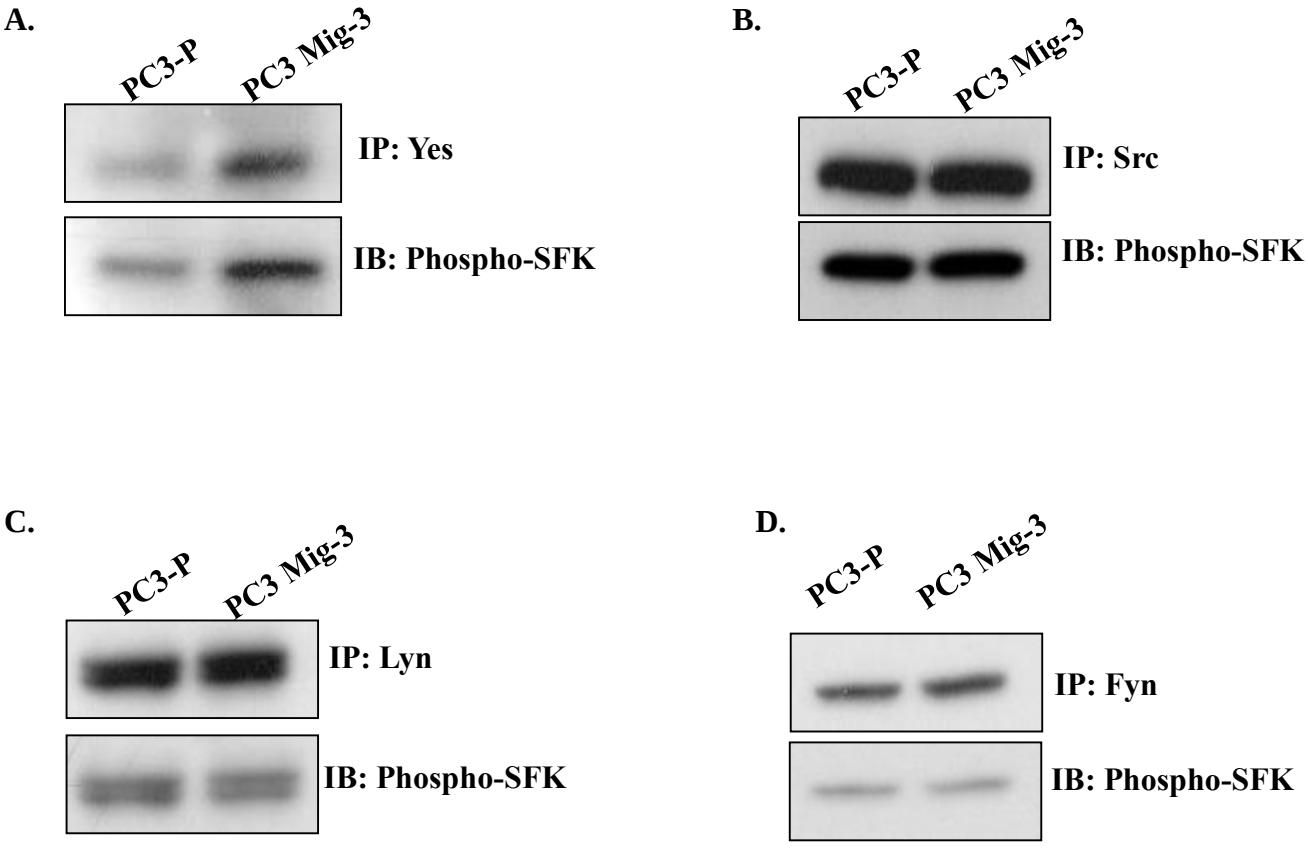

Figure 32: Immunoprecipitation to determine SFK activity. PC3-P and PC3 Mig-3 cells were grown in culture and lysed. Yes, Src, Lyn and Fyn was immunopreciptated from equal amounts of protein using specific antibodies for each kinase. Immunoblotting analysis was performed on the immunoprecipitated lysates to determine the levels of phospho SFK.

Yes kinase preferentially phosphorylates FAK Y861 in PC3 Mig-3 cells

Next, I investigated the role of Yes kinase in FAK Y861 phosphorylation. As shown in Figure 33, overexpression of Yes in parental PC3 cells with an expression vector as described in materials and methods did not increase phosphorylation of FAK Y397, FAK Y401, FAK Y577 and FAK Y576. However, FAK Y861 phosphorylation was increased by 2.6-fold. In contrast, overexpression of Src led to an equivalent increase in phosphorylation of all SFK sites, as shown in Figure 36.

In a second approach to determine if Yes preferentially phosphorylated FAK Y861, Yes was silenced by in PC3 Mig-3 cells using two Yes specific shRNA sequences. Knockdown of Yes kinase led to decreased expression of pFAK Y861 and in pFAK Y925 with no significant effect on expression of the other FAK tyrosine residues, as shown in Figure 34. In contrast, silencing Src led to decreased phosphorylation of all the SFK phosphorylated FAK tyrosine residues, represented in Figure 35. To examine the role of Yes in migration, we performed a migration assay PC3-P cells in which Yes was overexpressed and in PC3 Mig-3 cells in which Yes was silenced. I found that overexpression of Yes in PC3-P cells led to a 68% ($p<0.0001$) increase in migration in PC3-P cells (Figure 37), while knockdown of Yes in PC3 Mig-3 cells led to a 50% ($p<0.0001$) reduction in migration in PC3 Mig-3 cells (Figure 38). Collectively, these data indicate that migration in PC3 Mig-3 cells. These increases and decreases in migration correlate with the ability of Yes to phosphorylate FAK Y861, and to a lesser extent, FAK Y925.

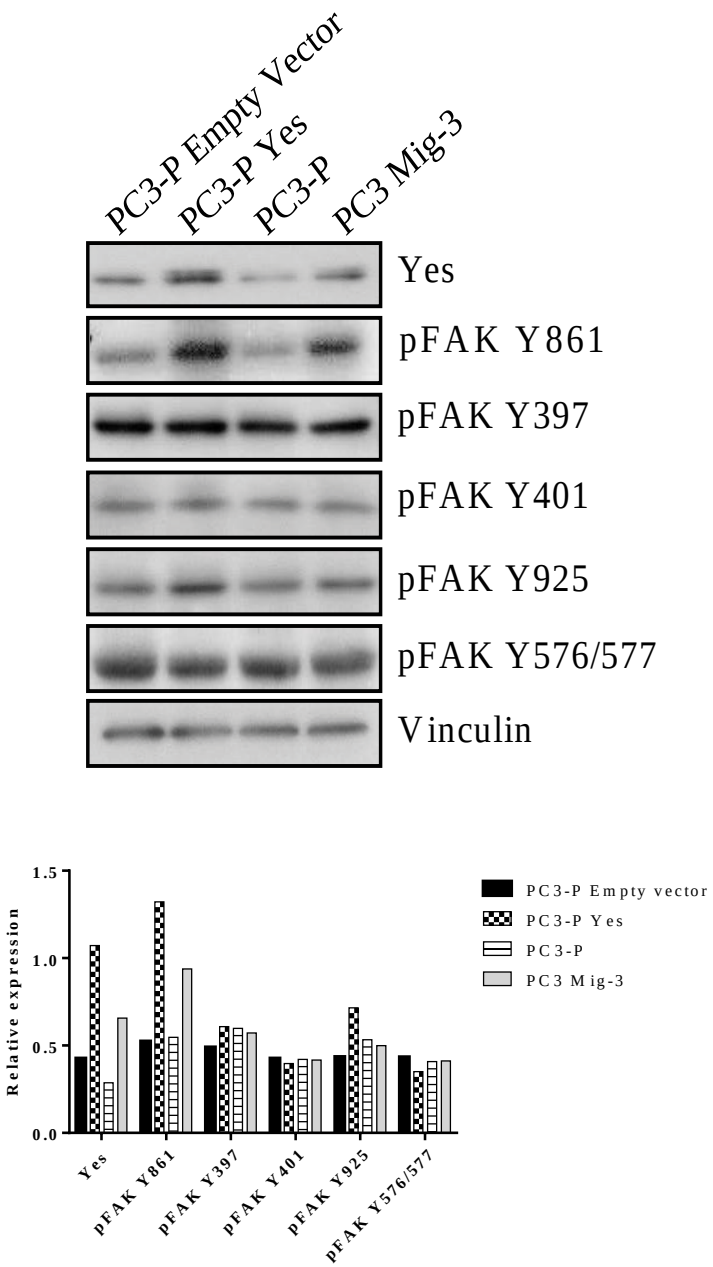

Figure 33: Overexpression of Yes kinase in PC3-P cells A. PC3-P cells were transfected using the PCMV6-XL5 control and Yes plasmid for 48 hours. The cells were lysed and 15µg of protein was subjected to immunoblot analysis for Yes and phospho FAK expression. **B.** The relative protein expression was determined after normalization against vinculin loading control using NIH ImageJ.

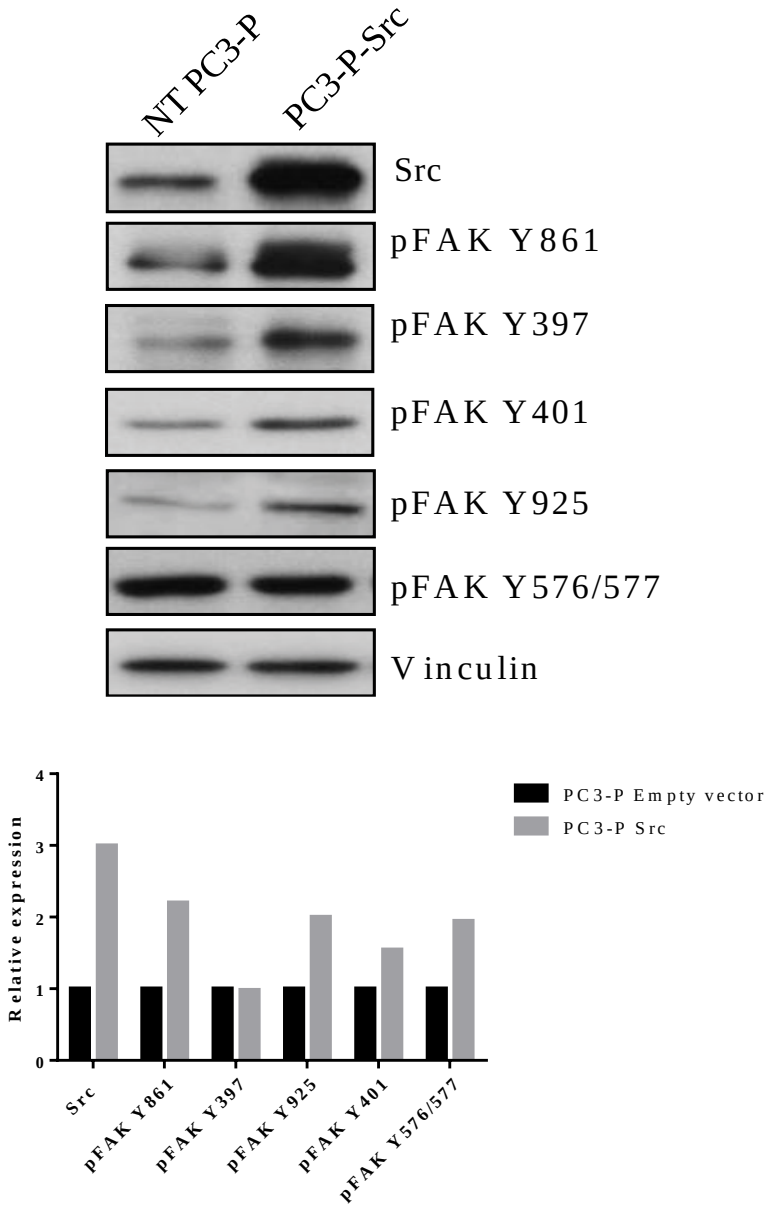

Figure 34: Overexpression of Src kinase in PC3 Mig-3 cells. PC3 Mig-3 cells were transfected with PCDNA3.1 Src expression vector and Non-targeting control plasmids for 24 hours and the cells were trypsinized after 48 hours of transfection. Cell lysates were subjected to immunoblot analyses for expression of Src and pFAK. Relative protein expression was determined after normalization to vinculin using NIH ImageJ.

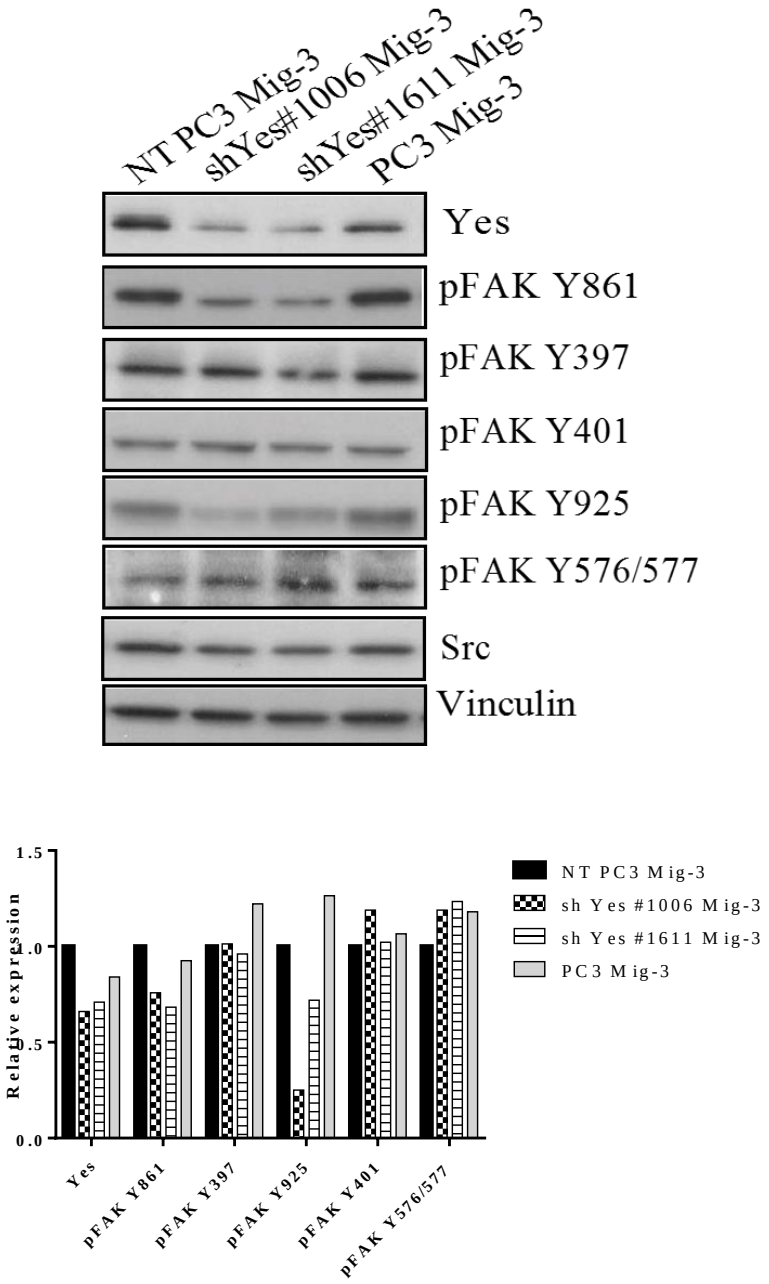

Figure 35: Knockdown of Yes in PC3 Mig-3 cells. PC3 Mig-3 cells were transfected with PLKO. puro shYes#1006 and shYes #1611plasmids for 48 hours. The cells were lysed and subjected to immunoblot analysis for Yes and pFAK expression. Relative protein expression was determined after normalization again vinculin loading control using NIH ImageJ.

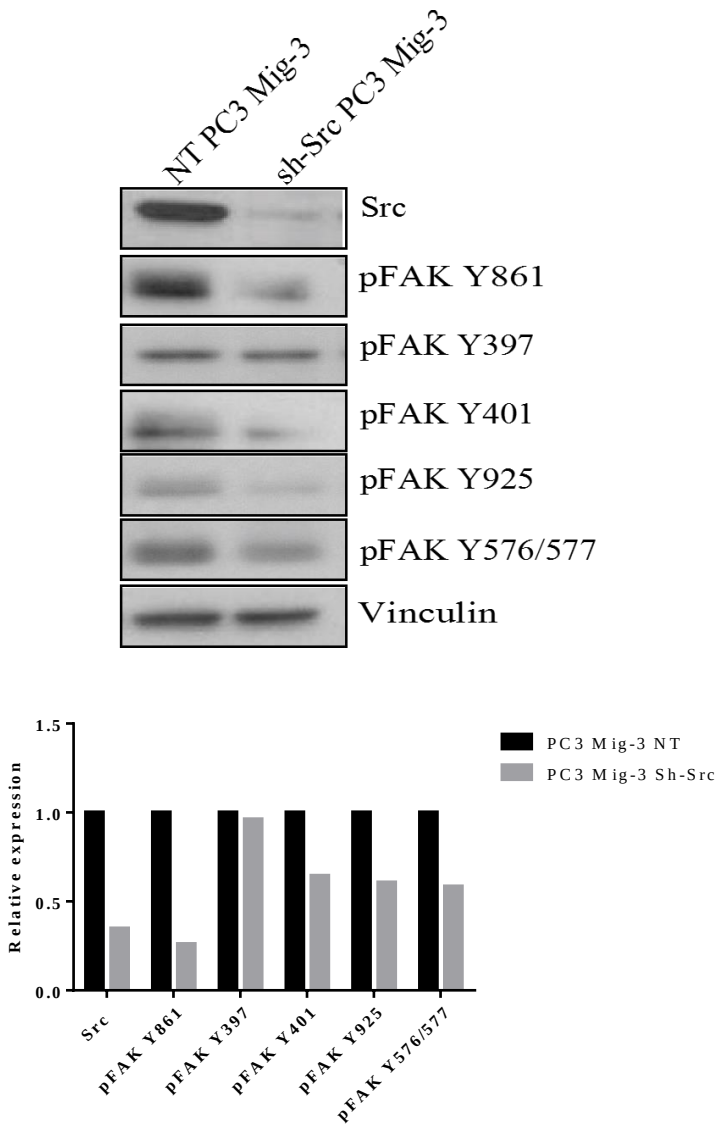

Figure 36: Knockdown of Src kinase in PC3 Mig-3 cells. PC3 Mig-3 cells were transfected with shSrc and Non-targeting control plasmids for 24 hrs. Cells were trypsinized after 48 hours of transfection. Cell lysates were subjected to immunoblot analyses for expression of Src and pFAK. Relative protein expression was determined after normalization to vinculin using NIH ImageJ.

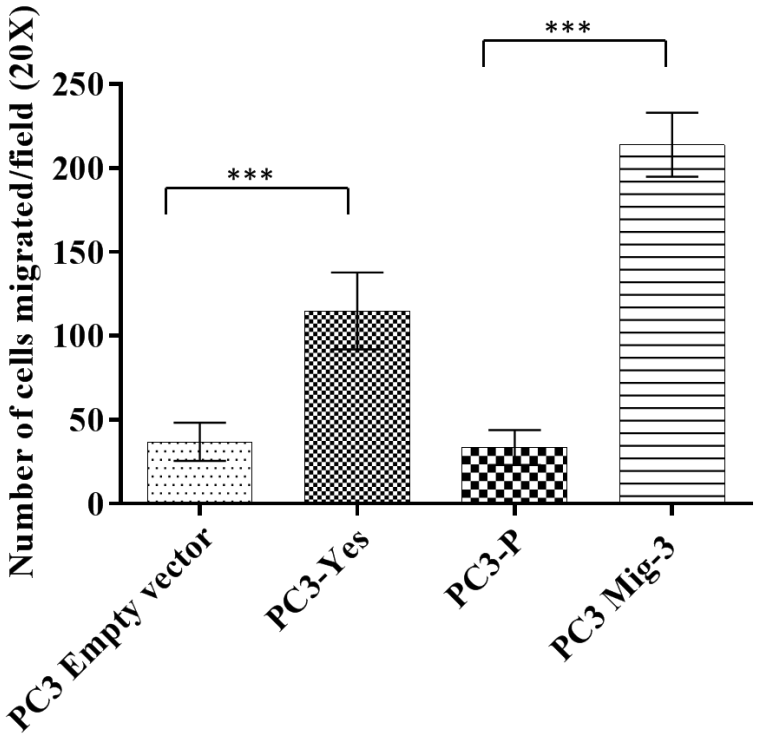

Figure 37: Migration assay of PC3-P cells after overexpression of Yes. PC3-P cells were transfected with PCMV6-XL5 control and Yes plasmids for 24 hours and the cells were plated in the Boyden chamber for 24 hours. After 24 hours, the cells were stained and counted to determine the number of migrating cells. Bars represent the average number of cells migrated from triplicate wells. ***$p<0.0001$ by Student's t-test, compared to the control group.

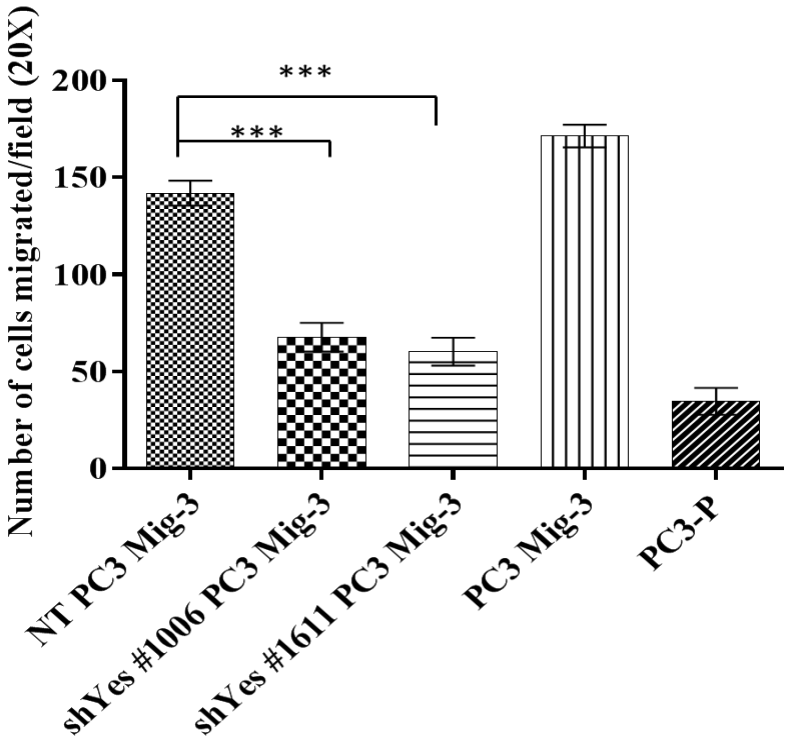

Figure 38: Migration assay of PC3-P cells after knockdown of Yes. PC3 Mig-3cells were transfected with shYes#1006, shYes#1611 and Non-targeting control plasmids for 24 hours and the cells were plated in the Boyden chamber for 24 hours for migration. After 24 hours, the cells were stained and counted to determine the number of migrating cells. Bars represent the average number of cells migrated from triplicate wells. ***$p<0.0001$ by Student's t-test, compared to the control group.

Src kinase and Yes kinase regulate FAK phosphorylation differently in SYF null mouse embryonic fibroblasts

While the above experiments provided strong evidence that Yes kinase preferentially phosphorylates FAK Y861 relative to the other FAK tyrosine sites, these experiments could not preclude potential roles of other SFKs expressed in prostate cancer cells. Therefore, to further determine whether Yes and Src differentially phosphorylated FAK, both were transiently overexpressed in the SYF (*src*-/-,*yes*-/-*fyn*-/-) mouse embryo fibroblasts using expression plasmids specific for Src and Yes as described in the methods. Overexpression of Src and Yes is shown in Figure 39. Overexpression of Src in the SYF cells led to increased phosphorylation of all the SFK-dependent tyrosine phosphorylation sites (Y 861, Y 407, Y 576, Y 577 and Y 925). However, overexpression of Yes kinase led to a 2-fold increase in phosphorylation of FAK Y861 with a lesser (1.4-fold) increase in phosphorylation of FAK Y 925 (Figure 39); other sites were not appreciably phosphorylated. These data are consistent with a novel role of Yes kinase in preferentially phosphorylating FAK Y861 and FAK Y925, the principal tyrosine sites mediating migration of cells.

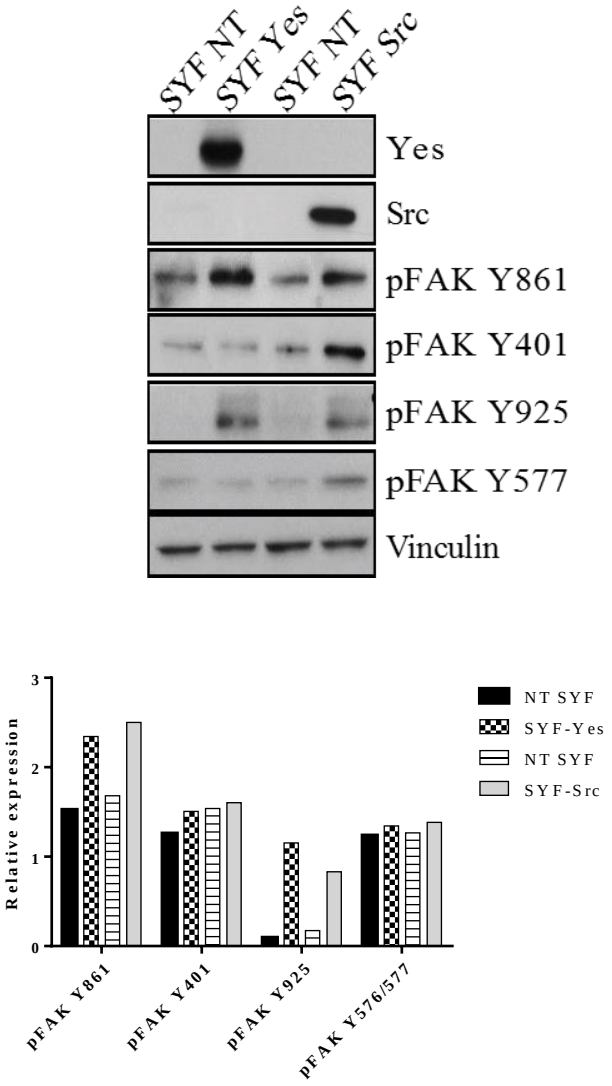

Figure 39: Overexpression of Src and Yes kinase in SYF mouse embryonic fibroblasts.

SYF MEF cells were transfected with PCDNA3.1 Src, pCMV6XL5-Yes and NT control plasmids for 24 hours and the cells were trypsinized and lysed after 48 hours of transfection. Cell lysates were subjected to immunoblot analyses for expression of Src and pFAK. Relative protein expression was determined after normalization to vinculin using NIH ImageJ.

Yes promotes prostate cancer lymph node metastasis in the orthotopic nude mouse model

To determine whether Yes overexpression promoted lymph node metastases in nude mouse models, intraprostatic injections were performed as described in materials and methods. For these experiments, control and Yes silenced cell lines with two different sequences were transduced with a plasmid directing luciferase expression. Following orthotopic injections, bioluminescence imaging of mice was performed weekly and mice were sacrificed when the primary tumors reached similar sizes (Figure 40, 42). A representative image of mice inoculated with cell lines expressing each construct is shown in Figure 44. Lymph node metastases were formed in all the groups and, with similar sized primary tumors as shown in Figure 40. NT PC3 Mig-3 cells formed 3.5 ±0.22 lymph node metastasis compared to 1.8± 0.3 lymph node metastases in the shYes#1006 group and 1.6± 0.2 lymph node metastases in the shYes#1006 group, indicated in Figure 41. Therefore, increased Yes expression is associated with prostate cancer lymph node metastases.

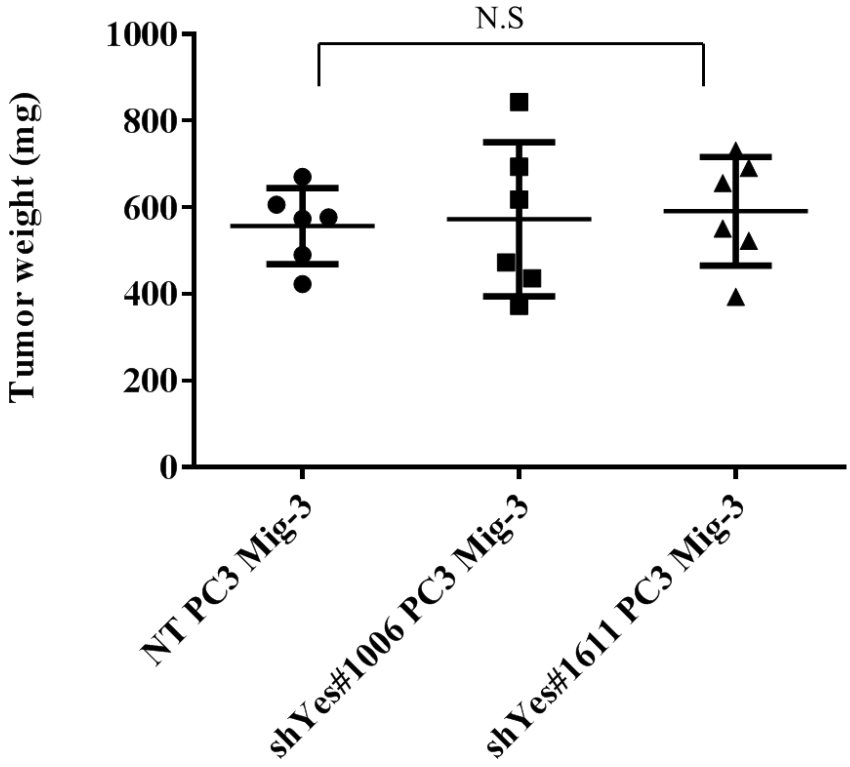

Figure 40: Tumorigenicity assay of PC3 Mig-3 cells after silencing Yes. Primary tumor weights after intraprostatic injection of $1X10^6$ NT PC3 Mig-3, shYes #1006 PC3 Mig-3 and shYes #1611 PC3 Mig-3 cells. The tumors were grown for 28 days and the mice were sacrificed.

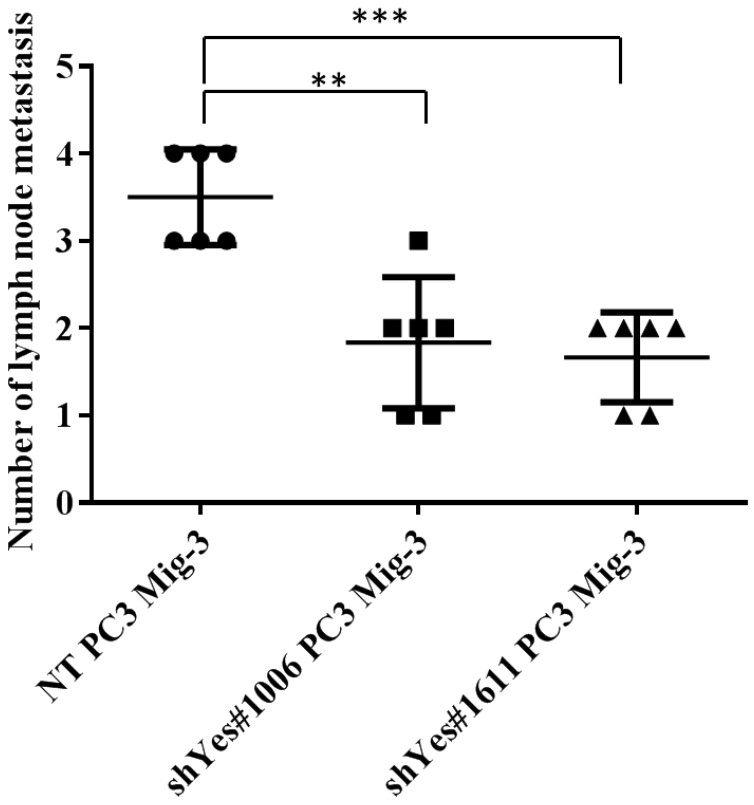

Figure 41: Tumorigenicity assay of PC3 Mig-3 cells after silencing Yes. Incidence of lymph node metastasis after intraprostatic injection of $1X10^6$ NT PC3 Mig-3, shYes #1006 PC3 Mig-3 and shYes #1611 PC3 Mig-3 cells. The tumors were grown for 28 days and the mice were sacrificed. **p<0.001, ***p<0.0001 by ANOVA and Tukey's test.

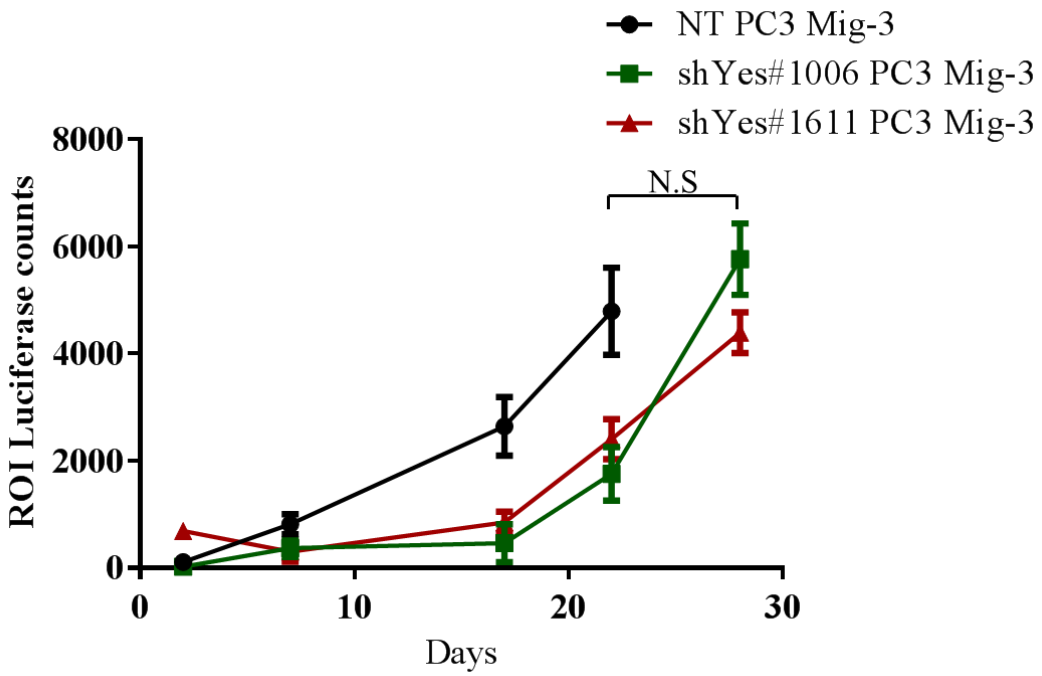

Figure 42: *In vivo* growth rate of PC3 Mig-3 cells after silencing Yes. Intraprostatic injections were performed using $1X10^6$ NT PC3 Mig-3, shYes#1006 PC3 Mig-3 and shYes#1611 PC3 Mig-3 cells. Tumor growth was monitored using luciferase imaging of the mice every 3 days after injection. Luciferase counts were calculated by selecting region of interests (ROIs) for each mouse. *$p<0.005$ by Student's t-test, compared to the control group.

NT PC3 Mig-3 **shYes PC3 Mig-3**

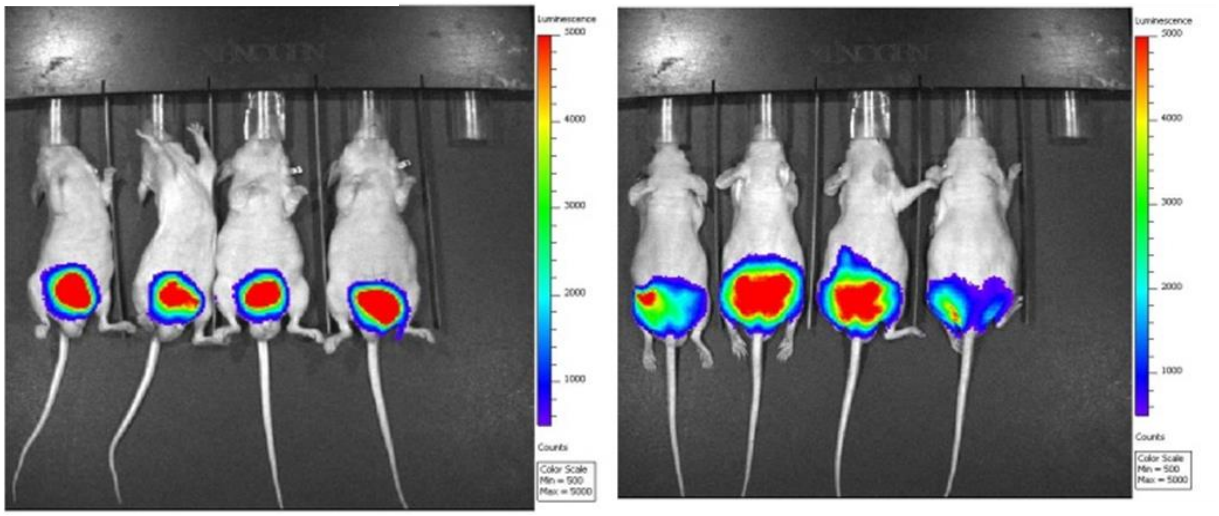

Figure 43: Bioluminescence imaging of PC3 Mig-3 cells after silencing Yes using luciferase. Representative images from the bioluminescence imaging using luciferase after intraprostatic injections were performed using $1X10^6$ NT PC3 Mig-3, shYes#1006 PC3 Mig-3 and shYes#1611 PC3 Mig-3 cells. The scales for imaging were standardized for each set.

Group	Average Tumor wt. (mg)/ range	Incidence of primary tumor	Average incidence of LN mets/ range	Incidence of LN Metastases
NT PC3 Mig-3	556.7 (490-670)	6/6	3.5 (3-4)**	6/6
sh Yes #1006 PC3 Mig-3	572.8 (436-694)	6/6	1.8 (1-3) **	6/6
sh Yes #1611PC3 Mig-3	604.7 (494-687)	6/6	1.6 (1-3) **	6/6

Table 3: Average weight and incidence of lymph node metastasis after knockdown of Yes in PC3 Mig-3 cells

ANOVA and Tukey's test, PC3 Mig-3 compared to PC3-P, **p<0.001

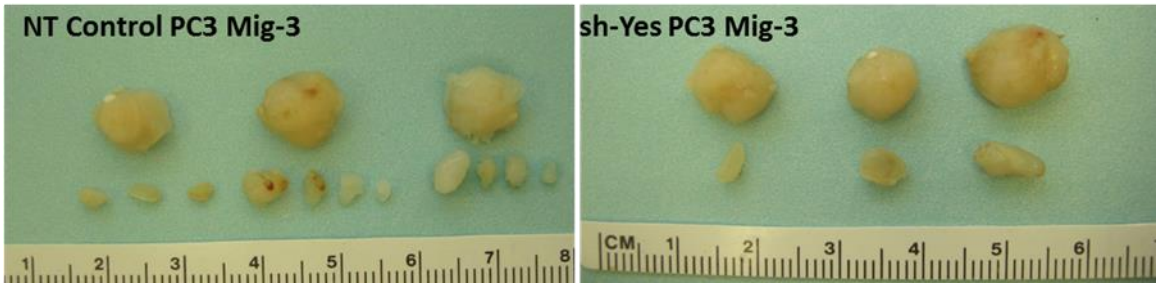

Figure 44: Representative primary tumors and lymph node metastases when mice were sacrificed. Luciferase-labeled NT Control PC3 Mig-3 and shYes PC3 Mig-3 cells (1×10^5) were orthotopically injected into the prostate. Mice were sacrificed when primary tumors reached similar sizes as monitored by bioluminescence imaging.

Chapter-6

Yes and pFAK Y861 expression in human prostate cancer

To determine the clinical relevance of pFAK Y861 and Yes expression in prostate cancer lymph node metastasis, I performed immunohistochemical analysis on formalin-fixed human prostate tumor specimens.

Correlation of pFAK Y861 expression in human prostate cancer patient specimens to survival

To examine the association of pFAK Y861 with patient survival, I collaborated with Dr. Chien-Jui Cheng and Dr. Sue-Hwa Lin. We examined pFAK Y861 expression in lymph node metastases of prostate cancer patients. The pFAK Y861 antibody was validated using a negative control experiment without the primary antibody. Patients were scored for positive (<10% of pFAK Y861 positive cells) and negative staining (>10% of pFAK Y861 positive cells) for pFAK Y861 expression. Representative images of lymph node metastases are shown in Figure 46. Patients with positive pFAK Y861 expression had an overall survival 6.13 ±0.99 years. In contrast patients with negative pFAK Y861 expression), had an overall survival of 11.69±1.67 years, (p=0.008) as represented in Figure 46. These data indicate that high expression of pFAK Y861 in prostate cancer patients correlate with poor survival.

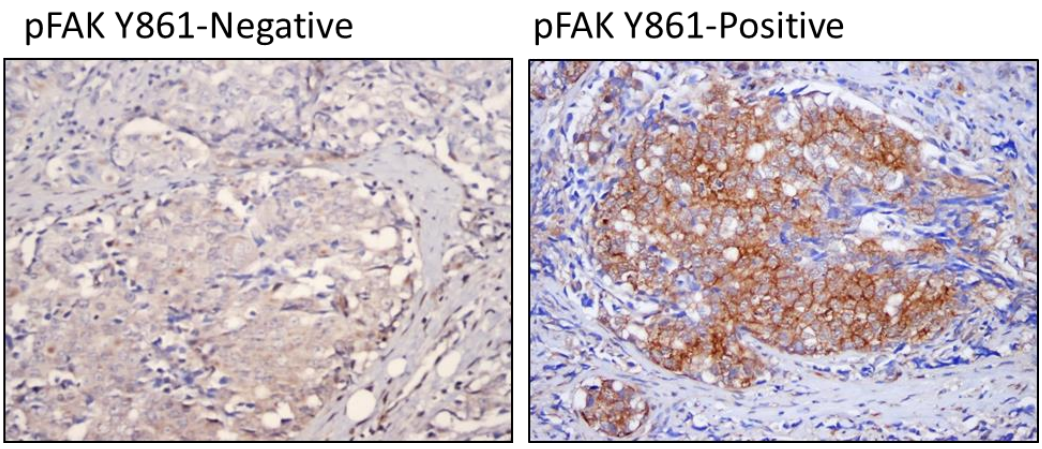

Figure 45: pFAK Y861 expression in lymph node metastases in human prostate cancer

Immunohistochemical staining of pFAK Y861 in lymph node metastases.

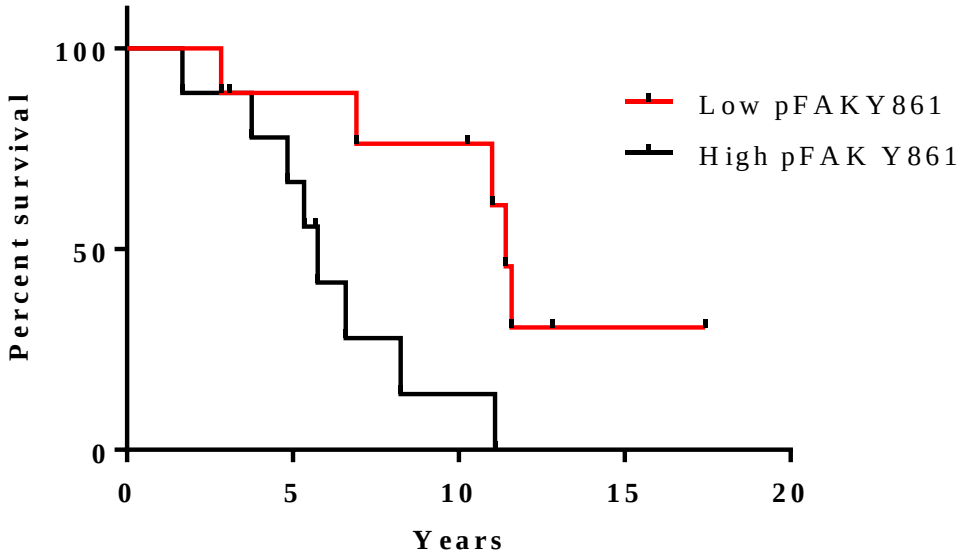

Figure 46: Survival analysis of patients with or without expression of pFAK Y861. The average survival time of cases with FAKpY861 expression is 6.13±0.99 years and in contrast, the average survival time of cases without FAKpY861 expression is 11.69±1.67 years. p=0.008 (logrank).

Yes expression in human prostate cancer patient specimens

To examine Yes kinase expression in prostate cancer primary tumors and matching lymph node metastases using a Yes-specific antibody, we obtained human prostate cancer primary tumor and lymph node metastases samples from the prostate cancer tissue bank at M. D. Anderson Cancer Center, under an approved IRB protocol. The Yes antibody was validated for specific staining by using a negative control experiment without using the primary antibody. Representative images of primary tumors and lymph node metastases are shown in Figure 47. We used 10 matching sample sets of primary tumors and lymph node metastases for the analysis. Yes expression was detected in all primary tumors and lymph node metastases. In addition, high expression was observed in lymphocytes. Average intensity of Yes expression was calculated after DAB extraction from each sample as described by Park *et al*. [114]. Yes expression in lymph node metastases in each set was significantly higher than the matching primary tumors ($p<0.05$-$p<0.00005$), indicated by the matching colors in the graph (Figure 48). The ratio of Yes expression in the primary tumor to its matching lymph node metastasis was determined. As shown in Figure 49, Yes expression was increased by 3.2-fold ($p<0.005$) in the lymph node metastases relative to the matching primary tumors, similar to what we observed in the PC3 Mig-3 and DU145 Mig-3 cells versus the parental prostate cancer cells.

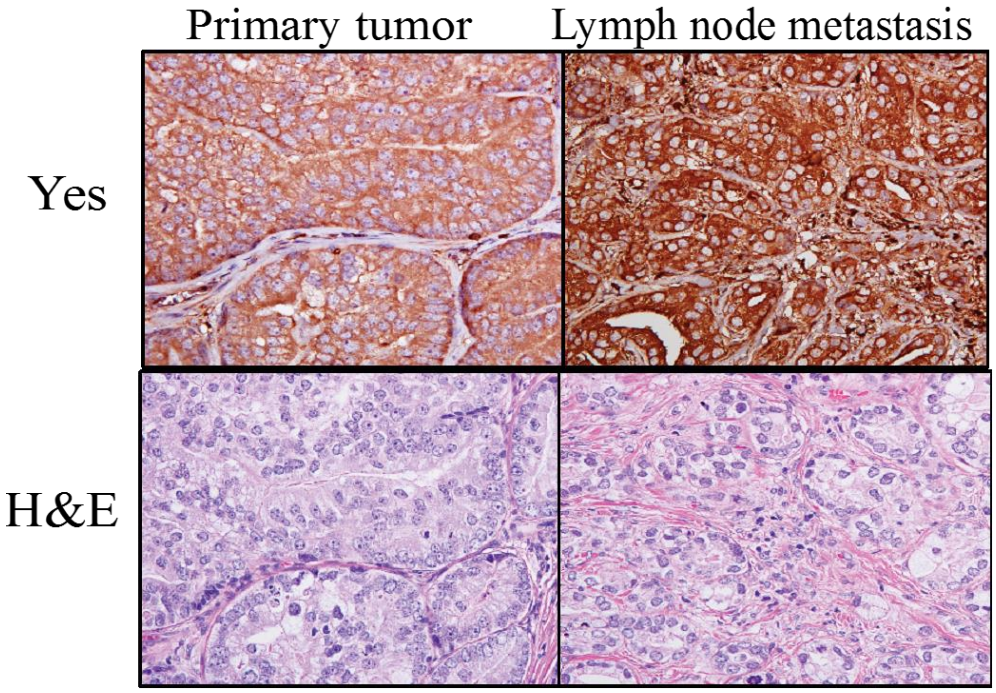

Figure 47: Yes expression in primary tumors and lymph node metastases in human prostate cancer. Immunohistochemical staining of Yes in primary tumor, lymph node metastases and matching H&E staining indicating the presence of tumor. The brown DAB staining indicates membranous localization of Yes kinase.

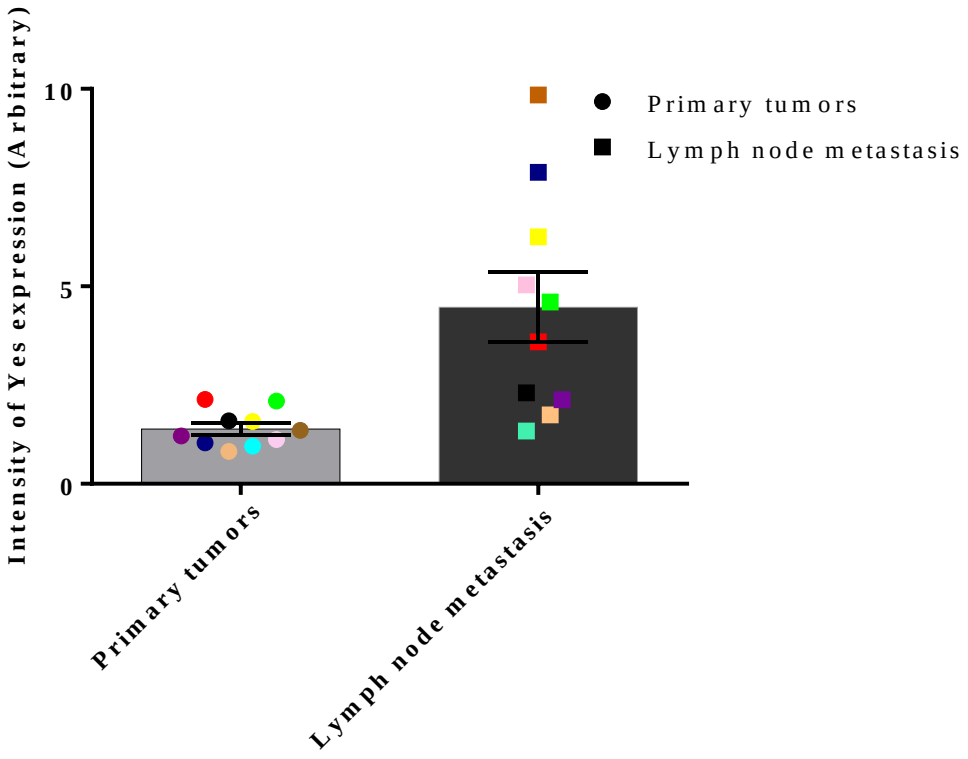

Figure 48: Quantification of Yes expression in primary tumors and lymph node metastases from human prostate cancer specimens. The graph represents average ratio of Yes expression in primary tumor to the matching lymph node metastasis. Similar color sets indicate matching lymph node metastasis has significantly higher Yes expression relative to primary tumors. * $p<0.05$, **$p<0.005$, **$p<0.0005$ by Student's t-test, compared to the control group.

Chapter-7

Discussion

Metastasis is the cause of mortality in the majority of prostate cancer patients. Because signature genetic alterations in prostate cancer are rare, understanding regulation of key gene products associated with metastasis, such as aberrant expression and activity of protein tyrosine kinases, is critical for prostate cancer progression. Activation of integrins and growth factor receptors result in activation of the FAK-SFK pathway, which is associated with increased migration and metastasis of prostate cancer cells. Additionally, in prostate cancer several pathways downstream of FAK are also activated, indicating that FAK is one of the central mediators of prostate cancer progression. FAK is overexpressed in metastasis but mutations in FAK are not found in human tumors and few if any studies have determined whether alterations in FAK either expression or phosphorylation are truly critical to metastasis. Since, FAK inhibitors are in clinical trials, understanding how FAK regulates metastasis of prostate cancer is critical. Hence, I investigated FAK and key elements that regulate FAK to understand its potential role in processes critical to metastasis.

Classical activation of FAK occurs after integrin clustering or growth factor receptor activation resulting in autophosphorylation of FAK Y397 and recruitment of SFKs [92]. The activated FAK-SFK complex then phosphorylates FAK Y401, FAK Y576, FAK Y577, FAK Y861 and FAK Y925. Phosphorylation of FAK at the SFK-dependent tyrosine residues discussed above, are known to be equivalent and the role of preferential phosphorylation of the FAK tyrosine residues in prostate cancer progression is unknown. Previous studies indicate that Src phosphorylates FAK *in vitro* [133] and other members of the Src family kinase are predicted to phosphorylate FAK similarly, however, the role of the different SFKs in regulation of FAK has not been investigated extensively. Hence, understanding the roles of individual SFKs in FAK phosphorylation is important, because increased expression of Src, Lyn and Fyn kinase,

the SFKs are all associated with prostate cancer progression [100, 107, 113, 115, 127]. However, Yes, also known to be expressed in prostate cancer has received much less attention.

Selection of highly migratory variants of prostate cancer cells

To understand the role of FAK in migration and metastasis of prostate cancer, and possible unique roles for SFKs in regulating FAK, I established cell models that specifically selected for isogenic variants with increased migration. While, in prior studies by other investigators, several isogenic cell lines had been isolated from mice with increased metastatic potential [134, 135], I selected cells through a Boyden chamber with the intent of specifically focusing on migration, to better understand specifically how FAK and FAK-SFK complexes that regulate this process. Surprisingly, the migration selection of cells selected for additional metastatic properties including increased invasion, decreased adhesion, and decreased proliferation in PC3 Mig-3 and DU145 Mig-3 cells relative to the parental cells. These data led me to examine the *in vivo* metastatic ability of PC3 Mig-3 cells in the orthotopic nude mode model for prostate cancer. I found that PC3 Mig-3 tumors had increased lymph node metastases relative to the PC3-P tumors confirming that migration selection of prostate cancer cells leads to selection of more metastatic cells that further highlighted the roles of the FAK/SFK signaling pathways. It is likely that this occurred because the parental PC3 cells that were used for selection of the PC3 Mig-3 cells are inherently metastatic. However, it is seems unlikely that this selection strategy would isolate a highly metastatic cell line from a non-tumorigenic immortalized line. Future studies could be to attempt this selection strategy in an immortalized non-tumorigenic cell line such as RWPE, to see if similar changes in FAK occurred, and which properties are altered due to the migration selection. This type of selection would seem unlikely

to increase all the properties I examined associated with metastasis, and may provide information as to the molecular alterations in earlier stages of prostate cancer progression.

Increased phosphorylation of FAK Y861 is a critical alteration associated with more migratory PC3 Mig-3 and DU145 Mig-3 cells.

Since we established two highly migratory cell models with increased metastatic potential, I next examined the alterations in FAK-SFK complexes that could be associated with the PC3 Mig-3 and DU145 Mig-3 cells. Classical activation of FAK requires autophosphorylation of FAK Y397 leading to phosphorylation of the remaining tyrosine sites on FAK. However, I found that in the highly migratory PC3 Mig-3 and DU145 Mig-3 cells, that only phosphorylation of FAK Y861 was increased independent of phosphorylation of FAK Y397, FAK Y401, FAK Y577, FAK Y576, and FAK Y925. Hence, I focused on understanding the role of increased phosphorylation of FAK Y861 in migration and metastasis of prostate cancer cells, discussed in the next sections. Interestingly, the total levels of FAK remained unaltered. This was an unexpected result given increases in FAK expression is observed in human prostate cancer metastases [126]. This leads to the question of whether overexpression of FAK leads to an increase in the number of FAK molecules phosphorylated, and therefore the phosphorylation, not the expression may be important in prostate cancer metastasis. This could be tested by overexpressing FAK in a low metastatic cell lines or in a genetically engineered mouse model that overexpresses FAK and then examining the levels of phosphorylated FAK Y861 along with the biological changes associated with increased FAK expression. Additionally, recent data also suggests that nuclear FAK functions as a transcription factor [136] , and whether this function is associated with tumor progression and metastasis would be an important question to address.

To directly test whether pFAK Y861 regulates migration of PC3 Mig-3 cells, we overexpressed the non-phosphorylatable FAK Y861F mutant in the PC3 Mig-3 cells using a lentiviral expression vector. Migration assays indicated that inhibition of phosphorylation of FAK Y861 lead to decreased migration of PC3 Mig-3 cells. Previous studies have indicated that phosphorylation of FAK Y861 is associated with migration of fibroblasts [93]; however no cause/effect relationship was established. Our studies have indicated that highly migratory prostate cancer cell lines may specifically increase phosphorylation of FAK Y861 and this might be important in FAK-mediated migration of cells.

To further, investigate the role of pFAK Y861 in prostate cancer metastasis, I examined pFAK Y861 expression in primary tumor and lymph node metastases, and I found a significant increase in expression of pFAK Y861 in the lymph node metastases relative to the primary tumors in the parental PC3 cells. These data indicate that similar to the *in vitro* selection, PC3-P cells with high expression of pFAK Y861 were selected to form lymph node metastasis with increased expression of pFAK Y861. On the contrary, PC3 Mig-3 primary tumors had high expression of pFAK Y861 and there was no further increase in pFAK Y861 in PC3 Mig-3 lymph node metastasis. This could be occurring as pFAK Y861 might be maximally activated in the PC3 Mig-3 primary tumors leading to increased lymph node metastasis in this group. These data confirm that pFAK Y861 expression is associated with metastasis of prostate cancer cells.

Previous studies from our laboratory have indicated that alterations in several other oncogenic proteins including Axl and Met are also associated with increased migration and metastasis of prostate cancer cells [131], and it was possible that these RTKs contributed to the increased phosphorylation of FAK Y861. Hence, I further investigated the role of Axl and Met

in PC3 Mig-3 cells in Chapter 4. Using the subcloning approach, I demonstrate that that in spite of increased expression of Axl and Met in the uncloned population of PC3 Mig-3 cells, subclones of the same cell line had differential expression of Axl, Met, and the only consistent alteration associated with increased migration of all the subclones was increased phosphorylation of FAK Y861. These data indicated that increased phosphorylation of FAK Y861 is a critical phenomenon occurring downstream of Axl and Met signaling. Our results suggest that Axl and Met could play a less dominant role in migration than the FAK-SFK complexes later in tumor progression, after cells have become metastatic. A better understanding of the roles of Met and Axl might require using cell lines lacking the ability to metastasize, in which their expression can be genetically manipulated. In line with these observations, work from our laboratory has shown that knockdown of Met in patient-derived xenografts from late-stage castrate resistant prostate cancer patients does not affect tumor growth, suggesting that Met-mediated effects may be at an earlier stage of progression than I studied. This possibility could be further analyzed by overexpression of Axl and Met in non-metastatic cells or in cells with lower intrinsic metastatic potential than I used in my thesis.

Yes is overexpressed and has increased activity in migratory cells relative to parental prostate cancer cells

To examine the mechanism of increased phosphorylation of FAK Y861, I investigated Src family kinases (SFKs), which are the principal kinases that phosphorylate FAK. SFKs are recruited to the phosphorylated tyrosine 397 of FAK via the SH2-SFK domain after activation and subsequently the FAK-SFK complex phosphorylates the remaining tyrosine residues of FAK. Although *in vitro* studies indicate that Src phosphorylates FAK [133], less is known about the role of other SFK members in FAK-mediated functions. As discussed in the introduction,

SFKs have structural and functional similarities; however, studies have identified different roles of SFKs in in prostate cancer progression [113, 116, 122, 127]. Hence, I examined the expression levels of the SFK members in PC3 Mig-3 cells. The data indicated that only Yes kinase was overexpressed and had increased activity in the PC3 Mig-3 and DU145 Mig-3 cells relative to the parental cells at both protein and RNA levels. Additionally, our previous data from the subcloning (Figure 21) indicated that increased expression of Yes kinase was a consistent alteration. This correlates with increased transcription of Yes. The mechanism by which transcription leads to overexpression of Yes in my migratory variants were increased was not addressed in this thesis. However, the cDNA array studies performed in collaboration with Dr. Woonyoung Choi and Dr. David McConkey indicated increased expression of several transcription factors such as *c-MYC, FOXA1* and *HEY1* in the PC3 Mig-3 cells relative to the parental cells. These transcription factors have binding sites on the Yes promoter and could be important in upregulating transcription of Yes (Figure 52).

The reasoning behind why selection of highly migratory cells also had increased expression and activity of Yes is also unknown. However I speculate that overexpression and over activity Yes kinase in the more migratory cells could be because that the other SFKs are close to maximally activated; and the specific migration selection selected for only the cells that had increased Yes activity required for preferential phosphorylation of pFAK Y861 and migration. Future studies could be to perform other selections for additional metastatic properties such as for adhesion, proliferation, or anoikis and examine whether alterations associated with other SFKs exist.

Yes preferentially phosphorylates FAK Y861 in PC3 Mig-3 cells

To directly investigate whether Yes phosphorylates FAK Y861, I first silenced the expression of Yes kinase in PC3 Mig-3 cells. Knockdown of Yes in the PC3 Mig-3 cells, preferentially downregulated pFAK Y861 expression and to some extent pFAK Y925 expression indicating that Yes specifically regulates both pFAK Y861 and pFAK Y925 in the PC3 Mig-3 model. Likewise, overexpression of Yes in PC3-P cells led to increased pFAK Y861 and pFAK Y925 expression. However, while Yes preferentially phosphorylated FAK Y861 and FAK Y925, the role of Src in phosphorylation of FAK in PC3 Mig-3 cells was not preferential to FAK Y861 and FAK Y925. I demonstrated that knockdown of Src in PC3 Mig-3 led to decreased phosphorylation of all the SFK-dependent FAK tyrosine sites and overexpression of Src lead to increased phosphorylation of all the SFK-dependent FAK tyrosine sites. I speculate that this Yes-mediated preferential phosphorylation of FAK Y861 and FAK Y925 in PC3 Mig-3 occurs because only Yes was overexpressed and had increased activity in PC3 Mig-3 cells relative to the parental cells. Additionally, previous reports indicate that Yes has weaker specific kinase activity against exogenous enolase relative to Src kinase in colorectal cancer cells [137], potentially explaining selective phosphorylation of only FAK Y861 and FAK Y925. Interestingly, FAK Y925 has also been associated with migration, and many of the signaling pathways activated through FAK Y861 phosphorylation are activated through FAK Y925 phosphorylation as well. So it is even more interesting that Yes also affects FAK Y925, further implicating its role in migration. It is unclear why the original selection did not change FAK Y925 phosphorylation. I speculate that other activating SFKs may have maximally phosphorylated this tyrosine residue and hence, increase in Yes activity after migration selection in PC3 cells did not further increase pFAK Y925 levels. Overlapping regulation of

pFAK Y861 and pFAK Y925 by Yes kinase is likely to occur due to easy accessibility of Yes kinase to these tyrosine residues as both FAK Y861 and FAK Y925 are present on the FAT domain of FAK that interacts with additional proteins that form the focal adhesion complex. Nevertheless, the role of pFAK Y925 in metastasis of prostate cancer cells could be investigated in the future using site-directed mutagenesis of pFAK Y925 in PC3 Mig-3 cells.

In spite of confirming the role in phosphorylation of FAK Y861 using Yes overexpression and Yes knockdown experiments, I could not negate the role of the remaining SFK members in phosphorylation of FAK Y861 and FAK Y925 in the PC3 Mig-3 cells. Hence, I used the SYF (*Src-/-, Yes-/-, Fyn-/-*) mouse embryonic fibroblasts model to demonstrate that overexpression of Yes kinase in the SYF MEF cells led to increased expression of only pFAK Y861 and pFAK Y925. However, overexpression of Src kinase led to equivalent overexpression of all the SFK-dependent of FAK phospho-tyrosine sites (Y401, Y577, Y576, Y861 and Y925), consistent with the PC3 cells. Additionally pFAK Y925 is also critically associated with FAK-mediated migration pathways, so despite the failure of the selection to increase FAK Y925 phosphorylation, these data suggests that increased Yes might be critical in regulating migration.

Yes-mediated migration of PC3 Mig-3 cells

Since, increased Yes expression and activity specifically phosphorylated pFAK Y861 that is associated with the highly migratory PC3 Mig-3 cells, I hypothesized that Yes promotes migration in prostate cancer cells. To test this hypothesis, I performed migration assays on PC3 Mig-3 and PC3-P cells after silencing and overexpression of Yes respectively. I found that Yes knockdown in PC3 Mig-3 cells leads to decreased migration, whereas overexpression of Yes in

PC3-P cells leads to increase in migration. I speculate that Yes regulates migration of prostate cancer cells by phosphorylation of pFAK Y861 and pFAK Y925, both of which recruit p130 Cas and Paxillin after phosphorylation leading to downstream pathways that regulate the migration signaling [138]. The role of Yes in phosphorylation and activation of these downstream signaling pathways mediating migration could be determined in the future by examining the expression of phospho p130Cas and phospho paxillin after knockdown and overexpression of Yes kinase in the PC3 Mig-3 cells. In Chapter 4 of this thesis, I also demonstrate that activation of Rho-A GTPases, which I predict is a possible downstream signaling mechanism of pFAK Y861 that regulates migration of PC3 Mig-3 cells. The data indicates that Rho-A was significantly more active in PC3 Mig-3 cells relative to the PC3-P cells additionally, Rho-A was downregulated in FAK Y861F Mig-3 cells, which had reduced migration *in vitro* (Figure 26). However, the role of Rho-A in migration of PC3 Mig-3 cells still remains unclear, and could be cell line dependent [139-141]. Hence, further studies are required to determine the role of additional proteins that are involved in regulation of Rho-A downstream of pFAK Y861.

Yes promotes lymph node metastases of prostate cancer cells

The data from Chapter 4 of this thesis indicate previously unknown roles of Yes kinase in prostate progression. Yes expression and activity was associated with increased migration of cells, however these data were correlative. To further investigate whether Yes affected metastasis *in vivo,* I performed an *in vivo* tumorigenicity assay using NT PC3 Mig-3 and shYes PC3 Mig-3 cells in the orthotopic nude mouse model for prostate cancer. The data indicated that shYes PC3 Mig-3 cells formed significantly fewer lymph node metastases relative to NT

PC3 Mig-3 cells similar to PC3-P cells. This provides a strong evidence that the increase in Yes was responsible for the increased lymph node metastases observed in the PC3 Mig-3 model.

Clinical significance of the study

Finally, to determine if the increased metastasis was a result of Yes expression and was relevant to human prostate cancer metastasis, I collaborated with Dr. Sue-Hwa Lin and Dr. Chein-Jui Cheng to examine pFAK Y861 expression in human tissues. We demonstrated that pFAK Y861 is overexpressed in lymph node metastasis of patients with poor survival (Figure 48, 49). I further demonstrated the clinical significance of Yes overexpression in prostate cancer progression by staining matched primary tumors and lymph node metastasis with antibody specific for Yes kinase. Increase in Yes expression in lymph node metastasis relative to the primary tumors (Figure 51) indicated that, the lymph node metastasis selected for cells overexpressing Yes kinase and I demonstrated that increased expression of Yes kinase was associated with prostate cancer lymph node metastasis. Since, very less information regarding Yes expression in matched primary tumors and lymph node metastases are currently available in The Cancer Genome Atlas (TCGA) databases, further confirmation for increased expression of Yes kinase in human prostate cancer progression can be determined by examining Yes overexpression at the RNA levels in matched primary and lymph node metastasis. mRNA levels of *yes* in patient samples can be determined after micro dissection of the tumor areas from the paraffin embedded tumor tissue and isolation of RNA, followed by RT-qPCR for *yes* expression using specific primers.

We specifically examined lymph node metastasis from prostate cancer patients as the spontaneous metastasis of prostate cancer in the mouse models occurs to the lymph node

metastasis. Although, lymph node metastasis is not lethal by itself, clinical studies from several institutions have indicated that lymph node metastasis is a poor prognostic factor of progression-free survival in patients and is critical in prostate cancer progression [142-145]. Whether, increased expression of pFAK Y861 and Yes kinase is important in bone metastasis can be determined experimentally, by performing intracardiac injections of PC3 Mig-3 and DU145 Mig-3 cells in the mice and examining whether PC3 Mig-3 cells colonize to the bone. Clinically, the significance of increased expression of pFAK Y861 and Yes kinase in bone metastasis of prostate cancer can be determined by performing immunohistochemistry to determine the expression of pFAK Y861 and Yes in human prostate cancer bone metastasis.

My study has unexpected clinical relevance, as a recent clinical trial investigating the role of Dasatinib, a small molecule inhibitor of SFKs did not show significant improvement in overall survival of metastatic castrate resistant prostate cancer patients. I demonstrate that increased expression and activity of only Yes kinase and not Src kinase is associated with a subset of prostate cancer cells, implicating that Src family kinases could be differentially upregulated in prostate cancer patients as well. This could be important as patients with upregulation of a specific SFK could respond differently to a pan-SFK inhibitor. Hence, stratification of patient cohorts depending of expression of different SFK members might be crucial for the success of future SFK inhibitor clinical trials and improvement of patient outcomes.

Future perspectives

This dissertation investigated the role of many proteins in prostate cancer metastasis. While the role of FAK and Src family kinase have been known to be associated with prostate cancer metastasis, my work is the first to identify the role of a specifically pFAK Y861 and Yes kinase in prostate cancer metastasis. However, many questions remain to be determined in the future.

In vitro migration selection of prostate cancer cells resulted in selection of cells with additional properties of metastasis. However, whether selection of cells using additional strategies, for example decreased adhesion, decreased proliferation, or increased anoikis would lead to selection of more metastatic cells could be another future study. As Src, Fyn and Lyn are known to play different roles in prostate cancer development, less is known regarding the role of Yes in this process. The role of Yes in promoting prostate cancer initiation and progression can be further examined by developing genetically engineered mouse models that overexpress Yes.

Since, we found increased expression of Yes kinase and pFAK Y861 in prostate cancer lymph node metastasis with the latter correlating to poor survival of patients, we can examine if increased expression of Yes kinase or pFAK Y861 in primary prostate tumor biopsies correlate with poor patient survival. Additionally, understanding whether increased expression of Yes and pFAK Y861 correlates with bone metastasis would be critical to investigate the role of these proteins in prostate cancer progression. This could be accomplished by immunohistochemical analysis of Yes and pFAK Y861 in human prostate cancer bone metastasis and by examining whether PC3 Mig-3 cells metastasize to the bone after performing

intracardiac injections of PC3 Mig-3 cells. This study could have a potential application of Yes and pFAK Y861 as biomarkers to detect prostate cancer progression.

Another approach towards using Yes and pFAK Y861 as biomarkers could be by detecting Yes kinase and phosphorylated FAK Y861 in the circulating tumor cells (CTCs). Although, whether Yes or pFAK Y861 are expressed in CTCs is not known, preliminary studies in our laboratory using antibodies against pFAK Y861 have indicated that expression of pFAK Y861 can be detected in PC3 prostate cancer cells experimentally introduced in mouse blood. Therefore, FAK phosphorylation and Yes expression may be a biomarker to predict prognosis in patients.

In spite of promising preclinical studies, the recent failure of dasatinib in a multinational phase-3 clinical trial indicates that not all the prostate cancer patients respond to a drug and selecting the patients that would respond to therapy is critical for improving overall survival of patients. Since, my study indicates different roles of Yes kinase in prostate cancer progression, a retrospective analysis of expression of different SFKs in the patients that responded to dasatinib and the ones that did not respond could be critical understanding the failure of the trial. Collectively, these studies would support my study that indicates that pFAK Y861 and Yes expression could not only be drivers of prostate cancer but also biomarkers for metastasis of prostate cancer

Conclusions

In this dissertation, I demonstrated that in the highly metastatic PC3 Mig-3 and DU145 Mig-3 cells, increased pFAK Y861 expression was associated with increased metastasis; however, the levels of total FAK remained unchanged. Using a non-phosphorylatable mutant of pFAK Y861, I demonstrated that pFAK Y861 is critical for migration of cells. Besides, increased phosphorylation of pFAK Y861 in lymph node metastasis of prostate cancer patients correlated with poor survival. These data demonstrate importance of pFAK Y861 in prostate cancer metastasis. Mechanistically, I demonstrated that specifically Yes kinase is responsible for preferential phosphorylation of pFAK Y861, indicating different roles of SFK members in phosphorylation of FAK in the highly migratory PC3 Mig-3 cells. Additionally, Yes kinase also promoted metastasis *in vivo* mouse model, directly correlating with its ability to increase tyrosine phosphorylation of FAK Y861. Finally, increased Yes kinase in lymph node metastases relative to matched primary tumors in human prostate cancer indicates the clinical relevance of these findings. In summary, I demonstrated that overexpression of Yes kinase promotes migration of prostate cancer cells through Yes-mediated preferential phosphorylation of pFAK Y861 (summarized in Figure 53). Therefore, I conclude that pFAK Y861 and Yes could be potential targets for development of novel therapies for prostate cancer metastasis.

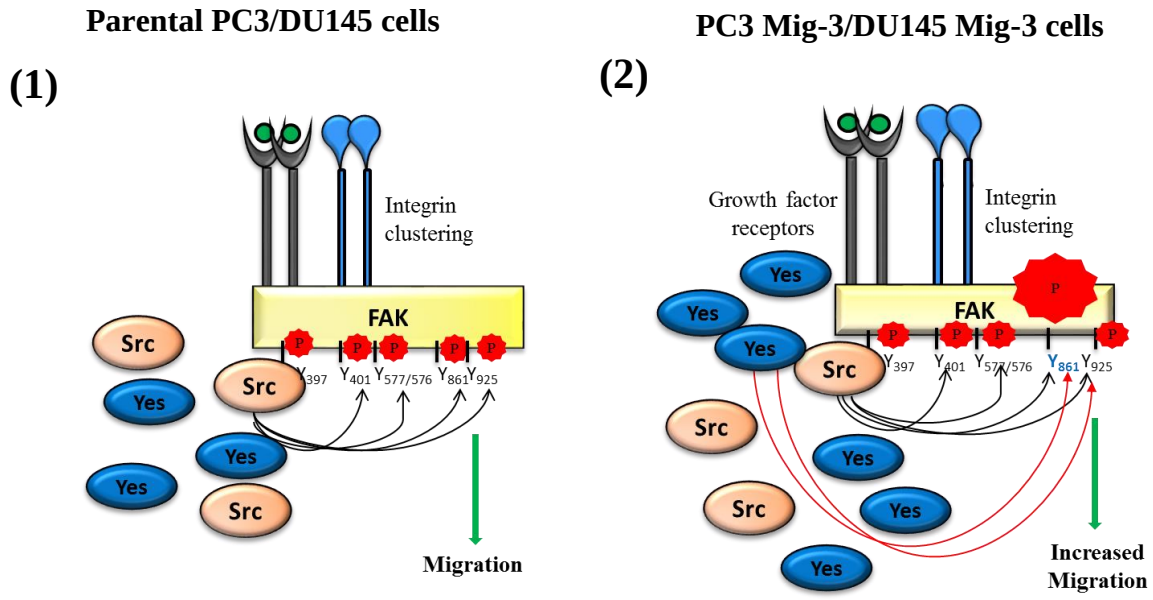

Figure 49: Model for preferential phosphorylation of pFAK Y861 in more migratory PC3 Mig-3 and DU145 Mig-3 cells. (1) In the parental PC3 and DU145 cells, Src phosphorylates all the SFK-dependent tyrosine kinase sites on FAK, (2) In the more migratory PC3 Mig-3 and DU145 Mig-3 cells, Yes kinase is over expressed and has increased activity leading to increased phosphorylation of FAK Y861 and increased migration of cells.

APPENDIX

Microarray analysis

RNA was isolated from the cells using the MirVana RNA extraction kit (Ambion/Life technologies, Austin,TX, USA). RNA was used for synthesis of biotin-labeled cRNA, using the Illumina RNA amplification kit (Ambion/Life Technologies, Austin, TX, USA). RNA purity and integrity were measured by NanoDrop ND-1000 and Agilent Bioanalyzer and only high quality RNA was used for the cRNA amplification, and then hybridized to Illumina-HT12 (Illumina, Inc., Hayward, CA, USA) chips. Slides were scanned with Bead Station 500X and signal intensities were quantified with GenomeStudio (Illumina, Inc.). Quantile normalization in the Linear Models for Microarray Data (LIMMA) package in the R language environment was used to normalize the data. BRB ArrayTools version 4.2 developed by National Cancer Institute was used to analyze the data as described by Choi *et al*.[146]. To identify molecular subtypes, we subjected the data obtained to unsupervised hierarchical cluster analysis using the 6700 probes that exhibited expression ratios of at least 2-fold relative to the median gene expression level across all samples in at least six samples. $p<0.001$ with FDR <0.1, 1.5 fold cut-off was used to determine differentially regulated genes in PC3 Mig-3 and PC3-P cells. To visualize gene expression patterns, specific gene expression values, adjusted to a median of zero, were used for clustering using Cluster 3.0 and TreeView (Eisen *et al.,* 1998). Functional and pathway analyses were performed using Ingenuity Pathway Analysis (IPA) software (Ingenuity® Systems, CA), which contains a database for identifying networks and pathways of interest in genomic data.

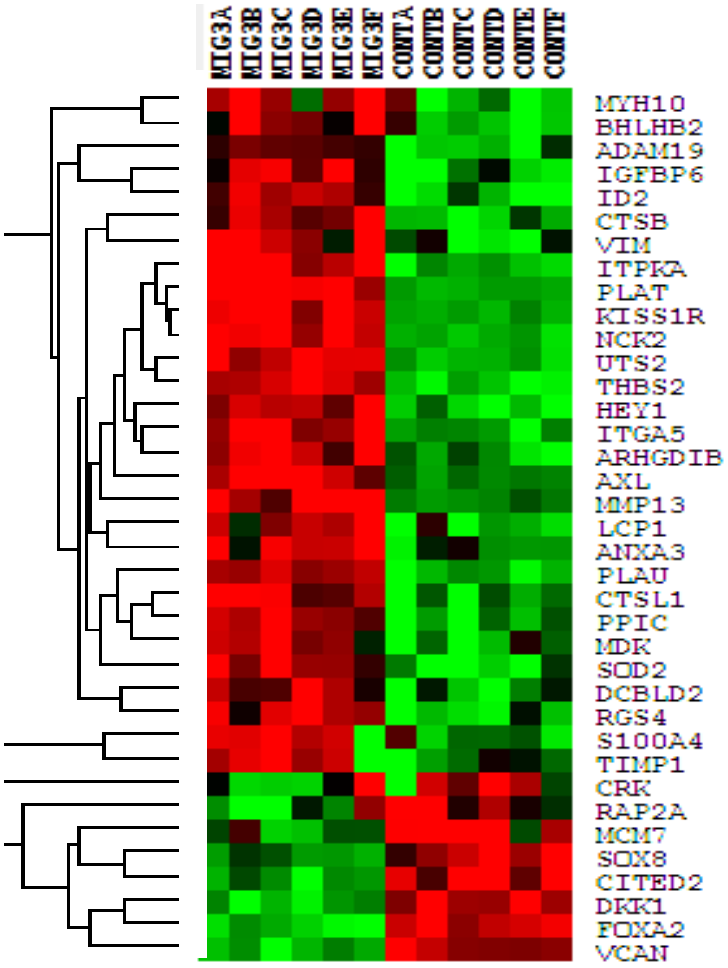

Figure 50: Heat-map of the migration and invasion regulating genes. Heat-map indicating the most differentially regulated genes that are involved in migration and invasion of cells.

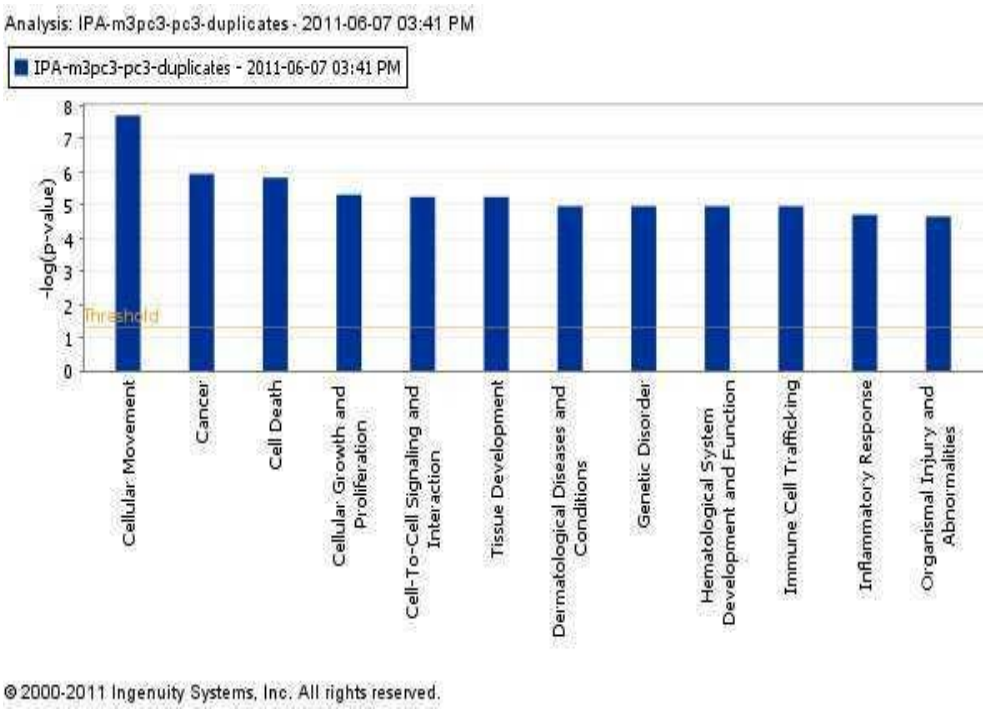

Figure 51: IPA pathway analysis. Pathway analysis indicating cellular movement signaling pathways as the most significantly altered pathway in the PC3 Mig-3 cells relative to the parental cells. $p<0.001$, False discovery rate <0.1

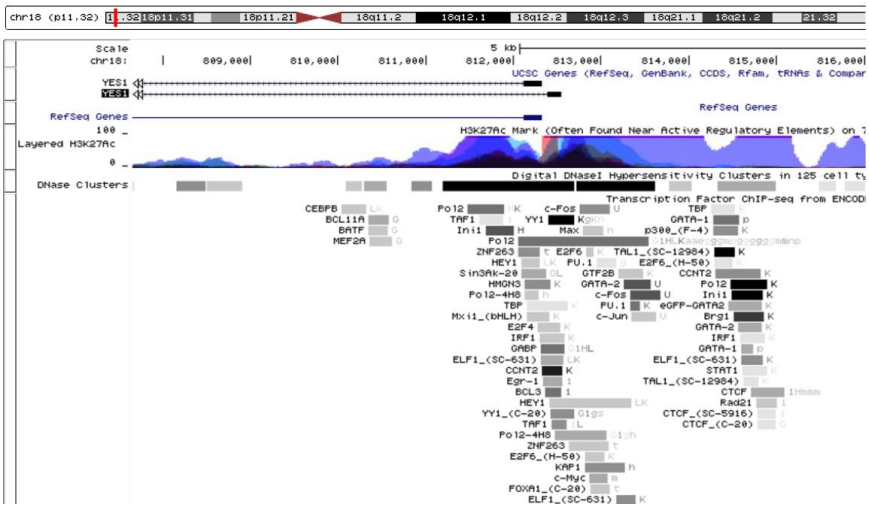

Figure 52: UCSC genome browser analysis of transcription factors binding to yes promoter. UCSC genome browser analysis indicating binding of several transcription factors including HEY1, FOXA1 and c-MYC to the Yes promoter region.

G-LISA Rho-A activation assay protocol

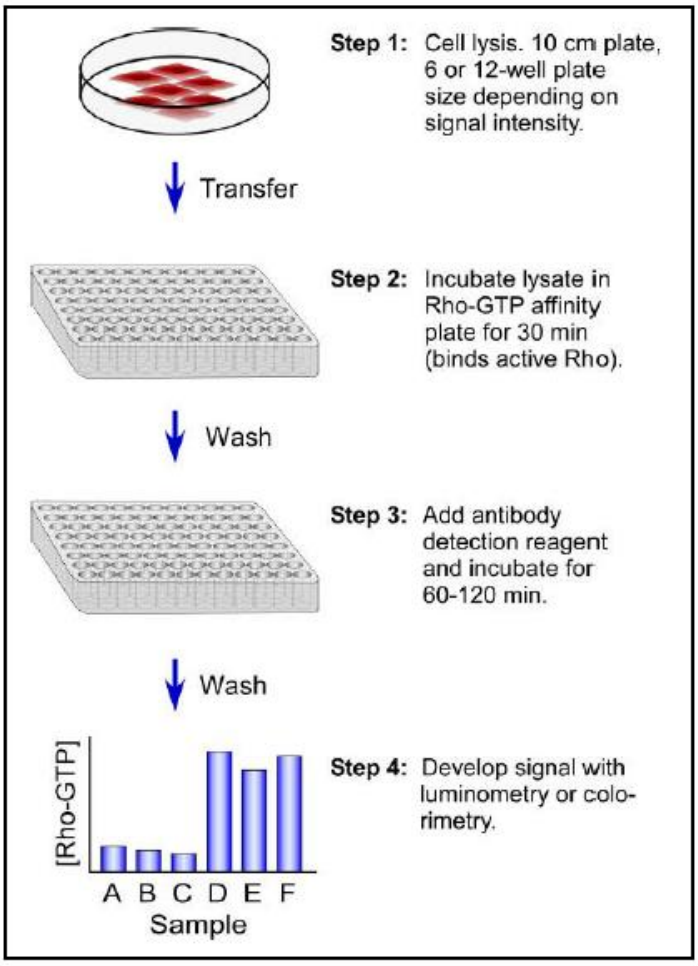

BIBLOGRAPHY

1. Siegel R, Ma J, Zou Z and Jemal A. Cancer statistics, 2014. CA: a cancer journal for clinicians. 2014; 64(1):9-29.
2. Cetnar JP and Beer TM. Personalizing prostate cancer therapy: the way forward. Drug discovery today. 2014; 19(9):1483-1487.
3. Koontz BF, Bossi A, Cozzarini C, Wiegel T and D'Amico A. A Systematic Review of Hypofractionation for Primary Management of Prostate Cancer. European urology. 2014.
4. Lund L, Svolgaard N and Poulsen MH. Prostate cancer: a review of active surveillance. Research and reports in urology. 2014; 6:107-112.
5. Moyad MA and Scholz MC. Short-term enzalutamide treatment for the potential remission of active surveillance or intermediate-risk prostate cancer: a case study, review, and the need for a clinical trial. Research and reports in urology. 2014; 6:71-77.
6. Ahmadi H and Daneshmand S. Androgen deprivation therapy for prostate cancer: long-term safety and patient outcomes. Patient related outcome measures. 2014; 5:63-70.
7. Tormey WP. The complexity of PSA interpretation in clinical practice. The surgeon : journal of the Royal Colleges of Surgeons of Edinburgh and Ireland. 2014.
8. Cary KC and Cooperberg MR. Biomarkers in prostate cancer surveillance and screening: past, present, and future. Ther Adv Urol. 2013; 5(6):318-329.
9. Loughlin KR. PSA velocity: A systematic review of clinical applications. Urologic oncology. 2014.
10. Saga Y, Furukawa K, Rogers P, Tung JS, Parker D and Boyse EA. Further data on the selective expression of Ly-5 isoforms. Immunogenetics. 1990; 31(5-6):296-306.

11. Brimo F, Montironi R, Egevad L, Erbersdobler A, Lin DW, Nelson JB, Rubin MA, van der Kwast T, Amin M and Epstein JI. Contemporary grading for prostate cancer: implications for patient care. European urology. 2013; 63(5):892-901.

12. Madan RA and Arlen PM. Recent advances revolutionize treatment of metastatic prostate cancer. Future oncology. 2013; 9(8):1133-1144.

13. Deng X, He G, Liu J, Luo F, Peng X, Tang S, Gao Z, Lin Q, Keller JM, Yang T and Keller ET. Recent advances in bone-targeted therapies of metastatic prostate cancer. Cancer treatment reviews. 2014; 40(6):730-738.

14. Ryan CJ, Smith MR, de Bono JS, Molina A, Logothetis CJ, de Souza P, Fizazi K, Mainwaring P, Piulats JM, Ng S, Carles J, Mulders PF, Basch E, Small EJ, Saad F, Schrijvers D, et al. Abiraterone in metastatic prostate cancer without previous chemotherapy. The New England journal of medicine. 2013; 368(2):138-148.

15. Scher HI, Fizazi K, Saad F, Taplin ME, Sternberg CN, Miller K, de Wit R, Mulders P, Chi KN, Shore ND, Armstrong AJ, Flaig TW, Flechon A, Mainwaring P, Fleming M, Hainsworth JD, et al. Increased survival with enzalutamide in prostate cancer after chemotherapy. The New England journal of medicine. 2012; 367(13):1187-1197.

16. Nakabayashi M, Werner L, Courtney KD, Buckle G, Oh WK, Bubley GJ, Hayes JH, Weckstein D, Elfiky A, Sims DM, Kantoff PW and Taplin ME. Phase II trial of RAD001 and bicalutamide for castration-resistant prostate cancer. BJU international. 2012; 110(11):1729-1735.

17. Mathew P. The bifunctional role of steroid hormones: implications for therapy in prostate cancer. Oncology. 2014; 28(5):397-404.

18. Westdorp H, Skold AE, Snijer BA, Franik S, Mulder SF, Major PP, Foley R, Gerritsen WR and de Vries IJ. Immunotherapy for prostate cancer: lessons from responses to tumor-associated antigens. Frontiers in immunology. 2014; 5:191.

19. Beer TM, Armstrong AJ, Rathkopf DE, Loriot Y, Sternberg CN, Higano CS, Iversen P, Bhattacharya S, Carles J, Chowdhury S, Davis ID, de Bono JS, Evans CP, Fizazi K, Joshua AM, Kim CS, et al. Enzalutamide in metastatic prostate cancer before chemotherapy. The New England journal of medicine. 2014; 371(5):424-433.

20. Kwon ED, Drake CG, Scher HI, Fizazi K, Bossi A, van den Eertwegh AJ, Krainer M, Houede N, Santos R, Mahammedi H, Ng S, Maio M, Franke FA, Sundar S, Agarwal N, Bergman AM, et al. Ipilimumab versus placebo after radiotherapy in patients with metastatic castration-resistant prostate cancer that had progressed after docetaxel chemotherapy (CA184-043): a multicentre, randomised, double-blind, phase 3 trial. The Lancet Oncology. 2014; 15(7):700-712.

21. Angelergues A, Maillet D, Flechon A, Ozguroglu M, Mercier F, Guillot A, Le Moulec S, Gravis G, Beuzeboc P, Massard C, Fizazi K, de La Motte Rouge T, Delanoy N, Elaidi RT and Oudard S. Prostate-specific antigen flare induced by cabazitaxel-based chemotherapy in patients with metastatic castration-resistant prostate cancer. European journal of cancer. 2014; 50(9):1602-1609.

22. Massari F, Maines F, Modena A, Brunelli M, Bria E, Artibani W, Martignoni G and Tortora G. Castration resistant prostate cancer (CRPC): state of the art, perspectives and new challenges. Anti-cancer agents in medicinal chemistry. 2013; 13(6):872-886.

23. Lee JL, Ahn JH, Choi MK, Kim Y, Hong SW, Lee KH, Jeong IG, Song C, Hong BS, Hong JH and Ahn H. Gemcitabine-oxaliplatin plus prednisolone is active in patients

with castration-resistant prostate cancer for whom docetaxel-based chemotherapy failed. British journal of cancer. 2014; 110(10):2472-2478.

24. Badrising S, van der Noort V, van Oort IM, van den Berg HP, Los M, Hamberg P, Coenen JL, van den Eertwegh AJ, de Jong IJ, Kerver ED, van Tinteren H and Bergman AM. Clinical activity and tolerability of enzalutamide (MDV3100) in patients with metastatic, castration-resistant prostate cancer who progress after docetaxel and abiraterone treatment. Cancer. 2014; 120(7):968-975.

25. Michaelson MD, Oudard S, Ou YC, Sengelov L, Saad F, Houede N, Ostler P, Stenzl A, Daugaard G, Jones R, Laestadius F, Ullen A, Bahl A, Castellano D, Gschwend J, Maurina T, et al. Randomized, placebo-controlled, phase III trial of sunitinib plus prednisone versus prednisone alone in progressive, metastatic, castration-resistant prostate cancer. Journal of clinical oncology : official journal of the American Society of Clinical Oncology. 2014; 32(2):76-82.

26. Boyd LK, Mao X and Lu YJ. The complexity of prostate cancer: genomic alterations and heterogeneity. Nature reviews Urology. 2012; 9(11):652-664.

27. Al Olama AA, Kote-Jarai Z, Berndt SI, Conti DV, Schumacher F, Han Y, Benlloch S, Hazelett DJ, Wang Z, Saunders E, Leongamornlert D, Lindstrom S, Jugurnauth-Little S, Dadaev T, Tymrakiewicz M, Stram DO, et al. A meta-analysis of 87,040 individuals identifies 23 new susceptibility loci for prostate cancer. Nature genetics. 2014.

28. Fraser M, Berlin A, Bristow RG and van der Kwast T. Genomic, pathological, and clinical heterogeneity as drivers of personalized medicine in prostate cancer. Urologic oncology. 2014.

29. Mazaris E and Tsiotras A. Molecular pathways in prostate cancer. Nephro-urology monthly. 2013; 5(3):792-800.

30. Schoenborn JR, Nelson P and Fang M. Genomic profiling defines subtypes of prostate cancer with the potential for therapeutic stratification. Clinical cancer research : an official journal of the American Association for Cancer Research. 2013; 19(15):4058-4066.

31. Gurel B, Ali TZ, Montgomery EA, Begum S, Hicks J, Goggins M, Eberhart CG, Clark DP, Bieberich CJ, Epstein JI and De Marzo AM. NKX3.1 as a marker of prostatic origin in metastatic tumors. The American journal of surgical pathology. 2010; 34(8):1097-1105.

32. Abate-Shen C, Banach-Petrosky WA, Sun X, Economides KD, Desai N, Gregg JP, Borowsky AD, Cardiff RD and Shen MM. Nkx3.1; Pten mutant mice develop invasive prostate adenocarcinoma and lymph node metastases. Cancer research. 2003; 63(14):3886-3890.

33. Bowen C, Bubendorf L, Voeller HJ, Slack R, Willi N, Sauter G, Gasser TC, Koivisto P, Lack EE, Kononen J, Kallioniemi OP and Gelmann EP. Loss of NKX3.1 expression in human prostate cancers correlates with tumor progression. Cancer research. 2000; 60(21):6111-6115.

34. Abate-Shen C, Shen MM and Gelmann E. Integrating differentiation and cancer: the Nkx3.1 homeobox gene in prostate organogenesis and carcinogenesis. Differentiation. 2008; 76(6):717-727.

35. Kim MJ, Bhatia-Gaur R, Banach-Petrosky WA, Desai N, Wang Y, Hayward SW, Cunha GR, Cardiff RD, Shen MM and Abate-Shen C. Nkx3.1 mutant mice recapitulate early stages of prostate carcinogenesis. Cancer Res. 2002; 62(11):2999-3004.

36. Abdulkadir SA, Magee JA, Peters TJ, Kaleem Z, Naughton CK, Humphrey PA and Milbrandt J. Conditional loss of Nkx3.1 in adult mice induces prostatic intraepithelial neoplasia. Mol Cell Biol. 2002; 22(5):1495-1503.

37. Aslan G, Irer B, Tuna B, Yorukoglu K, Saatcioglu F and Celebi I. Analysis of NKX3.1 expression in prostate cancer tissues and correlation with clinicopathologic features. Pathology, research and practice. 2006; 202(2):93-98.

38. Muniyan S, Ingersoll MA, Batra SK and Lin MF. Cellular prostatic acid phosphatase, a PTEN-functional homologue in prostate epithelia, functions as a prostate-specific tumor suppressor. Biochimica et biophysica acta. 2014; 1846(1):88-98.

39. Li J, Yen C, Liaw D, Podsypanina K, Bose S, Wang SI, Puc J, Miliaresis C, Rodgers L, McCombie R, Bigner SH, Giovanella BC, Ittmann M, Tycko B, Hibshoosh H, Wigler MH, et al. PTEN, a putative protein tyrosine phosphatase gene mutated in human brain, breast, and prostate cancer. Science. 1997; 275(5308):1943-1947.

40. Wang SI, Parsons R and Ittmann M. Homozygous deletion of the PTEN tumor suppressor gene in a subset of prostate adenocarcinomas. Clinical cancer research : an official journal of the American Association for Cancer Research. 1998; 4(3):811-815.

41. Steck PA, Pershouse MA, Jasser SA, Yung WK, Lin H, Ligon AH, Langford LA, Baumgard ML, Hattier T, Davis T, Frye C, Hu R, Swedlund B, Teng DH and Tavtigian SV. Identification of a candidate tumour suppressor gene, MMAC1, at chromosome

10q23.3 that is mutated in multiple advanced cancers. Nature genetics. 1997; 15(4):356-362.

42. Mithal P, Allott E, Gerber L, Reid J, Welbourn W, Tikishvili E, Park J, Younus A, Sangale Z, Lanchbury JS, Stone S and Freedland SJ. PTEN loss in biopsy tissue predicts poor clinical outcomes in prostate cancer. International journal of urology : official journal of the Japanese Urological Association. 2014.

43. Leinonen KA, Saramaki OR, Furusato B, Kimura T, Takahashi H, Egawa S, Suzuki H, Keiger K, Ho Hahm S, Isaacs WB, Tolonen TT, Stenman UH, Tammela TL, Nykter M, Bova GS and Visakorpi T. Loss of PTEN is associated with aggressive behavior in ERG-positive prostate cancer. Cancer epidemiology, biomarkers & prevention : a publication of the American Association for Cancer Research, cosponsored by the American Society of Preventive Oncology. 2013; 22(12):2333-2344.

44. Mulholland DJ, Tran LM, Li Y, Cai H, Morim A, Wang S, Plaisier S, Garraway IP, Huang J, Graeber TG and Wu H. Cell autonomous role of PTEN in regulating castration-resistant prostate cancer growth. Cancer cell. 2011; 19(6):792-804.

45. Stephan C, Ralla B and Jung K. Prostate-specific antigen and other serum and urine markers in prostate cancer. Biochim Biophys Acta. 2014; 1846(1):99-112.

46. Tomlins SA, Rhodes DR, Perner S, Dhanasekaran SM, Mehra R, Sun XW, Varambally S, Cao X, Tchinda J, Kuefer R, Lee C, Montie JE, Shah RB, Pienta KJ, Rubin MA and Chinnaiyan AM. Recurrent fusion of TMPRSS2 and ETS transcription factor genes in prostate cancer. Science. 2005; 310(5748):644-648.

47. Yoshimoto M, Cutz JC, Nuin PA, Joshua AM, Bayani J, Evans AJ, Zielenska M and Squire JA. Interphase FISH analysis of PTEN in histologic sections shows genomic

deletions in 68% of primary prostate cancer and 23% of high-grade prostatic intra-epithelial neoplasias. Cancer genetics and cytogenetics. 2006; 169(2):128-137.

48. Dang CV. MYC on the path to cancer. Cell. 2012; 149(1):22-35.

49. Koh CM, Gurel B, Sutcliffe S, Aryee MJ, Schultz D, Iwata T, Uemura M, Zeller KI, Anele U, Zheng Q, Hicks JL, Nelson WG, Dang CV, Yegnasubramanian S and De Marzo AM. Alterations in nucleolar structure and gene expression programs in prostatic neoplasia are driven by the MYC oncogene. The American journal of pathology. 2011; 178(4):1824-1834.

50. Koh CM, Bieberich CJ, Dang CV, Nelson WG, Yegnasubramanian S and De Marzo AM. MYC and Prostate Cancer. Genes & cancer. 2010; 1(6):617-628.

51. Gurel B, Iwata T, Koh CM, Yegnasubramanian S, Nelson WG and De Marzo AM. Molecular alterations in prostate cancer as diagnostic, prognostic, and therapeutic targets. Advances in anatomic pathology. 2008; 15(6):319-331.

52. Massard C and Fizazi K. Targeting continued androgen receptor signaling in prostate cancer. Clinical cancer research : an official journal of the American Association for Cancer Research. 2011; 17(12):3876-3883.

53. Dehm SM and Tindall DJ. Molecular regulation of androgen action in prostate cancer. Journal of cellular biochemistry. 2006; 99(2):333-344.

54. Logothetis CJ, Gallick GE, Maity SN, Kim J, Aparicio A, Efstathiou E and Lin SH. Molecular classification of prostate cancer progression: foundation for marker-driven treatment of prostate cancer. Cancer discovery. 2013; 3(8):849-861.

55. Valastyan S and Weinberg RA. Tumor metastasis: molecular insights and evolving paradigms. Cell. 2011; 147(2):275-292.

56. Fidler IJ. Seed and soil revisited: contribution of the organ microenvironment to cancer metastasis. Surgical oncology clinics of North America. 2001; 10(2):257-269, vii-viiii.

57. Killion JJ and Fidler IJ. The biology of tumor metastasis. Seminars in oncology. 1989; 16(2):106-115.

58. Langley RR and Fidler IJ. The seed and soil hypothesis revisited--the role of tumor-stroma interactions in metastasis to different organs. International journal of cancer Journal international du cancer. 2011; 128(11):2527-2535.

59. Klein CA. Parallel progression of primary tumours and metastases. Nature reviews Cancer. 2009; 9(4):302-312.

60. Friberg S and Mattson S. On the growth rates of human malignant tumors: implications for medical decision making. Journal of surgical oncology. 1997; 65(4):284-297.

61. van der Horst G, Bos L and van der Pluijm G. Epithelial plasticity, cancer stem cells, and the tumor-supportive stroma in bladder carcinoma. Molecular cancer research : MCR. 2012; 10(8):995-1009.

62. Nieto MA. Epithelial plasticity: a common theme in embryonic and cancer cells. Science. 2013; 342(6159):1234850.

63. Giampieri S, Manning C, Hooper S, Jones L, Hill CS and Sahai E. Localized and reversible TGFbeta signalling switches breast cancer cells from cohesive to single cell motility. Nature cell biology. 2009; 11(11):1287-1296.

64. Isaacs JT, Isaacs WB, Feitz WF and Scheres J. Establishment and characterization of seven Dunning rat prostatic cancer cell lines and their use in developing methods for predicting metastatic abilities of prostatic cancers. The Prostate. 1986; 9(3):261-281.

65. Mohler JL, Partin AW and Coffey DS. Prediction of metastatic potential by a new grading system of cell motility: validation in the Dunning R-3327 prostatic adenocarcinoma model. The Journal of urology. 1987; 138(1):168-170.

66. Partin AW, Schoeniger JS, Mohler JL and Coffey DS. Fourier analysis of cell motility: correlation of motility with metastatic potential. Proceedings of the National Academy of Sciences of the United States of America. 1989; 86(4):1254-1258.

67. Friedl P and Alexander S. Cancer invasion and the microenvironment: plasticity and reciprocity. Cell. 2011; 147(5):992-1009.

68. Huttenlocher A and Horwitz AR. Integrins in cell migration. Cold Spring Harbor perspectives in biology. 2011; 3(9):a005074.

69. Mitra SK, Hanson DA and Schlaepfer DD. Focal adhesion kinase: in command and control of cell motility. Nature reviews Molecular cell biology. 2005; 6(1):56-68.

70. Ilic D, Furuta Y, Kanazawa S, Takeda N, Sobue K, Nakatsuji N, Nomura S, Fujimoto J, Okada M and Yamamoto T. Reduced cell motility and enhanced focal adhesion contact formation in cells from FAK-deficient mice. Nature. 1995; 377(6549):539-544.

71. Brami-Cherrier K, Gervasi N, Arsenieva D, Walkiewicz K, Boutterin MC, Ortega A, Leonard PG, Seantier B, Gasmi L, Bouceba T, Kadare G, Girault JA and Arold ST. FAK dimerization controls its kinase-dependent functions at focal adhesions. The EMBO journal. 2014; 33(4):356-370.

72. Hall JE, Fu W and Schaller MD. Focal adhesion kinase: exploring Fak structure to gain insight into function. International review of cell and molecular biology. 2011; 288:185-225.

73. Frame MC, Patel H, Serrels B, Lietha D and Eck MJ. The FERM domain: organizing the structure and function of FAK. Nature reviews Molecular cell biology. 2010; 11(11):802-814.

74. Hogg PJ. Targeting allosteric disulphide bonds in cancer. Nature reviews Cancer. 2013; 13(6):425-431.

75. Arold ST, Hoellerer MK and Noble ME. The structural basis of localization and signaling by the focal adhesion targeting domain. Structure. 2002; 10(3):319-327.

76. Abu-Ghazaleh R, Kabir J, Jia H, Lobo M and Zachary I. Src mediates stimulation by vascular endothelial growth factor of the phosphorylation of focal adhesion kinase at tyrosine 861, and migration and anti-apoptosis in endothelial cells. The Biochemical journal. 2001; 360(Pt 1):255-264.

77. Lunn JA, Jacamo R and Rozengurt E. Preferential phosphorylation of focal adhesion kinase tyrosine 861 is critical for mediating an anti-apoptotic response to hyperosmotic stress. The Journal of biological chemistry. 2007; 282(14):10370-10379.

78. Slack JK, Adams RB, Rovin JD, Bissonette EA, Stoker CE and Parsons JT. Alterations in the focal adhesion kinase/Src signal transduction pathway correlate with increased migratory capacity of prostate carcinoma cells. Oncogene. 2001; 20(10):1152-1163.

79. Li S and Hua ZC. FAK expression regulation and therapeutic potential. Advances in cancer research. 2008; 101:45-61.

80. Mitra SK and Schlaepfer DD. Integrin-regulated FAK-Src signaling in normal and cancer cells. Current opinion in cell biology. 2006; 18(5):516-523.

81. Friedl P and Wolf K. Tumour-cell invasion and migration: diversity and escape mechanisms. Nature reviews Cancer. 2003; 3(5):362-374.

82. Serrels B, Serrels A, Brunton VG, Holt M, McLean GW, Gray CH, Jones GE and Frame MC. Focal adhesion kinase controls actin assembly via a FERM-mediated interaction with the Arp2/3 complex. Nature cell biology. 2007; 9(9):1046-1056.

83. Ilina O and Friedl P. Mechanisms of collective cell migration at a glance. Journal of cell science. 2009; 122(Pt 18):3203-3208.

84. Kraning-Rush CM and Reinhart-King CA. Controlling matrix stiffness and topography for the study of tumor cell migration. Cell adhesion & migration. 2012; 6(3):274-279.

85. Figel S and Gelman IH. Focal adhesion kinase controls prostate cancer progression via intrinsic kinase and scaffolding functions. Anti-cancer agents in medicinal chemistry. 2011; 11(7):607-616.

86. Raftopoulou M and Hall A. Cell migration: Rho GTPases lead the way. Developmental biology. 2004; 265(1):23-32.

87. Parri M and Chiarugi P. Rac and Rho GTPases in cancer cell motility control. Cell communication and signaling : CCS. 2010; 8:23.

88. Iden S and Collard JG. Crosstalk between small GTPases and polarity proteins in cell polarization. Nature reviews Molecular cell biology. 2008; 9(11):846-859.

89. Hamadi A, Bouali M, Dontenwill M, Stoeckel H, Takeda K and Ronde P. Regulation of focal adhesion dynamics and disassembly by phosphorylation of FAK at tyrosine 397. Journal of cell science. 2005; 118(Pt 19):4415-4425.

90. Tremblay L, Hauck W, Aprikian AG, Begin LR, Chapdelaine A and Chevalier S. Focal adhesion kinase (pp125FAK) expression, activation and association with paxillin and p50CSK in human metastatic prostate carcinoma. International journal of cancer Journal international du cancer. 1996; 68(2):164-171.

91. Rovin JD, Frierson HF, Jr., Ledinh W, Parsons JT and Adams RB. Expression of focal adhesion kinase in normal and pathologic human prostate tissues. The Prostate. 2002; 53(2):124-132.

92. Provenzano PP and Keely PJ. The role of focal adhesion kinase in tumor initiation and progression. Cell adhesion & migration. 2009; 3(4):347-350.

93. Lim Y, Han I, Jeon J, Park H, Bahk YY and Oh ES. Phosphorylation of focal adhesion kinase at tyrosine 861 is crucial for Ras transformation of fibroblasts. The Journal of biological chemistry. 2004; 279(28):29060-29065.

94. Kopetz S, Shah AN and Gallick GE. Src continues aging: current and future clinical directions. Clinical cancer research : an official journal of the American Association for Cancer Research. 2007; 13(24):7232-7236.

95. Kim MP, Park SI, Kopetz S and Gallick GE. Src family kinases as mediators of endothelial permeability: effects on inflammation and metastasis. Cell and tissue research. 2009; 335(1):249-259.

96. Park SI, Shah AN, Zhang J and Gallick GE. Regulation of angiogenesis and vascular permeability by Src family kinases: opportunities for therapeutic treatment of solid tumors. Expert opinion on therapeutic targets. 2007; 11(9):1207-1217.

97. Herynk MH, Zhang J, Parikh NU and Gallick GE. Activation of Src by c-Met overexpression mediates metastatic properties of colorectal carcinoma cells. Journal of experimental therapeutics & oncology. 2007; 6(3):205-217.

98. Lesslie DP, Summy JM, Parikh NU, Fan F, Trevino JG, Sawyer TK, Metcalf CA, Shakespeare WC, Hicklin DJ, Ellis LM and Gallick GE. Vascular endothelial growth

factor receptor-1 mediates migration of human colorectal carcinoma cells by activation of Src family kinases. British journal of cancer. 2006; 94(11):1710-1717.

99. Pan CC, Kumar S, Shah N, Hoyt DG, Hawinkels LJ, Mythreye K and Lee NY. Src-mediated Post-translational Regulation of Endoglin Stability and Function Is Critical for Angiogenesis. The Journal of biological chemistry. 2014; 289(37):25486-25496.

100. Summy JM and Gallick GE. Src family kinases in tumor progression and metastasis. Cancer metastasis reviews. 2003; 22(4):337-358.

101. Wang W, Liu Y and Liao K. Tyrosine phosphorylation of cortactin by the FAK-Src complex at focal adhesions regulates cell motility. BMC cell biology. 2011; 12:49.

102. Sausgruber N, Coissieux MM, Britschgi A, Wyckoff J, Aceto N, Leroy C, Stadler MB, Voshol H, Bonenfant D and Bentires-Alj M. Tyrosine phosphatase SHP2 increases cell motility in triple-negative breast cancer through the activation of SRC-family kinases. Oncogene. 2014.

103. Yang Y, Bai ZG, Yin J, Wu GC and Zhang ZT. Role of c-Src activity in the regulation of gastric cancer cell migration. Oncology reports. 2014; 32(1):45-49.

104. Kaplan KB, Swedlow JR, Morgan DO and Varmus HE. c-Src enhances the spreading of src-/- fibroblasts on fibronectin by a kinase-independent mechanism. Genes & development. 1995; 9(12):1505-1517.

105. Engen JR, Wales TE, Hochrein JM, Meyn MA, 3rd, Banu Ozkan S, Bahar I and Smithgall TE. Structure and dynamic regulation of Src-family kinases. Cellular and molecular life sciences : CMLS. 2008; 65(19):3058-3073.

106. Parsons SJ and Parsons JT. Src family kinases, key regulators of signal transduction. Oncogene. 2004; 23(48):7906-7909.

107. Vlaeminck-Guillem V, Gillet G and Rimokh R. SRC: marker or actor in prostate cancer aggressiveness. Frontiers in oncology. 2014; 4:222.

108. Chatzizacharias NA, Kouraklis GP, Giaginis CT and Theocharis SE. Clinical significance of Src expression and activity in human neoplasia. Histology and histopathology. 2012; 27(6):677-692.

109. Wheeler DL, Iida M and Dunn EF. The role of Src in solid tumors. The oncologist. 2009; 14(7):667-678.

110. Benati D and Baldari CT. SRC family kinases as potential therapeutic targets for malignancies and immunological disorders. Current medicinal chemistry. 2008; 15(12):1154-1165.

111. Summy JM and Gallick GE. Treatment for advanced tumors: SRC reclaims center stage. Clinical cancer research : an official journal of the American Association for Cancer Research. 2006; 12(5):1398-1401.

112. Jensen AR, David SY, Liao C, Dai J, Keller ET, Al-Ahmadie H, Dakin-Hache K, Usatyuk P, Sievert MF, Paner GP, Yala S, Cervantes GM, Natarajan V, Salgia R and Posadas EM. Fyn is downstream of the HGF/MET signaling axis and affects cellular shape and tropism in PC3 cells. Clinical cancer research : an official journal of the American Association for Cancer Research. 2011; 17(10):3112-3122.

113. Zardan A, Nip KM, Thaper D, Toren P, Vahid S, Beraldi E, Fazli L, Lamoureux F, Gust KM, Cox ME, Bishop JL and Zoubeidi A. Lyn tyrosine kinase regulates androgen receptor expression and activity in castrate-resistant prostate cancer. Oncogenesis. 2014; 3:e115.

114. Park SI, Zhang J, Phillips KA, Araujo JC, Najjar AM, Volgin AY, Gelovani JG, Kim SJ, Wang Z and Gallick GE. Targeting SRC family kinases inhibits growth and lymph node metastases of prostate cancer in an orthotopic nude mouse model. Cancer research. 2008; 68(9):3323-3333.

115. Goldenberg-Furmanov M, Stein I, Pikarsky E, Rubin H, Kasem S, Wygoda M, Weinstein I, Reuveni H and Ben-Sasson SA. Lyn is a target gene for prostate cancer: sequence-based inhibition induces regression of human tumor xenografts. Cancer research. 2004; 64(3):1058-1066.

116. Cai H, Smith DA, Memarzadeh S, Lowell CA, Cooper JA and Witte ON. Differential transformation capacity of Src family kinases during the initiation of prostate cancer. Proceedings of the National Academy of Sciences of the United States of America. 2011; 108(16):6579-6584.

117. Araujo JC, Trudel GC, Saad F, Armstrong AJ, Yu EY, Bellmunt J, Wilding G, McCaffrey J, Serrano SV, Matveev VB, Efstathiou E, Oudard S, Morris MJ, Sizer B, Goebell PJ, Heidenreich A, et al. Docetaxel and dasatinib or placebo in men with metastatic castration-resistant prostate cancer (READY): a randomised, double-blind phase 3 trial. The Lancet Oncology. 2013; 14(13):1307-1316.

118. Phillips R. Prostate cancer: Dasatinib fails to improve on docetaxel for metastatic CRPC. Nature reviews Urology. 2014; 11(1):5.

119. Saito YD, Jensen AR, Salgia R and Posadas EM. Fyn: a novel molecular target in cancer. Cancer. 2010; 116(7):1629-1637.

120. Gelman IH, Peresie J, Eng KH and Foster BA. Differential Requirement for Src Family Tyrosine Kinases in the Initiation, Progression, and Metastasis of Prostate Cancer. Molecular cancer research : MCR. 2014.

121. Summy JM, Sudol M, Eck MJ, Monteiro AN, Gatesman A and Flynn DC. Specificity in signaling by c-Yes. Frontiers in bioscience : a journal and virtual library. 2003; 8:s185-205.

122. Sato I, Obata Y, Kasahara K, Nakayama Y, Fukumoto Y, Yamasaki T, Yokoyama KK, Saito T and Yamaguchi N. Differential trafficking of Src, Lyn, Yes and Fyn is specified by the state of palmitoylation in the SH4 domain. Journal of cell science. 2009; 122(Pt 7):965-975.

123. Han NM, Curley SA and Gallick GE. Differential activation of pp60(c-src) and pp62(c-yes) in human colorectal carcinoma liver metastases. Clinical cancer research : an official journal of the American Association for Cancer Research. 1996; 2(8):1397-1404.

124. Suzman DL and Antonarakis ES. Castration-resistant prostate cancer: latest evidence and therapeutic implications. Therapeutic advances in medical oncology. 2014; 6(4):167-179.

125. Han NM, Fleming RY, Curley SA and Gallick GE. Overexpression of focal adhesion kinase (p125FAK) in human colorectal carcinoma liver metastases: independence from c-src or c-yes activation. Annals of surgical oncology. 1997; 4(3):264-268.

126. Calalb MB, Polte TR and Hanks SK. Tyrosine phosphorylation of focal adhesion kinase at sites in the catalytic domain regulates kinase activity: a role for Src family kinases. Molecular and cellular biology. 1995; 15(2):954-963.

127. Posadas EM, Al-Ahmadie H, Robinson VL, Jagadeeswaran R, Otto K, Kasza KE, Tretiakov M, Siddiqui J, Pienta KJ, Stadler WM, Rinker-Schaeffer C and Salgia R. FYN is overexpressed in human prostate cancer. BJU international. 2009; 103(2):171-177.

128. Zheng Y, Gierut J, Wang Z, Miao J, Asara JM and Tyner AL. Protein tyrosine kinase 6 protects cells from anoikis by directly phosphorylating focal adhesion kinase and activating AKT. Oncogene. 2013; 32(36):4304-4312.

129. Evdokimova V, Tognon C, Ng T and Sorensen PH. Reduced proliferation and enhanced migration: two sides of the same coin? Molecular mechanisms of metastatic progression by YB-1. Cell cycle. 2009; 8(18):2901-2906.

130. Paccez JD, Vasques GJ, Correa RG, Vasconcellos JF, Duncan K, Gu X, Bhasin M, Libermann TA and Zerbini LF. The receptor tyrosine kinase Axl is an essential regulator of prostate cancer proliferation and tumor growth and represents a new therapeutic target. Oncogene. 2013; 32(6):689-698.

131. Varkaris A, Corn PG, Gaur S, Dayyani F, Logothetis CJ and Gallick GE. The role of HGF/c-Met signaling in prostate cancer progression and c-Met inhibitors in clinical trials. Expert opinion on investigational drugs. 2011; 20(12):1677-1684.

132. Sequeira L, Dubyk CW, Riesenberger TA, Cooper CR and van Golen KL. Rho GTPases in PC-3 prostate cancer cell morphology, invasion and tumor cell diapedesis. Clinical & experimental metastasis. 2008; 25(5):569-579.

133. Calalb MB, Zhang X, Polte TR and Hanks SK. Focal adhesion kinase tyrosine-861 is a major site of phosphorylation by Src. Biochemical and biophysical research communications. 1996; 228(3):662-668.

134. Iguchi K, Ishii K, Nakano T, Otsuka T, Usui S, Sugimura Y and Hirano K. Isolation and characterization of LNCaP sublines differing in hormone sensitivity. Journal of andrology. 2007; 28(5):670-678.

135. Lim DJ, Liu XL, Sutkowski DM, Braun EJ, Lee C and Kozlowski JM. Growth of an androgen-sensitive human prostate cancer cell line, LNCaP, in nude mice. The Prostate. 1993; 22(2):109-118.

136. Lim ST. Nuclear FAK: a new mode of gene regulation from cellular adhesions. Molecules and cells. 2013; 36(1):1-6.

137. Park J and Cartwright CA. Src activity increases and Yes activity decreases during mitosis of human colon carcinoma cells. Molecular and cellular biology. 1995; 15(5):2374-2382.

138. Hauck CR, Hsia DA and Schlaepfer DD. The focal adhesion kinase--a regulator of cell migration and invasion. IUBMB life. 2002; 53(2):115-119.

139. Ren XD, Kiosses WB, Sieg DJ, Otey CA, Schlaepfer DD and Schwartz MA. Focal adhesion kinase suppresses Rho activity to promote focal adhesion turnover. Journal of cell science. 2000; 113 (Pt 20):3673-3678.

140. O'Connor K and Chen M. Dynamic functions of RhoA in tumor cell migration and invasion. Small GTPases. 2013; 4(3):141-147.

141. Hildebrand JD, Taylor JM and Parsons JT. An SH3 domain-containing GTPase-activating protein for Rho and Cdc42 associates with focal adhesion kinase. Molecular and cellular biology. 1996; 16(6):3169-3178.

142. Bianco FJ, Jr., Scardino PT and Eastham JA. Radical prostatectomy: long-term cancer control and recovery of sexual and urinary function ("trifecta"). Urology. 2005; 66(5 Suppl):83-94.

143. Cheng L, Zincke H, Blute ML, Bergstralh EJ, Scherer B and Bostwick DG. Risk of prostate carcinoma death in patients with lymph node metastasis. Cancer. 2001; 91(1):66-73.

144. Daneshmand S, Quek ML, Stein JP, Lieskovsky G, Cai J, Pinski J, Skinner EC and Skinner DG. Prognosis of patients with lymph node positive prostate cancer following radical prostatectomy: long-term results. The Journal of urology. 2004; 172(6 Pt 1):2252-2255.

145. Masterson TA, Bianco FJ, Jr., Vickers AJ, DiBlasio CJ, Fearn PA, Rabbani F, Eastham JA and Scardino PT. The association between total and positive lymph node counts, and disease progression in clinically localized prostate cancer. The Journal of urology. 2006; 175(4):1320-1324; discussion 1324-1325.

146. Choi W, Porten S, Kim S, Willis D, Plimack ER, Hoffman-Censits J, Roth B, Cheng T, Tran M, Lee IL, Melquist J, Bondaruk J, Majewski T, Zhang S, Pretzsch S, Baggerly K, et al. Identification of distinct basal and luminal subtypes of muscle-invasive bladder cancer with different sensitivities to frontline chemotherapy. Cancer cell. 2014; 25(2):152-165.

VITA

Tanushree Chatterji was born in Rajasthan, India, the daughter of Priyabrata Chatterji and Krishna Chatterji. After completing her high-school education in Mumbai, India in 2001, she entered University of Mumbai, Mumbai, India. She received the degree of Bachelor of Science with a major in pharmaceutical sciences from Mumbai University in May, 2002. She also earned the degree of Master of Science with a major in Biomedical and Pharmaceutical Sciences from Idaho State University, Idaho, USA in May, 2010. In August of 2010, she entered the Graduate School of Biomedical Sciences at the University Of Texas Health Science Center in Houston, TX.